Investigation of Antenna Elements and Arrays as Feed for Offset Reflector Antenna

Kaushik Debbarma

Investigation of Antenna Elements and Arrays as Feed for Offset Reflector Antenna

A

Thesis submitted

for the award of the degree of

DOCTOR OF PHILOSOPHY

By

Kaushik Debbarma

DEPARTMENT OF ELECTRONICS AND ELECTRICAL ENGINEERING

INDIAN INSTITUTE OF TECHNOLOGY GUWAHATI

GUWAHATI - 781 039, ASSAM, INDIA

March, 2021

Declaration

I hereby declare that the thesis entitled "**Investigation of Antenna Elements and Arrays as Feed for Offset Reflector Antenna**", submitted in the *Department of Electronics and Electrical Engineering, Indian Institute of Technology Guwahati, Assam, India*, for the award of the degree of **Doctor of Philosophy**, has been carried out by me under the supervision and guidance of Prof. Ratnajit Bhattacharjee. The results embodied in this thesis are original and have not been submitted to any other University or Institute for the award of any degree or diploma.

Dated:

Place: Guwahati

Kaushik Debbarma
Research Scholar
Dept. of Electronics and Electrical Engineering
Indian Institute of Technology Guwahati
Guwahati - 781039, Assam, India.

Certificate

This is to certify that the thesis entitled "**Investigation of Antenna Elements and Arrays as Feed for Offset Reflector Antenna**", submitted by **Kaushik Debbarma** (146102025), a research scholar in the *Department of Electronics and Electrical Engineering, Indian Institute of Technology Guwahati*, for the award of the degree of **Doctor of Philosophy**, is a record of an original research work carried out by him under my supervision and guidance. The thesis has fulfilled all requirements as per the regulations of the institute and in my opinion has reached the standard needed for submission. The results embodied in this thesis have not been submitted to any other University or Institute for the award of any degree or diploma.

Dated:

Guwahati.

Prof. Ratnajit Bhattacharjee
Professor
Dept. of Electronics and Electrical Engg.
Indian Institute of Technology Guwahati
Guwahati - 781 039, Assam, India.

To my lovely wife and parents

Acknowledgements

First and foremost, I wish to express my deepest gratitude to my thesis supervisor Prof. Ratnajit Bhattacharjee, for his excellent guidance throughout my PhD tenure. His work ethic and attention to details have been a source of great inspiration to me. My heartfelt thanks to him for his support and guidance during my difficult periods. He was always available and supportive during my moments of distress. I can not thank him enough for the patience shown by him while listening and clarifying my silliest of doubts. He has made an everlasting impression on my way of looking at problems, both professional and personal.

I want to thank my doctoral committee members: Prof. Rakhesh Singh Kshetrimayum, Dr. Nagarjuna Nallam, and Prof. Tarak Nath Dey for sparing time out of their busy schedule to evaluate my progress. They have enriched this work with their valuable suggestions and feedbacks. I would also like to thank Dr. Mahima Arrawatia and Dr. Debabrata Sikdar, for helping me with my research work in innumerable ways.

During my stay here in IIT Guwahati, I made many friends with whom I shared several precious memories that will stay with me forever. The comradery shared between me, Vivek, Alex, Vijith, Mathew, and Sishir is unbelievable, and I thank them all for their friendship. The encouragement and guidance received from seniors, Prateek, Pawan, Jitendra, and Anoop were immensely helpful in writing this thesis. Sports is essential for a healthy mind. Durga, Mirzaul, Anirban, and Vivek made sure that I was never short of any physical activity. My lab-mates and research scholars Arijit, Mohit, Ramanand, Rahul, and Prateek maintained the healthy and conducive lab environment necessary for good research.

Lastly, I extend my sincere thanks to all the staff members from EEE office and Academic office for helping me out in all sorts of ways during my stay at IITG.

Kaushik Debbarma

Abstract

This thesis presents an exhaustive study of microstrip antenna elements and arrays as feed for offset reflector antennas. Offset reflector antennas are popular due to their low aperture blockage and good isolation between the feed and the reflector. However, the asymmetry in offset reflector geometry also leads to depolarization of the incident waves on the reflector, thereby generating high cross-polarization in the asymmetric plane of the reflector. Such high cross-polar levels can be reduced by generating a higher order mode at an appropriate ratio in the reflector feed. This technique of cross-polar suppression is known as conjugate field matching (CFM) and is often employed in traditional matched horn feeds. Use of microstrip antennas as alternate feeds has generated much interest in the research community due to their low profile, light weight and low cost attributes. The TM_{21} mode, when generated at an appropriate ratio to the dominant mode in a circular microstrip patch antenna (CMPA), has shown cross-polar suppression attributes due to CFM.

This thesis investigates the performance of the matched feeds using microstrip antenna and arrays working on the principle of CFM. A total of 6 matched feed designs are proposed in this thesis, which includes the following:

- A dual-mode (TM_{11} and TM_{21}) CMPA generating both the modes at an appropriate ratio is designed for cross-polar reduction in the reflector pattern.
- A single layer centered circular array (CCA) of 9 elements as matched feed is proposed, which consists of 8 TM_{11} mode operating ring CMPA elements and a central TM_{21} mode generating CMPA.
- A dual-layer CCA matched feed of 10 elements is studied as matched feed, which is further investigated for reflector pattern reconfigurability in terms of beamwidth control and beam shifting. The top layer of CCA consists of 9 CMPAs each operating

in TM_{11} mode while the bottom layer contains a CMPA, placed below the central element and operates in TM_{21} mode.

- A dual-layer CCA matched feed of 10 elements similar to the previous design is investigated for dual-band application. The ring elements and the central dual-mode CMPA elements operate at 4 GHz and 6 GHz, respectively,
- A dual-mode matched feed is designed in which the TM_{21} mode is generated by an annular ring patch. The dimensions of the annular ring patch is adjusted for best cross-polar suppression at the operating frequency.
- A dual-mode matched feed is designed in which the top layer consists of a rectangular microstrip patch antenna generating TM_{10} mode and a CMPA generating TM_{21} mode.

In all the proposed matched feeds, the cross-polarization is reduced well below -30 dB while maintaining the sidelobe level better than -18 dB. The last two designs are also optimised for small offset reflectors (diameter less than 10λ) and specifically targeted for 5G sub-6 GHz band applications.

Keywords: Offset reflector antenna, conjugate field matching, centered circular array, matched feeds, dual-mode circular microstrip patch antenna, annular ring patch.

Contents

List of Figures **xix**

List of Tables **xxv**

List of Acronyms **xxvii**

List of Symbols **xxix**

1 Introduction **1**

1.1 Introduction to Reflector Antennas 2

1.1.1 Offset reflector antennas 2

1.2 Literature Survey on Reflector Feeds 5

1.2.1 Depolarization effect in offset reflector antennas 5

1.2.2 Literature review of conventional matched feeds 5

1.2.3 Literature review on alternate feeds for offset reflector 6

1.2.4 Literature review on some recent multi-mode microstrip antennas 8

1.3 Motivation and Problem Formulation 8

1.4 Contribution of the Thesis 9

1.5 Organization of the Thesis 10

1.6 Conclusion 12

2 Investigation of Conventional Microstrip Array Feeds **15**

2.1 Introduction 16

2.2 Aperture Field / Geometrical Optics Technique for Reflector Pattern calculation . . . 16

2.2.1 Reflector pattern of an offset reflector with $F/D = 0.6$ fed by a single circular microstrip patch feed 18

2.3 Conventional Array Feeds 19

2.3.1 Linear array 20

2.3.1.1 Number of antenna elements and inter-element spacing 20
2.3.1.2 Variation in element excitation 23
2.3.2 2-D Arrays of microstrip antennas 24
2.3.2.1 Circular array 25
2.3.2.2 3×3 square array 26
2.4 Conclusion 27

3 Introduction to Dual-mode CMPA Matched Feeds 29

3.1 Introduction 30
3.2 Review of Conjugate Field Matching 30
3.2.1 Focal plane fields of the offset reflector 30
3.2.2 TM_{21} mode as the asymmetric mode in the proposed matched feed 31
3.3 Proposed Dual-mode Matched Feed 32
3.3.1 Analytical expression for far-field pattern of the proposed matched feed 33
3.3.2 Secondary radiation pattern using GO 34
3.4 Investigation of Proposed Feed using CAD Simulators 37
3.4.1 Stacked Dual-mode CMPA 37
3.4.2 Reflector pattern using HFSS-PO 38
3.5 Conclusion 41

4 Circular Array Matched Feeds for Offset Reflector Antenna 43

4.1 Introduction 44
4.2 Single Layer CCA with TM_{21} Mode operating Centre Patch 45
4.2.1 Analytical expressions of the far-field pattern of the proposed feed 45
4.2.2 Proposed feed design in CAD simulator 47
4.3 CCA with Dual-Mode CMPA as Central Element 51
4.3.1 Analytical model of the proposed dual-layer CCA matched feed 52
4.3.1.1 Effect of array radius on cross-polarization 53
4.3.1.2 Offset reflector pattern for $F/D = 0.7$ 54
4.4 Beam Shifting and Beam Size Control using the Dual-layer CCA Matched Feed . . . 56
4.4.1 Beamwidth control 56
4.4.2 Beam-shifting in the reflector pattern 59

4.4.2.1 Large beam shift case: 0.4° beam shift . . . 59
4.4.2.2 Small beam shift case: 0.1° beam shift . . . 59
4.5 CCA Feed for Dual Band Application . . . 62
4.5.1 Design issues . . . 64
4.5.2 Proposed dual-band microstrip patch antenna feed . . . 65
4.5.2.1 Feed and reflector pattern at 6 GHz . . . 67
4.5.2.2 Feed and reflector pattern at 4 GHz . . . 69
4.5.3 Experimental validation . . . 72
4.6 Conclusion . . . 74
5 Matched MPA Feeds for Small Offset Reflector Antenna 75
5.1 Introduction . . . 76
5.2 Design and Analysis of First Matched Feed . . . 76
5.2.1 Working principle . . . 77
5.2.1.1 Analytical model . . . 77
5.2.1.2 HFSS model . . . 78
5.2.2 Reflector pattern analysis . . . 79
5.2.2.1 Using GO technique . . . 81
5.2.2.2 Using HFSS-PO . . . 82
5.2.3 Experimental Validation . . . 88
5.3 Design and Analysis of Second Matched Feed . . . 89
5.3.1 Working principle . . . 89
5.3.2 Simulation results and discussions . . . 91
5.3.3 Experimental validation . . . 93
5.4 Conclusion . . . 94
6 Summary of Thesis and Future Study 99
6.1 Summary of Work . . . 100
6.1.1 Dual-mode CMPA as matched feed . . . 100
6.1.2 Single layer CCA matched feed . . . 100
6.1.3 Dual layer CCA matched feed . . . 100
6.1.3.1 Beam shifting and beam size control . . . 100

6.1.3.2 Dual band application 101
6.1.4 Matched feeds using annular ring patches 101
6.1.5 Matched feed using RMPA for dominant mode and CMPA for TM_{21} mode . . 101
6.2 Future Scope of Investigation 101
6.2.1 Circularly polarized matched feeds 101
6.2.2 Multibeam offset reflectors 102
6.2.3 Investigation of other higher order modes for conjugate field matching 102
A Experimental Setup for Measuring Feed Antenna Pattern **103**
Bibliography **105**
List of Publications **111**

List of Figures

1.1 Offset reflector antenna configuration. 3

1.2 Thesis organization. 13

2.1 Reflector pattern obtained using both the GO technique and HFSS-PO at $\Phi = 90°$. . 19

2.2 Cross-polarization in the reflector pattern for different values of F/D obtained using the MATLAB code. 19

2.3 Variation in cross-polar levels in the reflector pattern with increase in inter-element spacing of the 2-element linear array feed along Y-axis with x-polarized CMPA elements. 20

2.4 Variation in cross-polar levels in the reflector pattern with increase in inter-element spacing of the 4-element linear array feed along Y-axis with x-polarized CMPA elements. 21

2.5 Variation in cross-polar levels in the reflector pattern with increase in inter-element spacing of the 6-element linear array feed along Y-axis with x-polarized CMPA elements. 21

2.6 Variation in cross-polar levels in the reflector pattern with increase in inter-element spacing of the 2-element linear array feed along X-axis with x-polarized CMPA elements. 22

2.7 Variation in cross-polar levels in the reflector pattern with increase in inter-element spacing of the 4-element linear array feed along X-axis with x-polarized CMPA elements. 23

2.8 Variation in cross-polar levels in the reflector pattern with increase in inter-element spacing of the 6-element linear array feed along X-axis with x-polarized CMPA elements. 23

2.9 (a) 3x3 square array and (b) simple circular array (SCA). 24

2.10 Radius of circular array vs cross-polarization level in the secondary radiation pattern using MATLAB code. 25

2.11 Radius of circular array vs cross-polarization level in the secondary radiation pattern using HFSS-PO. 26

2.12 Inter-element separation, d vs cross-polarization level in secondary radiation pattern using the MATLAB code. 26
2.13 Inter-element separation, d vs cross-polarization level in secondary radiation pattern using HFSS-PO. 27

3.1 Focal plane field configuration of symmetric and asymmetric components when fed by incident wave polarized in horizontal and vertical polarization. 31
3.2 Dual-mode circular microstrip patch antenna. 33
3.3 Variation in cross-polar levels with variation in C_2/C_1 ratio. 34
3.4 Cross-polar level at $C_2/C_1 = 0.5$ for X and Y-polarized circular microstrip antenna. . 35
3.5 Optimum excitation ratio C_2/C_1 for different values of F/D ratio for X and Y-polarization. 35
3.6 Optimum excitation ratio C_2/C_1 for different values of H for $F/D = 0.6$ for X and Y-polarization. 36
3.7 (a) Top view and side view of the dual-mode CMPA designed in HFSS and (b) Modal features of both the patch (upper patch on the left and lower at the right) when excited individually. 37
3.8 Return losses at both the ports obtained in HFSS and CST. 38
3.9 Variation in cross-polarization at the asymmetric plane with C_2/C_1 ratio. 39
3.10 Secondary field pattern of the offset reflector at the asymmetric plane when fed by the proposed matched feed design. 39
3.11 Primary feed pattern (at $\phi = 90°$) for optimized excitation ratio using both MATLAB code and HFSS-PO. 40
3.12 Cross-polar bandwidth in the secondary field pattern of the offset reflector with the proposed matched feed design. 40

4.1 Effect of variation in the excitation ratio between TM_{11} and TM_{21} modes on the cross-polar levels for different values of circular array radius. This study is performed using the MATLAB code for $F/D = 0.6$. 46

4.2 Effect of variation in the excitation ratio between the TM_{11} and TM_{21} mode on the cross-polar levels for different values of circular array radius. This study is performed using the MATLAB code for an array radius of 0.6λ. 46
4.3 CCA with TM_{21} operating central patch. 47
4.4 Parametric study of the effect of excitation ratio between the two modes on the cross-polarization at the asymmetric plane of the reflector pattern. 48
4.5 Secondary field pattern of the offset reflector at the asymmetric plane for the single layer CCA unmatched feed. 48
4.6 Secondary field pattern of the offset reflector at the asymmetric plane for the single layer CCA matched feed. 49
4.7 Field pattern (at $\phi = 90°$) of the proposed CCA feed using (4.1 and the two CAD simulators with optimized excitations. 49
4.8 Cross-polar bandwidth in the secondary field pattern of the offset reflector with the single layer CCA matched feed. 50
4.9 Gain pattern at $\Phi = 90°$ for the CCA feed design. 50
4.10 Gain versus frequency plot. 51
4.11 Proposed matched feed array dual-layered structure. The proposed structure consists of 10 CMPA elements. 52
4.12 Effect of variation in excitation ratio between the TM_{11} and TM_{21} mode for different values of circular array radius on cross-polarization. The F/D of the reflector is kept as 0.7 for this study. 53
4.13 Effect of variation in excitation ratio between the TM_{11} and TM_{21} mode for different values of $\frac{F}{D}$ ratio on cross-polarization. The array radius is kept as 0.6λ in this study. 54
4.14 Offset reflector pattern for $\frac{F}{D} = 0.7$ with unmatched CCA feed. 55
4.15 Offset reflector pattern for $\frac{F}{D} = 0.7$ with matched CCA feed. 55
4.16 Combinations of array elements for beamwidth control (a) only the central dominant and higher mode operating patches are excited (b) antenna element 2,4,6 and 8 along with the central dominant and higher mode operating patches are excited. 56
4.17 Beamwidth variation in reflector pattern (a) at $\Phi = 90°$ (b) at $\Phi = 0°$. 57
4.18 Reflector pattern at $\Phi = 0°$ (symmetric plane) for unmatched feed array. 58

4.19 Reflector pattern at $\Phi = 90^\circ$ (asymmetric plane) for matched feed array with proper excitation ratio between the two modes. 58
4.20 Reflector pattern beam shift in different direction on selective excitation of only a single CMPA array element. 60
4.21 Matched feed array (a) only CMPA 4 is excited along with the central TM_{11} and TM_{21} mode operating patches (b) only CMPA 8 is excited along with the central TM_{11} and TM_{21} mode operating patches. 61
4.22 Beam shift of 0.4° from the principal axis in the reflector pattern at $\Phi = 0^\circ$ (symmetric plane). 61
4.23 Reflector pattern for unmatched feed at $\Phi = 90^\circ$ (asymmetric plane). 62
4.24 Reflector pattern for matched feed at $\Phi = 90^\circ$ (asymmetric plane). 62
4.25 Matched feed array excitation (a) combination 1 (b) combination 2. 63
4.26 Beam shifting at $\Phi = 0^\circ$(symmetric plane) of the reflector pattern. Beam 1 corresponds to combination 1 and beam 2 corresponds to combination 2. 63
4.27 Reflector pattern for unmatched feed at $\Phi = 90^\circ$ (asymmetric plane). 64
4.28 Reflector pattern for matched feed at $\Phi = 90^\circ$ (asymmetric plane). 64
4.29 Proposed dual band dual-layer CCA reflector feed antenna 66
4.30 Cross-polar variation with the array radius for dual band antenna 67
4.31 Return losses of the proposed dual band antenna feed at both the operating frequencies 68
4.32 Return losses of the proposed dual band antenna feed at both the operating frequencies using CST. 68
4.33 Primary feed pattern of the proposed dual band antenna feed at 6 GHz obtained using both HFSS and CST. 69
4.34 Reflector pattern obtained using HFSS-PO at 6 GHz. 70
4.35 Feed pattern of the dual band CCA at 4 GHz obtained using HFSS and CST. 70
4.36 Reflector pattern of the offset reflector at 4 GHz. 71
4.37 Fabricated prototype of the central part of the dual band feed operating at 6 GHz. . . 72
4.38 Return losses of the proposed dual band antenna feed at both the operating frequencies. 72
4.39 Field pattern of the prototype when only port 1 is excited. 73
4.40 Field pattern of the prototype when only port 2 is excited. 73

5.1 Geometry of the proposed feed design (a) side view along X-axis and (b) top view. . . 79
5.2 Nature of field distribution in AR for different values of a_1 given by (a) 3 mm (b) 4 mm (c) 5 mm (d) 6 mm and (e) 7 mm. 80
5.3 Offset reflector antenna configuration. 80
5.4 Optimum excitation ratio (magnitude) for different a_1 81
5.5 Variation in reflector cross-polarization for different excitation ratios for $a_1 = 5$ mm . 81
5.6 Simulated reflector pattern obtained using the analytical feed model (for $a_1 = 5$ mm) . 82
5.7 Reflector cross-polar performance with variation in excitation ratio for different feed dimensions. 83
5.8 Aperture H-fields generated at the upper circular patch due to the AR with inner radius given by(a) $a_1 = 3$ mm (b) $a_1 = 4$ mm (c) $a_1 = 5$ mm (d) $a_1 = 6$ mm and (e) $a_1 = 7$ mm. 84
5.9 Nature of transverse H-field distribution in the proposed matched feed for $a_1 = 5$ mm. 84
5.10 Normalized offset reflector pattern at $\Phi = 90°$ obtained using HFSS-PO. 85
5.11 -30 dB cross-polar bandwidth of the ORA illuminated by the proposed matched feed. 85
5.12 Gain v/s frequency plot. 86
5.13 Radiation pattern of the proposed feed with the optimized excitation ratio and $a_1 = 5$ mm. 86
5.14 Fabricated prototype of the proposed feed. 87
5.15 Comparison of the measured return losses of the proposed feed with the simulated results obtained in both HFSS and CST. 87
5.16 Feed pattern of the proposed structure when only port 1 is excited. 88
5.17 Feed pattern of the proposed structure when only port 2 is excited. 88
5.18 Proposed matched feed in HFSS. 91
5.19 Aperture field distribution of the proposed feed when (a) only port 1 is excited, (b) only port 2 is excited and (c) both the ports are excited. 91
5.20 Reflector pattern at the asymmetric plane ($\Phi = 90°$) obtained for an ORA with $\frac{F}{D} = 0.6$ using GO MATLAB code 92
5.21 Reflector pattern at the asymmetric plane ($\Phi = 90°$) obtained for an ORA with $\frac{F}{D} = 0.6$ using HFSS-PO 93

5.22 Feed pattern of the proposed dual-mode matched feed with optimized excitation ratio between the two modes (TM_{10} mode and TM_{21} mode). 94
5.23 An image of the matched feed prototype fabricated on FR4. 95
5.24 Return loss of the proposed matched obtained using HFSS, CST and measurement. . . 95
5.25 Feed pattern when only port 1 is excited and port 2 is terminated by a 50 Ω matched load. 96
5.26 Feed pattern when only port 2 is excited and port 1 is terminated by a 50 Ω matched load. 96

A.1 (a) Illustrative diagram of the experimental setup (b) Photograph of the experimental setup for pattern measurement of the proposed feed with annular ring patch at the bottom. 104

List of Tables

1.1 Different mode combination for optimum field matching in matched feeds using multi-mode horns 6

2.1 Variation in cross-polarization with variation in number of elements and inter-element spacing obtained using HFSS-PO 22

2.2 Variation in cross-polarization with variation in number of elements and inter-element spacing obtained using HFSS-PO 22

2.3 Variation in cross-polarization with variation in element excitation distribution in an offset reflector with $F/D = 0.6$ 24

3.1 Performance of ORA fed by the proposed feed 41

4.1 Performance analysis of the matched feed designs for an offset reflector with $F/D = 0.6$ and operating at 20 GHz 51

4.2 Offset reflector dimensions 51

4.3 Variation of the simulated reflector gain with frequency 54

4.4 Offset reflector dimensions 64

4.5 Dual band feed parameters 67

4.6 Offset reflector performance at 6 GHz 69

4.7 Offset reflector performance at 4 GHz 71

4.8 Performance analysis of the dual layer CCA matched feed 71

5.1 Different stacked patch dimensions with varying a_1 resonating at 3.5 GHz 79

5.2 Cross-polarization in the reflector pattern at 3.5 GHz for different values of a_1 83

5.3 Performance of ORA fed by the proposed feed 86

5.4 Cross-polarization at $\Phi = 90°$ in the reflector pattern when the F/D of the ORA is varied 92

5.5 Performance of ORA fed by the proposed feed 93

List of Acronyms

AR	Annular ring
CAD	Computer-Aided Design
CCA	Centered Circular Array
CFM	Conjugate Field Matching
CMPA	Circular Microstrip Patch Antenna
GO	Geometrical Optic
RMPA	Rectangular Microstrip Patch Antenna
SCA	Simple Circular Array
TM mode	Transverse Magnetic mode
ORA	Offset Reflector Antenna

List of Symbols

J_n	Bessel function of first kind
$J_n{}'$	Derivative of Bessel function of first kind
α	Offset angle of the reflector
a_{mn}	Effective radius of circular microstrip patch antenna operating in TM_{mn} mode
F	Focal length of the parent paraboloid
D	Diameter of projected aperture of the reflector at the focal plane
H	Offset height of the reflector
θ^*	Half illumination angle
k_0	Free space wave number
a_1	Inner radius of the annular ring patch
b_1	Outer radius of the annular ring patch
a	Radius of the circular microstrip patch antenna
h	Height of the substrate
ϵ_r	Dielectric constant of the substrate
λ	Free space wavelength

1

Introduction

Contents

1.1 Introduction to Reflector Antennas 2
1.2 Literature Survey on Reflector Feeds 5
1.3 Motivation and Problem Formulation 8
1.4 Contribution of the Thesis 9
1.5 Organization of the Thesis 10
1.6 Conclusion 12

1.1 Introduction to Reflector Antennas

Reflector antennas have found widespread application in satellite communication, radar, weapon systems, radiometry, cellular communication, medical applications, space communication, etc. due to their high gain and narrow beamwidth attributes. These electrically large antennas (usually $20 - 70\lambda$ in diameter) are mostly used at frequencies higher than 1 GHz. At lower frequencies, the physical size of these reflector antennas becomes bulky and present handling issues. A typical reflector antenna section is basically a conic section i.e. it is either a parabola or a hyperbola or an ellipse or a circle [1]. These conic sections are used to generate reflector antennas through rotation around either of the primary axes or translation along one of the primary axes. The main objective of these reflector antennas is to collimate the microwave energy radiating from the feed into a narrow beam, with very small amount of spillover energy.

Reflector antennas have a very long and enriched history. From legends, it is believed that parabolic reflectors were used by Archimedis to concentrate sun's heat rays and burn the Roman enemy ships in 212-215 B.C. The parabolic reflectors were also used in the earlier experiments conducted by Marconi for his first patent in 1893 A.D. [1]. The extensive use of reflectors for developing radars during the second world war, has led to the development of reflectors with various shapes. The different techniques for their analysis were also developed during this period. After second world war, the demand for parabolic reflectors grew for deep space exploration, radio astronomy and satellite tracking. Parabolic reflectors were deployed all around the globe for deep space exploration, such as the 64-m radio astronomy antenna at Parkes in 1961 A.D. In modern times, reflectors are used for almost all the wireless point-to-point communications, digital broadcast satellite systems, space exploration, etc.

1.1.1 Offset reflector antennas

Reflector antennas can be classified into single reflector and multi-reflector antennas. Examples of multi-reflector antennas include cassegrain and gregorian reflector antennas. In multi-reflector arrangement, the feed is placed behind the main reflector and illuminates the sub-reflectors first. In the single reflector antenna, the feed is placed in front of the reflector and can be further classified as axial and offset fed reflectors. Although, the primary feed blocks the aperture of the reflector in both the front fed cases, an offset reflector reduces the aperture blockage by placing the feed at an offset angle (α). These offset fed reflector further improves the isolation between feed and reflector,

compared to its center fed counterpart. The offset fed reflectors are also easily deployable in satellites and on the move applications. A typical offset reflector is shown in Fig. 1.1. In Fig. 1.1, primed and unprimed coordinates correspond to parent paraboloid and offset coordinates, respectively. The secondary coordinate system for the offset reflector is given by (r,Ψ,Φ). Further, the reflector shown in Fig. 1.1 is arranged such that the asymmetric plane is along $\Phi = 90°$ and the symmetric plane is along $\Phi = 0°$. Feed and reflector coordinates are represented by unprimed and primed coordinates. Features like low sidelobe level, good aperture efficiency and high isolation between the feed and the reflector make offset reflector a preferred option in low noise applications e.g. as VSAT (very small aperture terminal) [2,3] in satellite broadcasting systems. In addition to VSAT, such offset reflectors also find applications in conventional satellite systems [1,4], and radars [5,6]. Large sized reflector antennas are deployed for space exploration all over the globe.

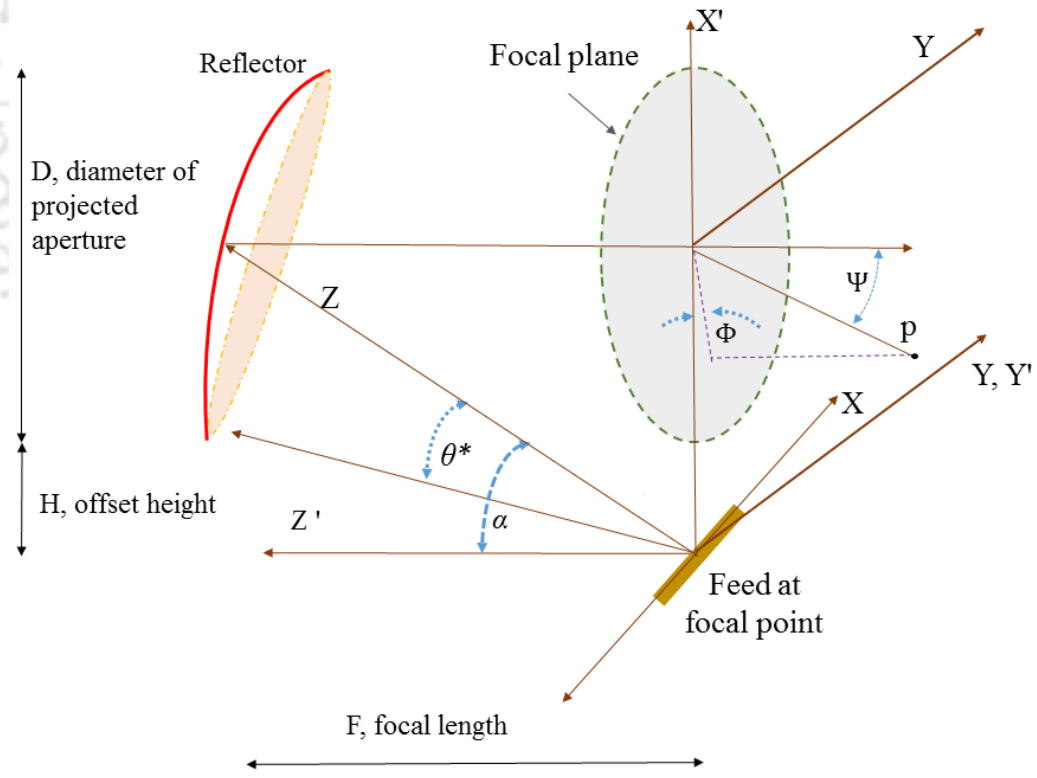

Figure 1.1: Offset reflector antenna configuration.

Even with all the advantages of an offset reflector, it has one major disadvantage, which needs careful consideration during its design. An offset reflector tends to suffer from depolarization effect inherited due to its offset feed. This effect is severe for offset reflectors with small F/D ratio (F/D< 1).

They produce high cross-polarization (> -25 dB) at the asymmetric plane of the reflector pattern, when illuminated by a pure linearly polarized feed [2,7]. In case of a pure circularly polarized wave excitation, the main beam of the reflector pattern is squinted due to the depolarization effect [8]. In recent times, the commercial communication systems usually employ polarization diversity for better utilization of the available frequency spectrum. In such a scenario, the high cross-polarization component will severely affect the quality of signals due to cross-talk. Further, even if the communication systems does not employ polarization diversity, reduction in cross-polar components will improve the overall efficiency of the antenna system. Thus, a proper mechanism to improve the cross-polar performance in the reflector radiation pattern presents an attractive research problem. Several cross-polarization mitigation techniques are reported in literature, some of which include the following:

- Since, high cross-polarization occurs mainly in offset reflectors with small F/D, maintaining large focal-length-to-diameter ratio (F/D) and small tilt angle comes as an automatic choice to minimize cross-polarization. However, in such cases, the reflector system becomes bulkier and unsuitable for applications with space constraints. [2, 9].

- Polarization selective grid is another option used to suppress the cross-polarization in the reflector pattern [10, 11]. It is placed between the feed and the reflector for cross-polar improvement. In [10], Gregorwich et al. have investigated polarization selective reflector (PRS) system by placing a wire reflector in front of the main reflector for cross-polar reduction. Two types of polarization selective grids, namely straight strip grid and a curved strip grid are investigated by Nakamura et al. in [11]. However, such grids add to the complexity level of the reflector arrangement.

- Use of the conventional dielectric lens in front of feed horn is a way of reducing the cross-polar power of an offset reflector antenna [12]. However, presence of a dielectric lens increases the noise temperature and the system gain gets reduced.

- In [13, 14], Rudge et al. proposed a technique of improving the cross-polarization in the reflector pattern by combining higher order modes with the fundamental modes of a horn at an appropriate ratio. The reflector feeds employing this technique are known as matched feeds.

This thesis further explores the concept of optimal field matching in the design and analysis of multi-mode microstrip patch antenna elements and arrays as matched feed for offset reflector antennas.

1.2 Literature Survey on Reflector Feeds

1.2.1 Depolarization effect in offset reflector antennas

As discussed previously, the depolarization effect in offset reflectors are responsible for high cross-polarization in the asymmetric plane of the reflector pattern. The extent of this depolarization effect depends on the value of the offset angle (α). For a large α, the depolarization effect will be high, which in turn will produce high cross-polarization and beam squinting in the reflector pattern for linear and circularly polarized wave excitations, respectively. In [15], Chu et al. demonstrated the dependance of the cross-polarized radiation on α using mathematical and experimental results. The reflected field from the parabolic reflector using the geometrical optics [16], can be expressed as:

$$\vec{E}_r = -\vec{E}_f + 2\hat{n}(\vec{E}_f.\hat{n}) \tag{1.1}$$

where, $\vec{E}_f$ is the primary feed pattern and $\hat{n}$ is the unit normal to the reflector surface. Further, using a balanced feed it is shown that the cross-polarization and beam-squint becomes zero when $\alpha = 0^\circ$ for linearly and circularly wave excitations, respectively.

1.2.2 Literature review of conventional matched feeds

A class of primary feed for offset reflectors is reported by Rudge et al in [14] to overcome this depolarization effect in offset reflectors. This primary feed reported in [14] for an offset reflector antenna is a tri-mode (TE_{11}, TM_{11} and TE_{21}) smooth-walled cylindrical horn antenna. This primary feed is also known as matched feed and works on the principle of conjugate field matching (CFM). CFM is achieved in this primary feed by addition of selected higher order modes (specifically the TE_{21} mode) such that the asymmetric field component of the feed aperture is similar to that of the focal plane electric field distributions in the offset reflector antenna. The excitation ratio between the higher order modes and the dominant mode of the primary horn feed is then varied to obtain the optimal field matching. At an optimum excitation ratio between the higher order modes and the dominant mode, cross-polarization is reduced in the reflector pattern. Further details of CFM is provided in chapter 3. It may be noted that good cross-polarization is achieved in [14] without increasing any complexity or mass in the overall reflector design. This concept of field matching is later employed by several other multi-mode horn feeds and are well documented in literature [5, 13, 17–31]. The matched horn feeds reported in literature are of different shapes. Rectangular matched horns reported in [5, 32]

for offset reflectors. In [5], Sharma et al have designed a rectangular matched feed by adding the TE_{11} mode at an appropriate ratio to the dominant TE_{01} mode. The matched feed is designed for both linear and circular polarizations and has shown significant cross-polar improvement. In [32], Jana et al designed a dual-mode (TE_{11} and TM_{11}) rectangular matched feed for offset reflector to achieve good cross-polar suppression upto 18 dB. Smooth walled-circular horn generating TE_{11} and TE_{21} modes at an optimum ratio is discussed by Pour et al in [33]. This matched feed has reduced the cross-polarization below -47 dB at both the planes ($\Phi = 90°$ and $\Phi = 45°$). Corrugated over-moded horns use higher order hybrid asymmetric modes for achieving conjugate field matching [23, 28]. the cross-polarization in the reflector pattern obtained for an optimum ratio of HE_{21} and HE_{11} modes is better than -35 dB in both of the reported matched feeds. A summary of different mode combination used for cylindrical, rectangular and corrugated horn is given in Table 1.1.

Table 1.1: Different mode combination for optimum field matching in matched feeds using multi-mode horns

Feed structure type	Plane of symmetry (x)	Plane of asymmetry (y)
Smooth-walled cylinder	TE_{11}+TM_{11}+TE_{21}	TE_{11}+TM_{11}+TE_{21}
Rectangular waveguide	TE_{10}+TE_{20}	TE_{01}+TE_{11}/TM_{11}
Corrugated cylinder	HE_{11}+HE_{21}	HE_{11}+HE_{21}

Apart from the mode combinations given in 1.1, Michael et al. have proposed the use of TM_{01} or TE_{01} mode instead of TE_{21} mode in [34, 35] for cross-polar suppression in the reflector pattern. Recently, multihole directional couplers are proposed in [36] for design of broadband dual-polarized matched feeds. The traditional multi-mode horns as matched feeds discussed earlier offer good cross-polar suppression in the reflector pattern. However, these conventional feeds are often bulky, heavy and have high profiles. Thus, for applications requiring lighter offset reflector system, there are some alternate feeds investigated in literature. The most prominent among those alternate feeds are microstrip based feeds. A review of the literature on such alternate feeds using microstrip antennas is discussed in the next subsection.

1.2.3 Literature review on alternate feeds for offset reflector

Microstrip antenna due to its advantages such as: low profile, light weight, low radar cross-section, ease in reproduction by the printed circuit technology, etc. is reported as alternate feed for offset reflector in [37, 38, 38–55]. In [39, 40], Kona et al. have investigated stacked microstrip patch arrays as feeds for spaceborne reflector antennas. These feeds are designed to operate at L-band frequencies

of 1.413 GHz and 1.26 GHz for radiometer and radar applications, respectively. The inter-element spacing and amplitude excitation of the microstrip array is optimized using PSO (particle swarm optimization) algorithm. The cross-polarization in the reflector pattern is around -25 dB and is insufficient for some of the modern day communication systems. In [42], a multilayered suspended planar array is reported as dual-polarized reflector feed for direct broadcast satellite systems. The gain and beamwidth of the reflector antenna fed by the planar array is found to be comparable with that of a conventional horn feed. However, discussion on cross-polar performance of reflector pattern when illuminated by such array feed is lacking. In [44], a pair of rectangular patches known as doublet is used to reduce the cross-polarization in the reflector pattern. These pair of rectangular patches are excited using both the vertical and horizontal polarization at an appropriate ratio. The excitation ratio is maintained such that the cross-polarization in the reflector pattern gets reduced. Although, the 'doublet' feed reduces cross-polarization, the feeding network required for such an array is complex. In [56], a focal plane array of sequentially rotated linearly polarized elements is proposed as feed for an offset reflector with $F/D = 0.3$. The amplitude and phase of the array elements are optimized to reduce beam squinting in the reflector pattern. Though, the focal plane array has successfully reduced the beam squinting by 0.0935 degree, the circuit components required to implement the required element excitation is very complex. Thus, the alternate feeds using microstrip antennas reported either overlooks cross-polarization in the reflector pattern or a complex feed network is required to achieve a good cross-polarization.

In [57, 58], Kanso et al. proposed electro-magnetic bandgap (EBG) antennas as feed for offset reflector antennas with very high F/D (> 1.2). These EBG antennas are in turn fed by either horn or microstrip antennas for multibeam and dual-band applications. Although, the reflector antenna with EBG feeds provide good directivity, they are developed only for smaller offset angles. Further, the use of microstrip or horns to feed these EBG antennas further increases the complexity level. The existing literature for alternate feeds is limited to arrays of dominant mode operating microstrip patches. However, these misrostrip based feed for the offset reflectors can be designed by adopting an approach similar to the traditional multimode horn feeds. Some of the existing multi-mode micrsotrip antennas used for applications other than as reflector feeds are discussed next. This review will lay down the base of multimode microtrip antenna feeds for the offset reflectors.

1.2.4 Literature review on some recent multi-mode microstrip antennas

In [59–65], multi-mode generating CMPA are reported recently in literature for MIMO applications [60], beam scanning applications [61, 63] and for increasing the gain of an antenna [59, 65]. In [60], two compact CMPA designs are presented for MIMO applications, namely a dual-mode (TM_{11} and TM_{01} mode) CMPA and a tri-mode (TM_{11}, TM_{01} and TM_{21} mode) CMPA. Multimode microstrip patch antennas are widely popular for beam scanning applications due to their pattern reconfigurability features. The pattern reconfigurability is achieved in such antennas by selective excitation of dominant or higher order modes. The higher order modes selected for beam scanning applications are usually conical pattern generating modes. Juyal et al. in [59, 65] have used higher order modes generating broadside pattern at an appropriate ratio with the dominant mode of microstrip antennas for gain enhancement.

1.3 Motivation and Problem Formulation

From the literature survey done on the offset reflector antenna feeds, it can be inferred that conventional multi-mode horn antennas of different geometries as matched feed can suppress the cross-polarization in the reflector pattern. However, these multi-mode horns are heavy and have high profile. Alternated feeds for offset reflector with lower profile and light weight are desirable for certain applications such as satellite and space communications. Although, EBG antennas and microstrip antenna arrays are discussed as viable alternatives to the bulky horn antennas in some recent literature, matched feeds using multi-mode microstrip antennas are seldom discussed. Moreover, some multi-mode microstrip antennas are already reported in literature for applications such as MIMO and pattern reconfiguration. Hence, a thorough investigation of multi-mode microstrip antennas as matched feeds for offset reflectors presents an attractive research problem. Following are some of the problem statements formulated for design of new matched feeds for offset reflector antennas using microstrip antennas:

- ☞ Investigation of dual-mode microstrip patch antennas with different geometries as matched feed for offset reflector antennas.

- ☞ Investigation of arrays with multi-mode microstrip patch antenna elements as matched feeds for offset reflector antennas.

☞ Investigation of array feeds for offset reflectors which can provide pattern reconfigurability along with reduced cross-polarization.

☞ Investigation of dual-band array feeds for offset reflectors with cross-polarization better than -30 dB.

☞ Investigation of matched feeds for smaller reflectors (diameter$\leq 10\lambda$) for 5G applications.

1.4 Contribution of the Thesis

The thesis contains a detailed study of the various factors influencing the cross-polar suppression using optimum field matching. A dual-mode (TM_{11} and TM_{21}) circular microstrip patch antenna has been investigated as matched feed for offset reflector antenna. Three new circular array designs are proposed as reflector feed in this thesis for single frequency, dual frequency and beam reconfigurability applications. A dual-mode (TM_{11} and TM_{21}) microstrip patch antenna in which annular ring patch generates the TM_{21} mode at an appropriate ratio is reported as matched feed. Another matched feed using rectangular and circular microstrip patch antenna is designed for cross-polar suppression. The reflector feeds are extensively analyzed using analytical, simulation and experimental results. Finally, the key contributions of the thesis can be summarized as:

- Investigation of conventional antenna arrays as offset reflector feeds using aperture method and HFSS-PO. (**Chapter 2**)
- Design of a dual-mode circular microstrip patch antenna (CMPA) as matched feed. (**Chapter 3**)
- Design of a single layer circular array matched feed. (**Chapter 4**)
- Design of a matched feed with pattern reconfigurable properties. (**Chapter 4**)
- Design of a dual-band offset reflector feed. (**Chapter 4**)
- Design of a matched feed using annular ring antennas for generating higher order mode. (**Chapter 5**)
- Design of a matched feed using rectangular microstrip patch antenna (RMPA) for dominant mode and CMPA for higher order mode. (**Chapter 5**)

1.5 Organization of the Thesis

The rest of the thesis is organized as follows:

Chapter 2: Investigation of Conventional Microstrip Array Feeds

This chapter presents an initial investigation of antenna arrays with only fundamental mode operating microstrip antennas as feed for an offset reflector antenna. A MATLAB code is developed using GO (geometrical optics/aperture integration) technique to calculate the secondary radiation pattern of the offset reflector antenna for a given feed pattern. Antenna array parameters such as amplitude and inter-element spacing are varied to study their effect on the cross-polar performance in the reflector pattern. Both linear and planar array configurations with TM_{11} mode CMPA elements are investigated exhaustively as offset reflector feeds. This study led to the conclusion that, from the perspective of cross-polar reduction of offset antennas, conventional arrays can only provide limited improvement.

Chapter 3: Introduction to Dual-mode Circular Microstrip Patch Antenna Feeds

In this chapter, performance of a dual-mode circular microstrip patch antenna (CMPA) as matched feed for an offset reflector antenna is investigated. The proposed dual-mode CMPA is a stacked configuration of two CMPA patch layers. The upper patch operates in the fundamental mode (TM_{11} mode), where as an asymmetric higher order mode (TM_{21} mode) is generated by the lower patch. The excitation ratio between the two modes is optimized for an optimum match between the asymmetric field component at the feed aperture and the projected aperture of the reflector.

Analytical expressions for the radiation pattern of the proposed dual-mode CMPA feed is obtained using basic cavity model. The analytical feed model is then used to calculate the secondary radiation pattern of the offset reflector using the MATLAB code developed in the previous chapter. The matched feed is simulated in both HFSS and CST, and the corresponding reflector pattern is obtained in HFSS-PO.

Chapter 4: Circular Array of Circular microstrip Patch Antenna as Matched Feeds

This chapter will discuss three different centered circular array (CCA) structures as matched feed for offset reflectors. A single-layer CCA of 9 CMPA elements is investigated as matched feed for offset reflector antennas. The CCA consists of 8 TM_{11} mode operating CMPA and the central CMPA element generating TM_{21} mode. The asymmetric higher order mode is generated at an appropriate ratio to obtain the required conjugate field match. The proposed feed has reduced the cross-polarization in

the reflector pattern below −33 dB.

A dual-layered microstrip based matched feed array for an offset reflector is also proposed which can be used for controlling the beam-width and beam-shift of the reflector pattern. The top layer of the proposed feed consists of 9 circular microstrip antennas operating in TM_{11} mode arranged in a centered circular array configuration. The second layer contains a circular microstrip antenna operating in TM_{21} mode and located below the central element of the circular array. The excitation ratio between the higher order mode and dominant mode patches is varied to achieve a low cross-polar level at the asymmetric plane by using the concept of conjugate field matching. The effect of circular array radius on the reflector pattern of the offset reflector with focal length to diameter (F/D) ratio equal to 0.7 is investigated to find the optimum radius of the circular array. An investigation has been done to show that by exciting selective array antenna elements, beamwidth and beam shift reconfigurability in the reflector pattern can be achieved, while maintaining the cross-polar level below -38 dB. A maximum beam shift of 0.4° (approximately 31% of 3 dB beamwidth) from the principal axis has been achieved in the reflector pattern.

A dual layer centered circular array is investigated as dual-band feed for an offset reflector with $F/D = 0.8$. The proposed feed consists of a central dual-mode (TM_{11} and TM_{21}) CMPA operating at 6 GHz and a ring of 8 TM_{11} mode generating CMPA elements operating at 4 GHz. The reflector cross-polarization at 6 GHz is reduced by having an optimum ratio between the two modes. Further, the optimum radius of the circular array is also obtained such that the cross-polar levels at both 4 GHz and 6 GHz are below -30 dB. The reflector gain is better than 37 dBi at both the resonant frequencies for an offset reflector with a projected diameter of 2.5 m and $F/D = 0.8$

Chapter 5: Other Matched MPA Feeds for Offset Reflector Antenna

This chapter discusses in brief two more microstrip matched feeds, designed for 5G application. The offset reflector under study is relatively smaller (10λ) in comparison to the previously discussed reflectors and the feed is designed for 5G sub-6 GHz frequency band. The smaller dimension is chosen due to the space constraint in base stations for cellular communication. The first proposed stacked microstrip feed consists of a circular patch generating TM_{11} mode at the top and an annular ring patch under it generating TM_{21} mode. Generation of both these modes at an appropriate ratio provides good cross-polarization in the reflector pattern. A parametric study is performed to obtain the required mode excitation ratio and patch dimensions of the proposed matched feed to achieve the optimum

cross-polarization. An asymmetric coupled field is generated on the upper patch from the lower patch for certain combinations of both the patch dimensions. The strength of this coupled field and its effect on the overall cross-polarization is investigated by varying the inner radius of the annular ring patch. It is found that this coupled field has significant impact on the cross polar performance of the offset reflector. The coupled field has a field configuration similar to TE_{21} mode. The second proposed feed consists of a dominant mode operating rectangular patch at the top layer and a TM_{21} mode operating circular patch at the bottom layer. Both the microstrip patches are excited using two different ports and the excitation ratio between the two ports is varied to obtain the conjugate field matching, required for cross-polar suppression in the reflector pattern. Optimum excitation ratio between the two generated modes are obtained through a parametric study for three different F/D (focal length to diameter) values of $0.4, 0.6$ and 0.8. The proposed matched feed is a low cost matched feed designed on FR4 substrate and its feed pattern is obtained using HFSS and CST. The reflector pattern of the offset reflector is calculated using geometrical optics technique and verified in HFSS-PO. The cross-polarization in the reflector pattern obtained using both the geometrical optics and HFSS-PO are better than -40 dB for an offset reflector with $F/D = 0.6$. A prototype of the proposed matched feed is fabricated and the measured results show good agreement with the simulation results.

Chapter 6: Summary of thesis and future work

This chapter discusses the summary of the works reported in this thesis. Further scope of investigation on certain extended topics of the current problem is provided in this chapter.

The organization of the thesis is also summarized in Fig. 1.2.

1.6 Conclusion

This chapter presents a brief introduction to offset reflector antennas and the high cross-polarization associated with them. A literature survey of various matched feeds and alternate feeds for offset reflectors is provided followed by the motivation for the thesis. The problem statements for the thesis are discussed in this chapter. Further, major contributions of the thesis are also highlighted, followed by the organization of the thesis.

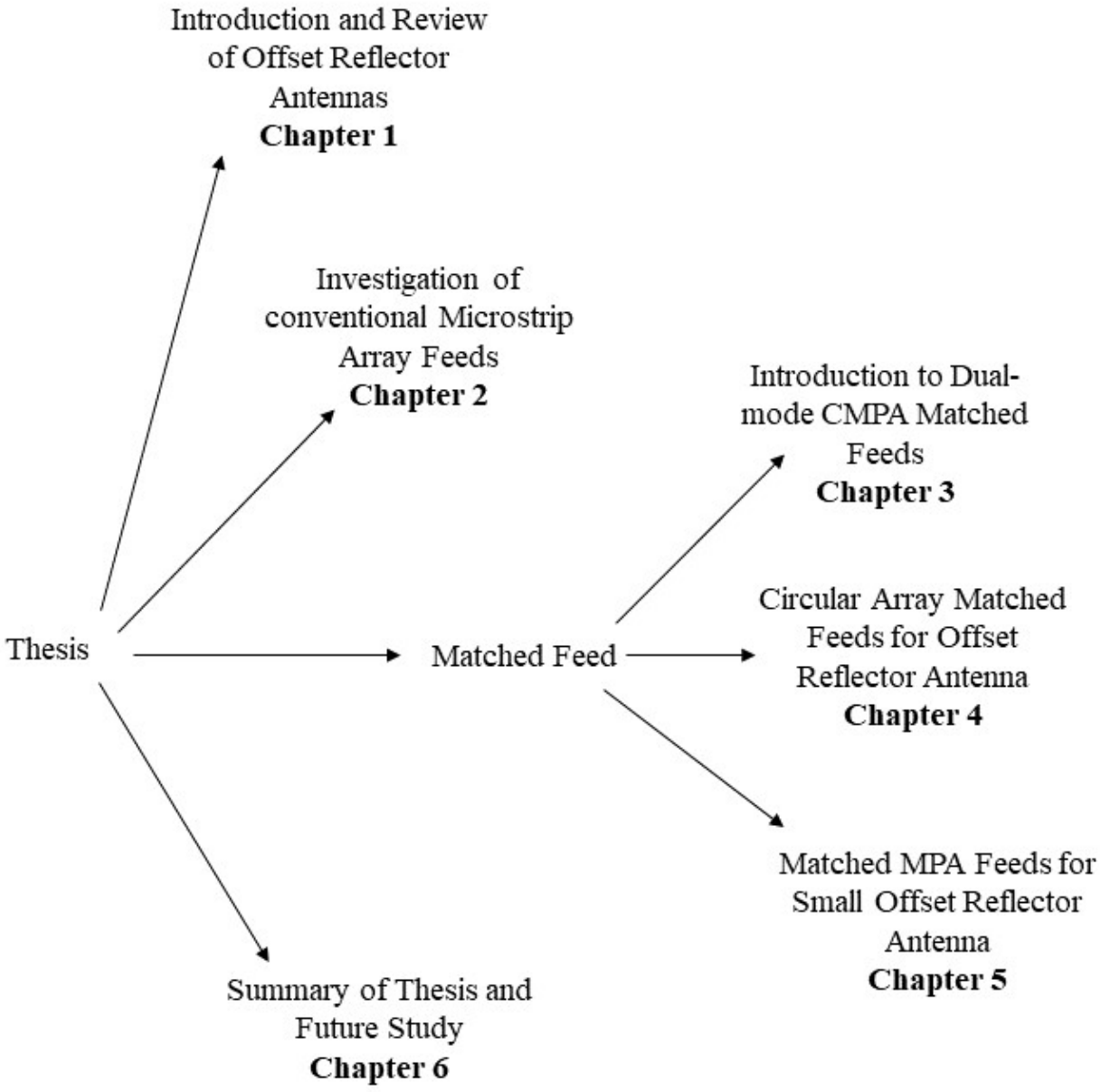

Figure 1.2: Thesis organization.

2

Investigation of Conventional Microstrip Array Feeds

Contents

2.1 Introduction 16
2.2 Aperture Field / Geometrical Optics Technique for Reflector Pattern calculation 16
2.3 Conventional Array Feeds 19
2.4 Conclusion 27

2.1 Introduction

The literature review discussed in the previous chapter, presents microstrip antenna elements and arrays as viable alternatives to the traditional horn feeds. Their light weight and low profile nature make them an attractive option in applications with space and weight constraints. However, a major challenge for such microstrip based reflector feeds in case of compact offset reflectors ($F/D \leq 0.8$), is to obtain a cross-polar performance similar to that of the traditional horn feeds. An array provides the flexibility of changing its radiated field by controlling a number of parameters. It would be interesting to get an insight into how the variation of different array parameters effect the cross-polar performance of an offset reflector antenna. With this motivation, in this chapter, an investigation of the various aspects of conventional microstrip antenna arrays effecting the cross-polar performance when used as feed for offset reflectors is performed. A MATLAB code is developed based on the GO technique to calculate the reflector pattern from a given analytical feed pattern when the reflector parameters (focal length, diameter and offset height) are known. The investigation of the microstrip based reflector feed initiated with the study of a basic dominant mode operating circular microstrip patch antenna (CMPA) as feed for the offset reflectors using both the MATLAB code and HFSS. Thereafter, the various aspects of a microstrip antenna array feeds influencing the reflector cross-polar performance are considered. The performance of these antenna array feeds are obtained by varying amplitude excitation ratio, inter-element spacing, and types of array configuration. The analysis of these array feeds are done for an offset reflector operating at 20 GHz, with a projected diameter (D) = 0.75 m and clearance height (H) = 0.075 m.

2.2 Aperture Field / Geometrical Optics Technique for Reflector Pattern calculation

Analysis of microstrip based feeds using only the commercial CAD simulators such as HFSS and CST, requires a lot of computational time. On the other hand, study of the proposed microstrip feeds using the cavity model analysis saves a lot of computational time and resource. Further, in [2], Rudge et al. has shown that the focal plane fields of the offset reflector can be calculated from the analytical model of the proposed feeds using some basic axis transformations. Ray optics or geometric optics principles are used to find the aperture fields at the focal plane, taking into account the reflection

of radiated field of the feed by the reflector. Fields outside the projected aperture is assumed to be zero. Thereafter, the far-field pattern of the reflector is found from numerical integration of the focal plane fields. Calculation of radiated field from the focal plane field is known as the aperture field integration. Thus, using the analytical model of the proposed feeds and the GO technique, an initial estimation of the reflector pattern for the offset reflector illuminated by the proposed microstrip feed can be obtained. The GO technique can predict the cross-polar components till -50 dB and first sidelobe quite accurately [66, 67]. It may be noted that the proposed feed and the corresponding reflector pattern can also be obtained using HFSS. In HFSS, the reflector pattern is obtained using the surface current integration technique/ physical optics (PO) which is different from the GO technique. Thus, investigation of the cross-polarization in the reflector pattern using both HFSS-PO and the GO technique are used in this thesis to validate the proposed microstrip feed performance.

A MATLAB code has been developed by us based on the GO (geometrical optics/aperture integration) technique discussed in [2] to calculate the secondary radiation pattern of the offset reflector antenna for a given feed pattern. The mathematical details of the MATLAB code is given below.

Calculation of the focal plane aperture fields of the offset reflector from the given analytical feed pattern by using the following expressions:

$$\begin{bmatrix} E_{ay}(\theta,\phi) \\ E_{ax}(\theta,\phi) \end{bmatrix} = K \begin{bmatrix} -a_1 & b_1 \\ b_1 & a_1 \end{bmatrix} \begin{bmatrix} E_{\theta}(\theta,\phi) \\ E_{\phi}(\theta,\phi) \end{bmatrix} \tag{2.1}$$

where,

$$a_1 = (\cos\alpha + \cos\theta)\sin\phi,$$

$$b_1 = \sin\theta\sin\alpha - \cos\phi(1 + \cos\theta\cos\alpha),$$

and

$$K = exp(-2kF/2F)$$

The reflector pattern can be calculated easily from the aperture fields obtained in (2.1) by solving the following expression numerically,

$$f(\theta,\phi) = \int_0^{2\pi}\int_0^{\theta^\star} E_a exp(-jkR\sin\Psi)\rho^2\sin\theta d\theta d\phi \tag{2.2}$$

where,

$$\rho = \frac{2F}{1 + \cos\theta\cos\alpha - \sin\theta\sin\alpha\cos\phi},$$

and

$$R = x_0\cos\Phi - \rho((\sin\theta\cos\alpha\cos\phi + \sin\alpha\cos\theta)\cos\Phi - \sin\theta\sin\phi\sin\Phi).$$

This MATLAB code can be used to calculate the reflector pattern of reflector with any dimensions, if the analytical pattern of the feed is known. This proves extremely useful in cases of conventional microstrip antenna elements and arrays, which have well defined analytical patterns.

2.2.1 Reflector pattern of an offset reflector with $F/D = 0.6$ fed by a single circular microstrip patch feed

The reflector pattern of an offset reflector fed by an x-polarized CMPA is obtained using both the MATLAB code and in HFSS-PO, for validation of the MATLAB code. The analytical field pattern of a single CMPA operating in the fundamental mode (TM_{11}) mode is obtained using the basic cavity model and is expressed as:

$$\begin{bmatrix} E_{\theta mn}(\theta,\phi) \\ E_{\phi mn}(\theta,\phi) \end{bmatrix} = \begin{bmatrix} -j^m\cos m\phi(J_{m-1}(u_{mn}) - J_{m+1}(u_{mn})) \\ j^m\cos\theta\sin m\phi(J_{m-1}(u_{mn}) + J_{m+1}(u_{mn})) \end{bmatrix}$$

and

$$u_{mn} = k_0 a_{mn}\sin\theta.$$

The values of a_{mn} (effective patch radius) can be calculated from the roots of the Bessel function and are also available in [68]. Fig. 2.1 shows both the co-polar and the cross-polar component of the reflector pattern obtained using the MATLAB code and HFSS-PO. The simulation results obtained using both the techniques are in good agreement within the main beam of the co-polar component. It may be noted that the primary feed generating only the fundamental mode will be termed as unmatched feed in this thesis.

Further, the cross-polarization obtained at the asymmetric plane of the offset reflector with $F/D = 0.6$ is almost -22 dB. The cross-polar performance of the unmatched feed for different F/D is shown in Fig. 2.2. Thus, the cross-polar performance of the unmatched feed is poor for low F/D ratio and

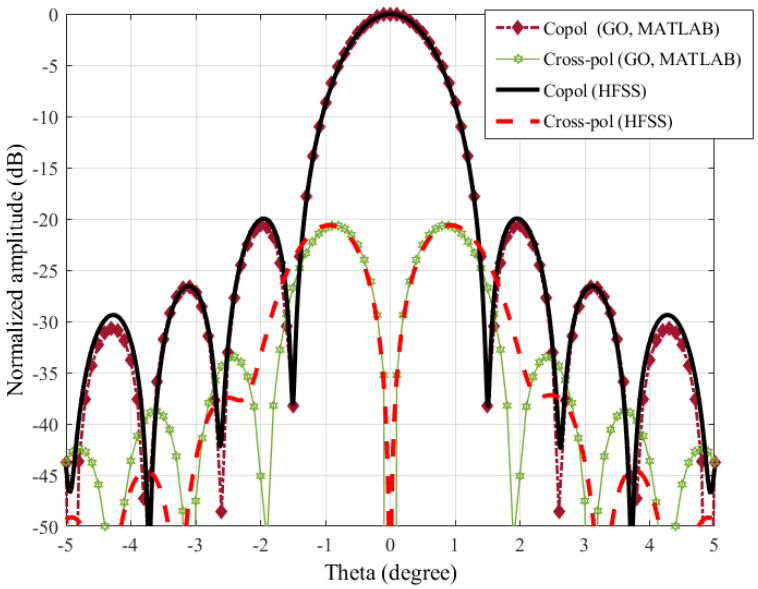

Figure 2.1: Reflector pattern obtained using both the GO technique and HFSS-PO at $\Phi = 90°$.

requires significant improvement.

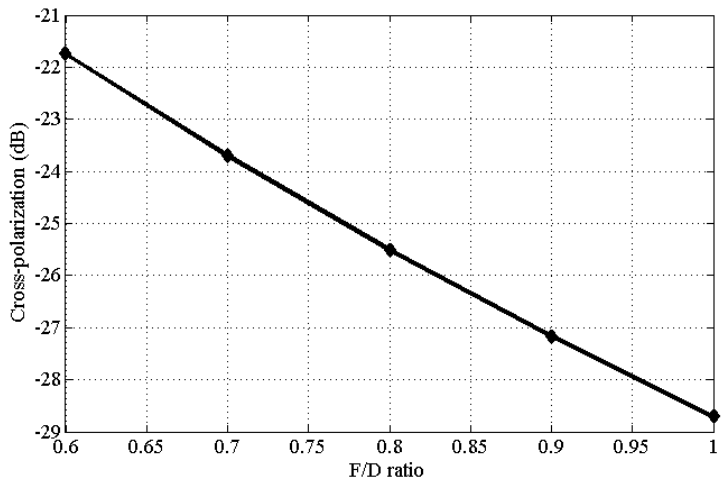

Figure 2.2: Cross-polarization in the reflector pattern for different values of F/D obtained using the MATLAB code.

2.3 Conventional Array Feeds

A single unmatched CMPA feed shows poor cross-polar performance for offset reflectors with $F/D \leq 0.8$. The nature of feed pattern for arrays with only the TM_{11} mode can be varied by

changing the array parameters (i.e. excitation distribution, inter-element spacing and the number of array elements). In this section, the reflector cross-polar performance of the unmatched array feed is investigated to obtain the optimum array parameters for linear (1-D) arrays and planar (2-D) arrays.

2.3.1 Linear array

At first, an investigation of the reflector pattern of an offset reflector antenna fed by a linearly polarized 1-D microstrip array feed is performed. Here, we consider X-polarized CMPA elements which are either placed along Y-axis or X-axis. The analytical expression of the array factor for a linear array with N-elements along the plane of symmetry can be obtained as:

$$AF = \begin{cases} 2\sum_{n=1}^{N} I(n)\cos[(2n-1)u] & \text{N is even} \\ 2\sum_{n=1}^{N} I(n)\cos[2(n-1)u] & \text{N is odd} \end{cases} \tag{2.3}$$

where,

$$u = \begin{cases} \frac{\pi d}{\lambda}\sin\theta\cos\phi & \text{elements placed along X-axis} \\ \frac{\pi d}{\lambda}\sin\theta\sin\phi & \text{elements placed along Y-axis} \end{cases}$$

and d is the inter-element spacing between the array elements.

2.3.1.1 Number of antenna elements and inter-element spacing

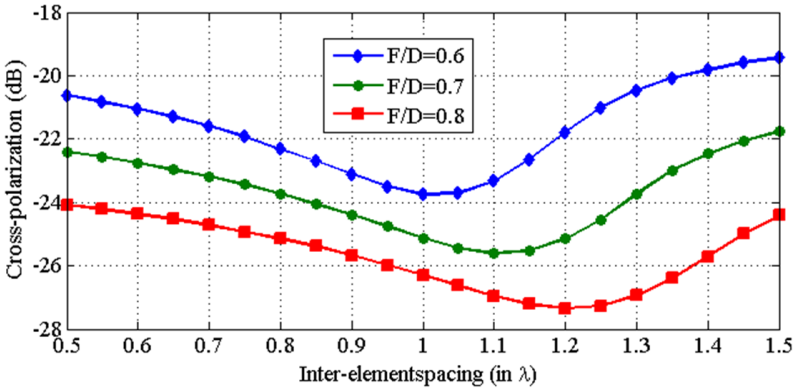

Figure 2.3: Variation in cross-polar levels in the reflector pattern with increase in inter-element spacing of the 2-element linear array feed along Y-axis with x-polarized CMPA elements.

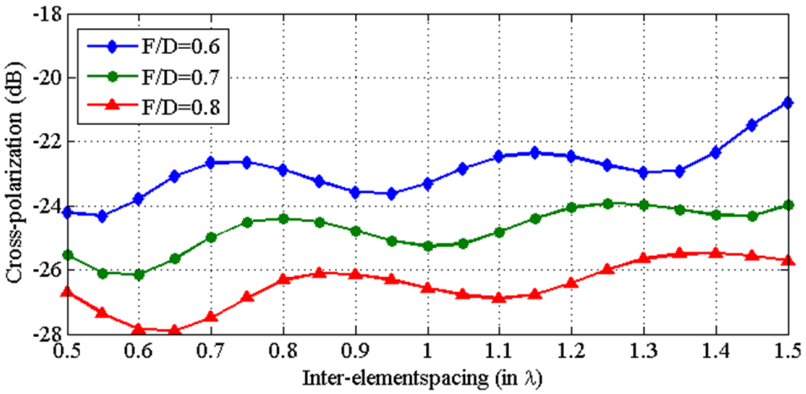

Figure 2.4: Variation in cross-polar levels in the reflector pattern with increase in inter-element spacing of the 4-element linear array feed along Y-axis with x-polarized CMPA elements.

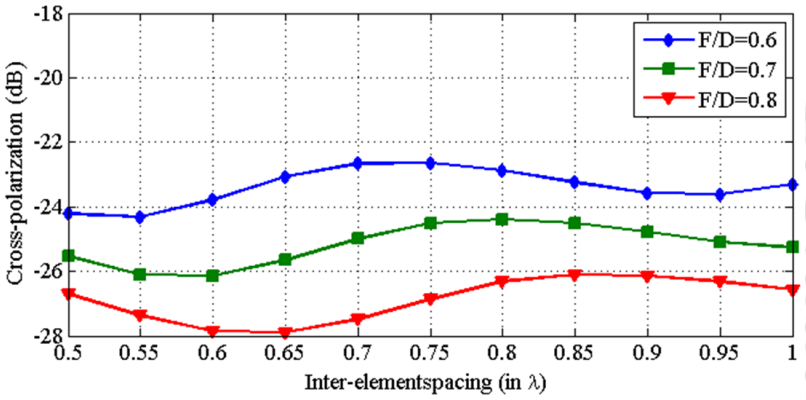

Figure 2.5: Variation in cross-polar levels in the reflector pattern with increase in inter-element spacing of the 6-element linear array feed along Y-axis with x-polarized CMPA elements.

The number of antenna elements and the inter-element spacing are varied to investigate the cross-polar variation in the reflector pattern. Fig. 2.3, 2.4 and 2.5 shows the variation in cross-polar performance with increase in the inter-element spacing (d) for 2, 4 and 6 element linear array along Y-axis obtained using the MATLAB code. Irrespective of the number of array elements, the cross-polar performance is found to be improved marginally (2-3 dB) for certain values of 'd'. This improvement can be attributed to the variation in the main beam and first few sidelobes of the feed pattern which are dependent on the value of 'd'. It may be noted that λ here represents the free space wavelength. The cross-polar variation in the reflector pattern for 2, 4 and 6 element array feed is also obtained using HFSS-PO for $F/D = 0.6$ and is given in Table. 2.1. The nature of cross-polar variation obtained in HFSS-PO is similar to the variation obtained using the MATLAB code.

A similar investigation on the cross-polar performance of the linear array along X-axis is performed

Table 2.1: Variation in cross-polarization with variation in number of elements and inter-element spacing obtained using HFSS-PO

d / No. of elements	0.5λ	0.6λ	0.7λ	0.8λ	λ
2	-21.19 dB	-22.81 dB	-22.54 dB	-22.74 dB	-22.12 dB
4	-22.88 dB	-21.68 dB	-19.68 dB	-22.4 dB	-21.17 dB
6	-22.67 dB	-21.76 dB	-23.06 dB	-22.03 dB	-22.49 dB

using both the MATLAB and HFSS-PO. The cross-polar variation obtained using the MATLAB code is shown in Fig. 2.6, 2.7 and 2.8. Table 2.2 shows the variation obtained using HFSS-PO.

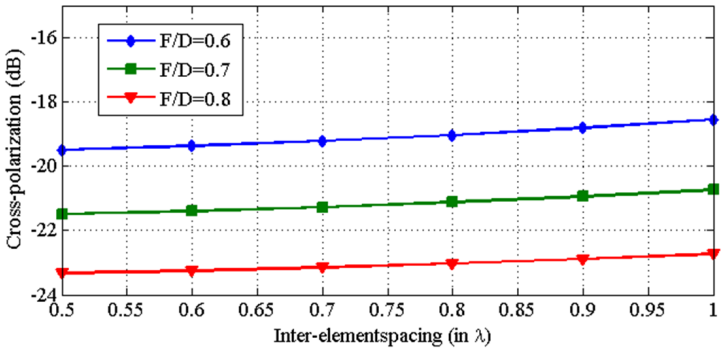

Figure 2.6: Variation in cross-polar levels in the reflector pattern with increase in inter-element spacing of the 2-element linear array feed along X-axis with x-polarized CMPA elements.

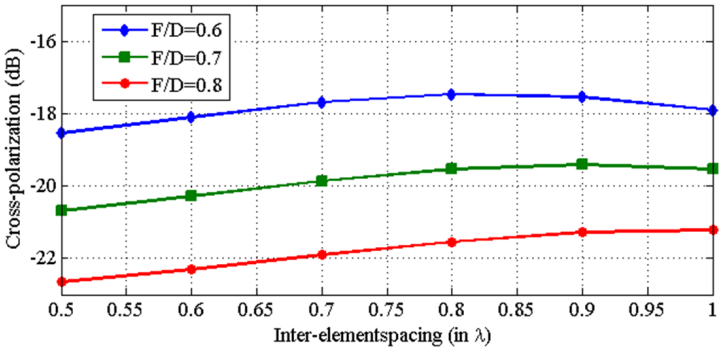

Figure 2.7: Variation in cross-polar levels in the reflector pattern with increase in inter-element spacing of the 4-element linear array feed along X-axis with x-polarized CMPA elements.

As shown in Table 2.2, the cross-polarization in the asymmetric plane of the reflector pattern

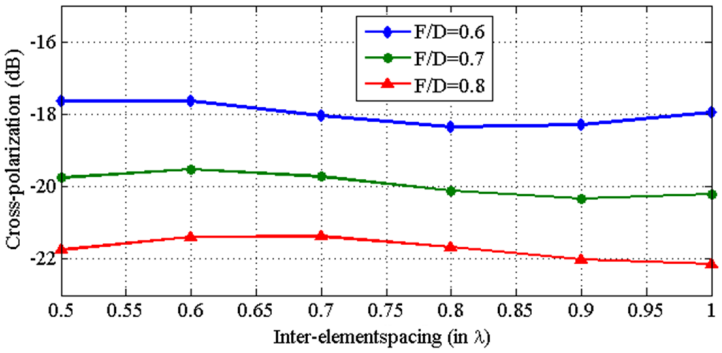

Figure 2.8: Variation in cross-polar levels in the reflector pattern with increase in inter-element spacing of the 6-element linear array feed along X-axis with x-polarized CMPA elements.

Table 2.2: Variation in cross-polarization with variation in number of elements and inter-element spacing obtained using HFSS-PO

No. of elements \ d	0.5λ	0.6λ	0.7λ	0.8λ	λ
2	-18.19 dB	-18.81 dB	-19.54 dB	-18.73 dB	-18.56 dB
4	-19.38 dB	- 19.05 dB	-19.68 dB	-19.26 dB	-19.81 dB
6	-20.27 dB	-20.57 dB	-19.13 dB	-19.71 dB	-19.67 dB

does not vary significantly with the variation in inter-element spacing and the number of elements. Thus, it is observed that variation in 'd' in a linear array feed have marginal effect on the cross-polar performance in the reflector pattern.

2.3.1.2 Variation in element excitation

Variation in the amplitude excitation distribution determines the feed beamwidth and the sidelobe level, which may further effect the cross-polar performance of the reflector. Three types of element excitation distributions are studied for cross-polarization: uniform distribution, binomial distribution and Dolph-Tschebyscheff distribution. The linear array feed consists of 6 CMPA elements placed at an equal spacing of 0.5λ. Cross-polar performance of an offset reflector with $F/D = 0.6$ is studied for the three types of element excitation distribution in the linear array feed.

As shown in Table 2.3, the cross-polar performance in the reflector pattern improves marginally in case of binomial distribution of excitation. Thus, for a linear array feed , the variation in the array parameters has an incremental effect on the overall cross-polar performance.

Table 2.3: Variation in cross-polarization with variation in element excitation distribution in an offset reflector with $F/D = 0.6$

	Uniform distribution	Binomial distribution	Dolph-Tschebyscheff distribution
Cross-polarization (HFSS-PO)	-20.27 dB	-21.81 dB	-20.54 dB
Cross-polarization (MATLAB code)	-18.03 dB	-18.50 dB	-18.27 dB

2.3.2 2-D Arrays of microstrip antennas

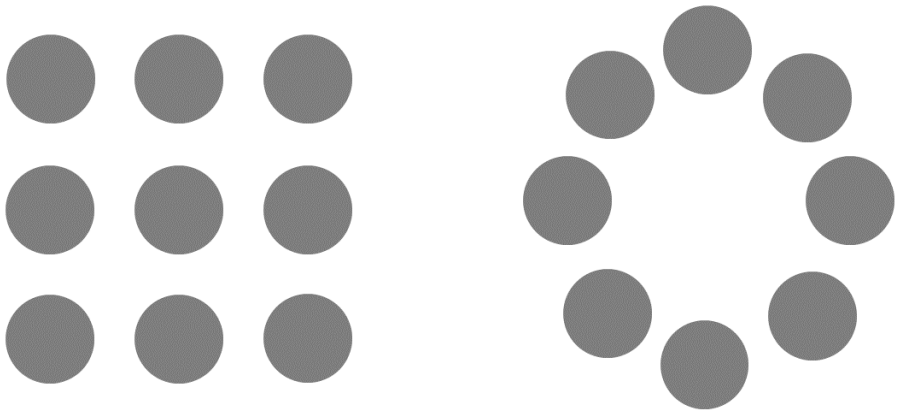

(a) (b)

Figure 2.9: (a) 3x3 square array and (b) simple circular array (SCA).

In comparison to the linear arrays, the 2-D planar arrays as feed for the offset reflector antennas, offer more degrees of freedom which can be utilized to achieve better cross-polar suppression. In planar arrays, square arrays and circular arrays are investigated in this section. The inter-element spacing between the array elements in an array may play an important role in improving the cross-polar level. The effect of inter-element spacing in both the types of 2-D array configurations as feed for the offset reflector is investigated. Both the square array and the simple circular array (SCA) configuration are shown in Fig 2.9. The array configurations in Fig 2.9(a) have nine elements each while the simple circular array configuration in Fig 2.9(b) has eight elements. All the elements of the array are excited uniformly and are operating at 20 GHz.

2.3.2.1 Circular array

The radius of the SCA configuration is varied in order to obtain the best cross-polar performance in the secondary radiation pattern of the reflector. The analytical expression for the array factor of a simple circular array can be obtained as:

$$AF = \sum_{n=1}^{N} I(n) \exp jk_0 r \sin\theta \cos(n\xi - \phi). \tag{2.4}$$

where, ξ is the angular separation between array elements. The parametric study of the array radius for different F/D using the MATLAB code is shown in Fig. 2.10. Fig. 2.10 shows the cross-polar performance for different values of array radius(in λ) for an offset reflector with $F/D = 0.6$. The best cross-polar performance for $F/D = 0.6$ is achieved using the MATLAB code and the HFSS-PO for an operating frequency of 20 GHz is -25.98 dB and -25.48 dB, respectively. The optimum cross-polarization obtained using both the MATLAB code and HFSS are relatively close in terms of array radius as well. The parametric study shows that by placing the CMPA elements at an optimum position (optimum array radius), the cross-polarization can be improved by almost 4-5 dB.

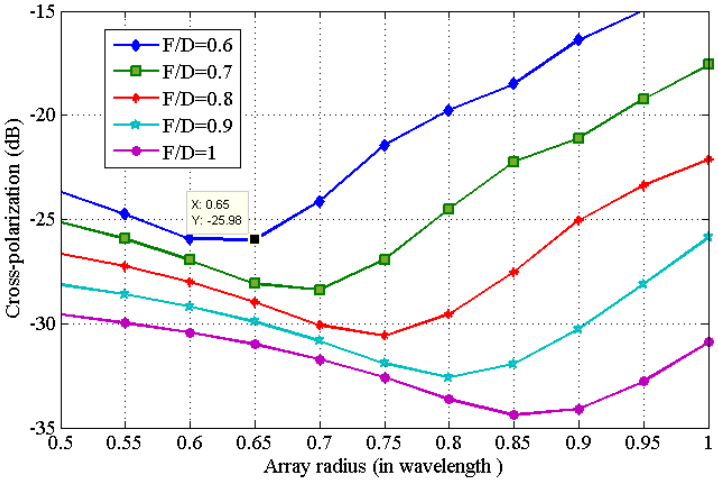

Figure 2.10: Radius of circular array vs cross-polarization level in the secondary radiation pattern using MATLAB code.

2.3.2.2 3×3 square array

The next planar array configuration investigated is a 3×3 square array. A parametric study on the inter-element space, d is performed to obtain the optimum cross-polar performance in the reflector

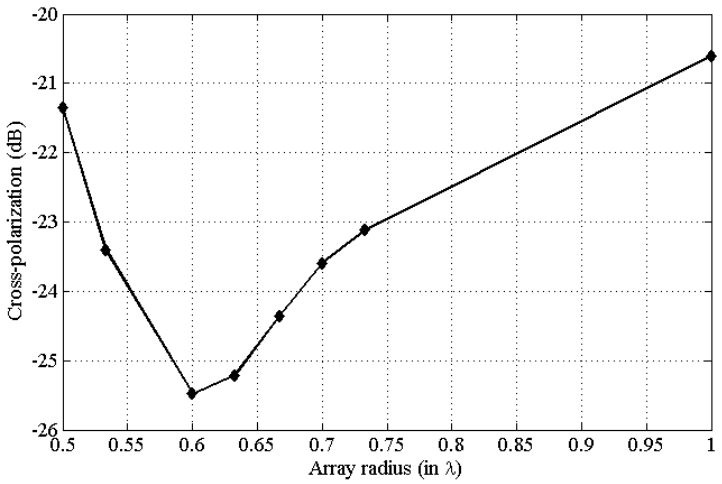

Figure 2.11: Radius of circular array vs cross-polarization level in the secondary radiation pattern using HFSS-PO.

pattern. It is found that the best cross-polar performance is achieved using the MATLAB code when the array feed has an inter-element spacing of 0.5λ as given in Fig.2.12. Fig. 2.13 shows that using HFSS, the optimum cross-polarization in the reflector pattern is obtained when the inter-element separation is 0.6λ.

Similar to its circular counterpart, the 3×3 array shows an improvement of 4-5 dB in the reflector cross-polarization for an optimum inter-element spacing. Thus, both the planar array feeds show an improvement in cross-polarization with respect to the linear arrays. However, the -25 dB cross-

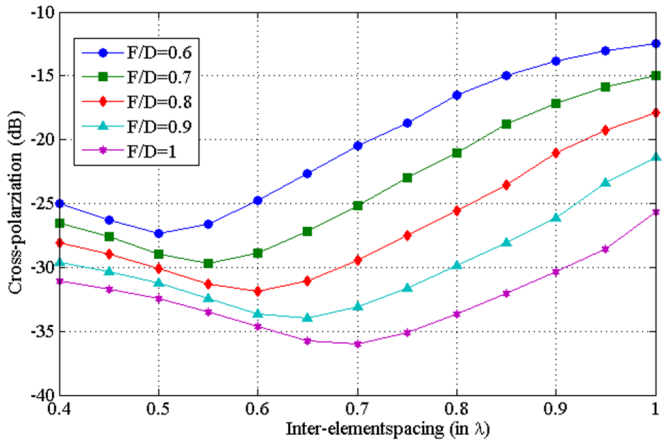

Figure 2.12: Inter-element separation, d vs cross-polarization level in secondary radiation pattern using the MATLAB code.

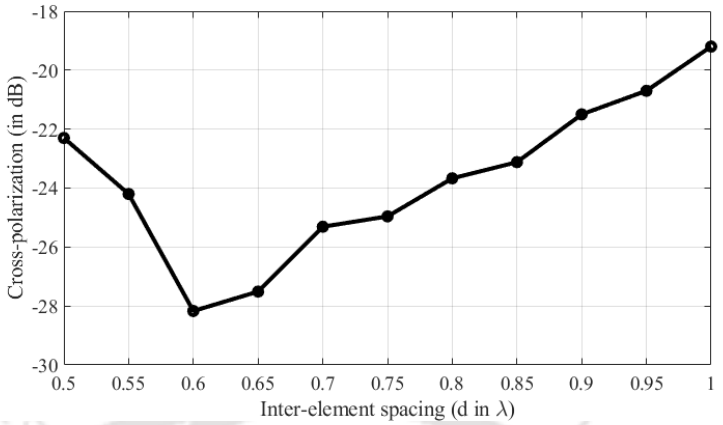

Figure 2.13: Inter-element separation, d vs cross-polarization level in secondary radiation pattern using HFSS-PO.

polarization obtained for an offset reflector with $F/D = 0.6$ is poor and needs further improvement.

2.4 Conclusion

An investigation of various aspects of array parameters influencing the reflector cross-polarization is performed. From the parametric study performed using both the GO-MATLAB code and the HFSS-PO, it is observed that arrays with only dominant mode operating antenna elements are unable to improve the cross-polarization by more than 5 dB when the F/D ratio is kept small. Hence, the subsequent chapters will incorporate a higher order mode microstrip patch antenna with an appropriate excitation ratio to improve the cross-polarization.

3

Introduction to Dual-mode CMPA Matched Feeds

Contents

3.1 Introduction 30
3.2 Review of Conjugate Field Matching 30
3.3 Proposed Dual-mode Matched Feed 32
3.4 Investigation of Proposed Feed using CAD Simulators 37
3.5 Conclusion 41

3.1 Introduction

This chapter introduces a dual-mode (TM_{11} and TM_{21}) circular microstrip patch antenna (CMPA) as matched feed for offset reflectors. The analytical radiation pattern of the proposed dual-mode CMPA matched feed is obtained using the basic cavity model. The choice of TM_{21} mode for cross-polar suppression is justified through the concept of conjugate field matching. The offset reflector pattern is obtained from the analytical pattern of the proposed dual-mode CMPA using the MATLAB code developed in the previous chapter. A more exclusive analysis of the proposed CMPA matched feed is carried out in HFSS and CST, and the corresponding offset reflector performance is evaluated using HFSS-PO. The analysis of the proposed feed is done for an offset reflector with $D = 50\lambda$, operating at the Ka-band uplink frequency of 20 GHz.

3.2 Review of Conjugate Field Matching

Conjugate field matching (CFM) is a widely popular technique for cross-polar suppression in the reflector pattern of an offset reflector. It works on the principle of conjugate matching between the feed aperture field and the focal plane aperture field of the reflector. In case of an optimum field match, the cross-polarization due to the asymmetry of the offset reflector gets cancelled. Thus, prior information about the nature of field distribution at the focal plane is helpful in choosing the appropriate higher order mode of microstrip patch antennas for matched feed design.

3.2.1 Focal plane fields of the offset reflector

D. J. Bem discussed the nature of the field distributions in the focal plane region of an offset reflector fed by horizontal and vertical polarization in [69]. As per his analysis, cross-polar lobes are created at the plane of asymmetry due to the offset nature of the reflector along the plane of asymmetry. The transverse field components at the focal plane of the offset reflector when illuminated by a pure linearly polarized feed is obtained though physical optics and is expressed as:

$$E_{ax}(u', \phi_0) = 2\frac{J_1(u')}{u'} + j\frac{D\sin\alpha}{F}\frac{J_2(u')}{u'}\cos\phi_0 \tag{3.1}$$

$$E_{ay}(u', \phi_0) = -j\frac{D\sin\alpha}{F}\frac{J_2(u')}{u'}\sin\phi_0 \tag{3.2}$$

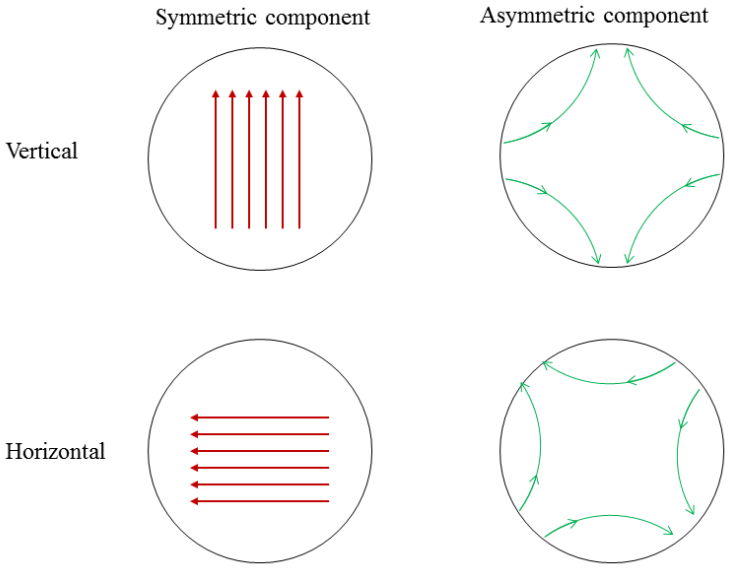

Figure 3.1: Focal plane field configuration of symmetric and asymmetric components when fed by incident wave polarized in horizontal and vertical polarization.

where, $J_n(u')$ is the Bessel function of order n and u' represents the normalized distance to a point in the focal plane. (r', ϕ_0) are the polar coordinates in the focal plane of the reflector and its origin is at the geometrical focus. The multiplying constants are suppressed in 3.1and 3.2 for simplification. The magnitude of these cross-polar lobes depend on the offset angle α at which the feed is placed. At $\alpha = 0$, the field distributions are similar to that of axial fed reflectors. The asymmetric component of the focal plane fields will be due to the asymmetric component in the feed aperture fields. A representative diagram of the focal plane distribution of the offset reflector fed by incident waves of both horizontal and vertical polarization, is given in Fig. 3.1.

3.2.2 TM_{21} mode as the asymmetric mode in the proposed matched feed

Now, an appropriate higher order mode in the CMPA is to be selected which has field distributions similar to the asymmetric field component at the focal plane for an optimal field match. As observed from Fig. 3.1, the asymmetric field component resembles a TM_{21} mode distribution in CMPA. The transverse aperture fields of TM_{21} mode for a CMPA are obtained from [68, 70] and expressed as:

$$H_x(u, \phi') = K \frac{J_2(u)}{u} \sin 2\phi' \cos \phi' - K' J_2'(u) \cos 2\phi' \sin \phi' \tag{3.3}$$

$$H_y(u, \phi') = K \frac{J_2(u)}{u} \sin 2\phi' \sin \phi' + K' J_2'(u) \cos 2\phi' \cos \phi' \tag{3.4}$$

where,

$$K = -j\frac{2\omega\epsilon}{k_0}, \tag{3.5}$$

$$K' = -j\frac{\omega\epsilon}{k_0},$$

(u) represents a normalized distance parameter and $(\phi^{'})$ represents a polar angle. At $\phi^{'} = \frac{\pi}{2}$, the transverse aperture fields of TM_{21} mode can be expressed as

$$H_x(u, \phi^{'}) = K' J_2^{'}(u) \tag{3.6}$$

$$H_y(u, \phi^{'}) = 0 \tag{3.7}$$

It may be noted that $J_2^{'}(u)$ and $\frac{J_2(u)}{u}$ have very similar general characteristics [2]. Based on the similar field characteristics found in between the transverse asymmetric components of the focal plane distribution and the aperture field distribution of a TM_{21} mode, we investigated a dual-mode (TM_{11} and TM_{21}) CMPA as matched feed for offset reflectors. In the dual-mode CMPA, the TM_{21} mode is excited at an appropriate ratio to the TM_{11} mode of CMPA for cross-polar suppression.

Further investigation on the performance of the dual-mode CMPA as matched feed is detailed in the subsequent sections.

3.3 Proposed Dual-mode Matched Feed

As discussed in the previous chapter, a conventional un-matched antenna array with less number of patch elements, seldom provides a cross-polarization better than -30 dB for compact offset reflectors with $F/D \leq 0.6$. A different approach towards solving this problem is required and the solution is found in the dual nature between the aperture field configuration of the microstrip and the horn antennas. Thus, similar to the TE_{21} mode in dual-mode horns reported in [33], TM_{21} mode in CMPA is also capable of cross-polar reduction. Further, this notion is already verified in the previous section. This section will analyze the performance of the proposed dual-mode CMPA as matched feed using its analytical feed pattern.

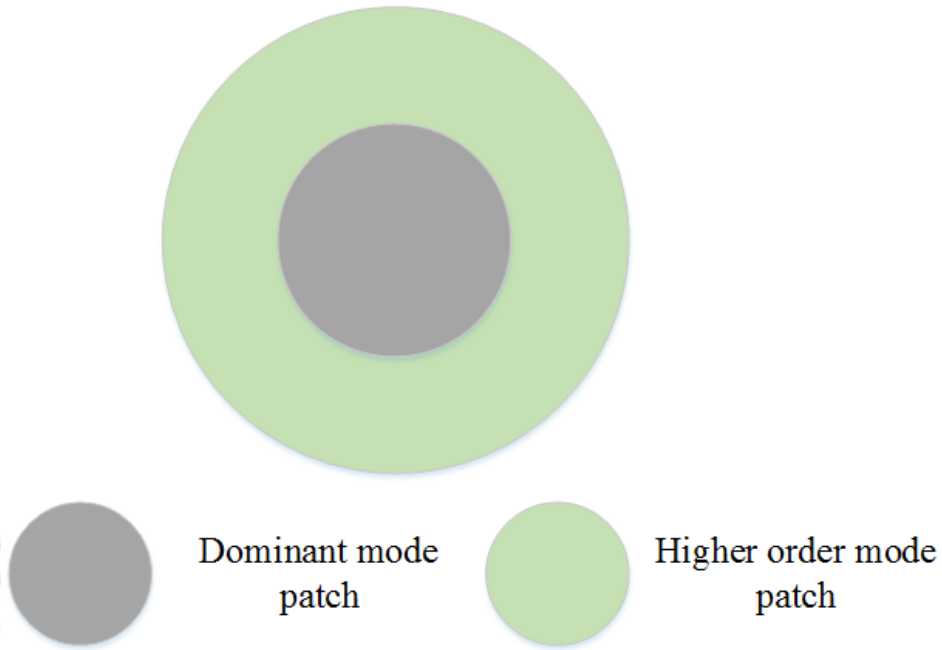

Figure 3.2: Dual-mode circular microstrip patch antenna.

3.3.1 Analytical expression for far-field pattern of the proposed matched feed

The proposed dual-mode CMPA consists of two separate patch layers arranged as a stacked patch antenna. The lower patch will generate TM_{21} mode and the TM_{11} will be generated by the upper patch antenna as given in Fig. 3.2.

The field pattern for an x-polarized dual-mode CMPA can be expressed using the cavity model for the patch as:

$$\begin{bmatrix} E_\theta(\theta,\phi) \\ E_\phi(\theta,\phi) \end{bmatrix} = \begin{bmatrix} E_{\theta 11}(\theta,\phi) \\ E_{\phi 11}(\theta,\phi) \end{bmatrix} + (-j)\frac{C_2}{C_1} \begin{bmatrix} E_{\theta 21}(\theta,\phi) \\ E_{\phi 21}(\theta,\phi) \end{bmatrix} \tag{3.8}$$

where,

$$\begin{bmatrix} E_{\theta mn}(\theta,\phi) \\ E_{\phi mn}(\theta,\phi) \end{bmatrix} = \begin{bmatrix} -j^m \cos m\phi (J_{m-1}(u_{mn}) - J_{m+1}(u_{mn})) \\ j^m \cos\theta \sin m\phi (J_{m-1}(u_{mn}) + J_{m+1}(u_{mn})) \end{bmatrix}$$

and

$$u_{mn} = k_0 a_{mn} \sin\theta.$$

Here, a_{mn} represents the radius of the CMPA operating in TM_{mn} mode. The values of a_{11} and a_{21} for the proposed dual-mode CMPA are obtained using cavity model analysis given in [68]. The excitation ratio C_2/C_1 between the two modes generated by the circular patch antenna can be varied to obtain the required conjugate field matching for any offset reflector antenna configuration. As an example, the proposed matched feed performance is evaluated by illuminating an offset reflector with projected diameter of 50λ and an offset height of 5λ, at an operating frequency of 20 GHz (Ka-band).

3.3.2 Secondary radiation pattern using GO

The secondary radiation pattern of the offset reflector is calculated from the analytical feed pattern using the MATLAB code developed in the earlier chapter. A parametric study is performed to obtain the optimum C_2/C_1 ratio between the two modes for reduction in the cross-polar radiation of an offset

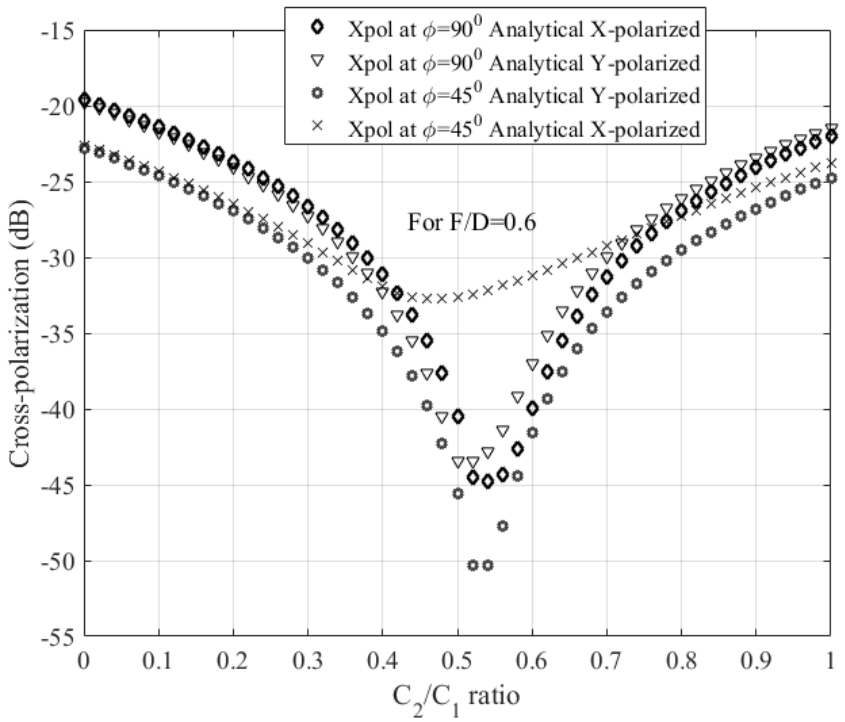

Figure 3.3: Variation in cross-polar levels with variation in C_2/C_1 ratio.

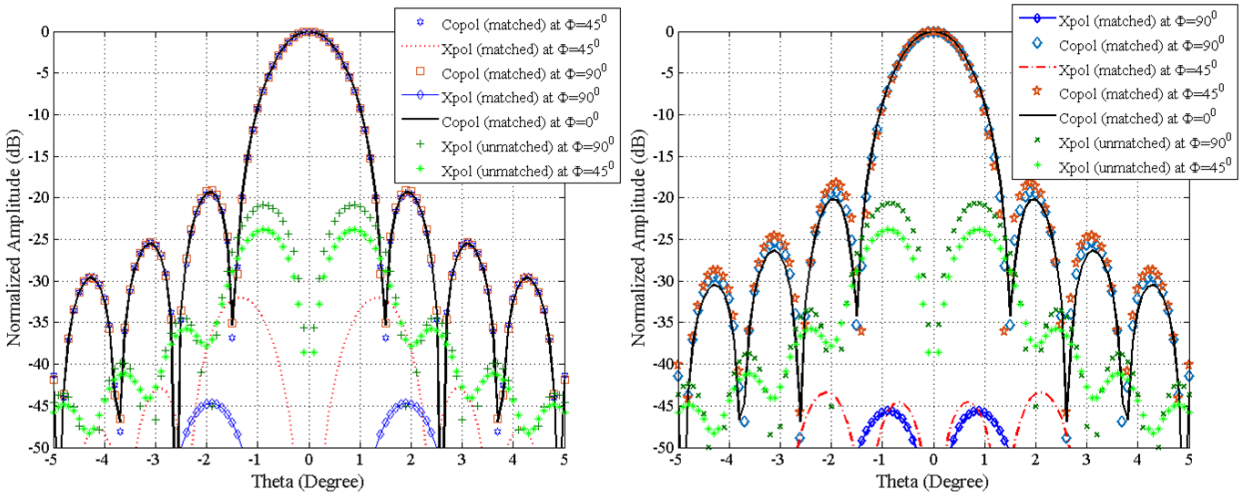

Figure 3.4: Cross-polar level at $C_2/C_1 = 0.5$ for X and Y-polarized circular microstrip antenna.

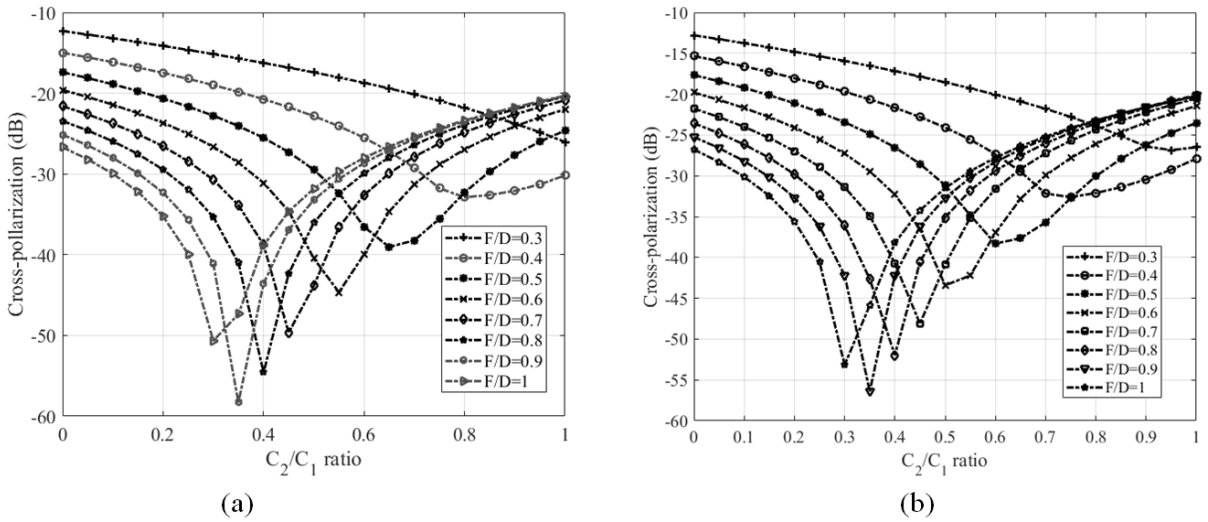

Figure 3.5: Optimum excitation ratio C_2/C_1 for different values of F/D ratio for X and Y-polarization.

reflector with $F/D = 0.6$.

The variation in cross-polarization at both the asymmetric ($\Phi = 90°$) and diagonal ($\Phi = 45°$) planes with different C_2/C_1 ratio is shown in Fig. 3.3. An optimum cross-polarization suppression is obtained for the mode excitation ratio of $C_2/C_1 = 0.5$ at all the planes for both the x and y-polarized waves. The secondary radiation pattern of the offset reflector with $F/D = 0.6$ fed by the dual-mode CMPA for y-polarized waves and x-polarized wave are given in Fig. 3.4. The cross-polar performance is better than -40 dB at all the planes except at diagonal plane for an x-polarized wave. A cross-polar

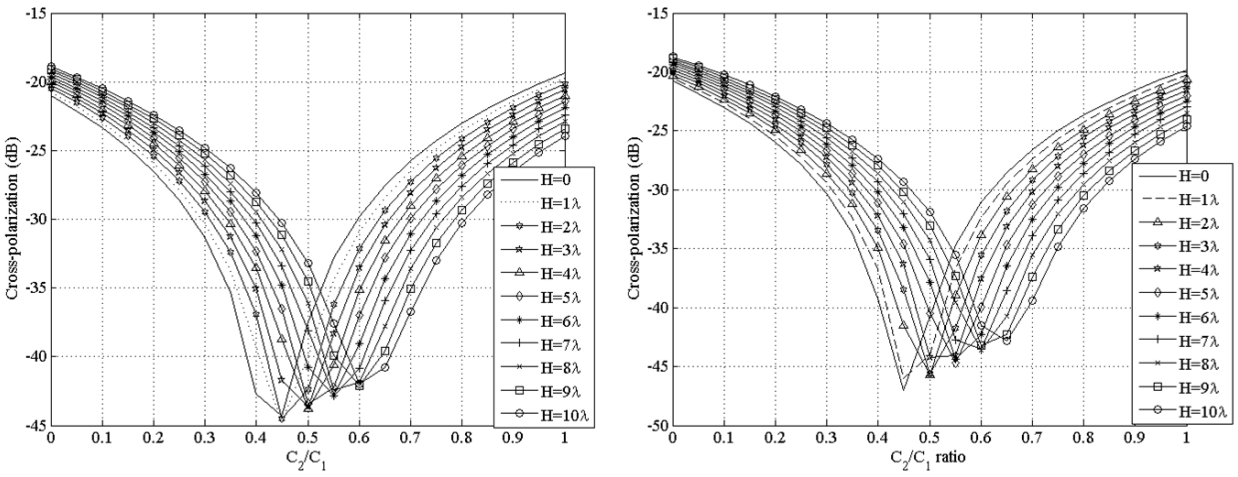

(a) (b)

Figure 3.6: Optimum excitation ratio C_2/C_1 for different values of H for $F/D = 0.6$ for X and Y-polarization.

suppression of more than 23 dB over the un-matched CMPA feeds is achieved at the asymmetric plane for both the polarizations.

Values of C_2/C_1 required for other F/D ratios are also obtained and shown in Fig. 3.5. The magnitude of the TM_{21} mode component required to achieve a match field decreases as the offset angle (α) increases. Further, the extent of the cross-polar reduction in the reflector pattern for smaller F/D is less.

The variation in cross-polarization with respect to increase in offset height (H) for $F/D = 0.6$ in for y-polarized case and x-polarised case shows similar results in Fig. 3.6. The trends are as expected since an increase in H value increases the offset angle which in turn will require higher magnitude of TM_{21} mode for cross-polar compensation. The investigation of the proposed dual-mode CMPA feed using the analytical feed pattern presents its case as matched feed for the offset reflector. However, the simple analytical feed pattern does not include the coupling between the two patch layers, which may effect its performance as a matched feed. For a more exclusive analysis of the dual-mode CMPA, commercial CAD simulators (HFSS and CST) are used in the subsequent section.

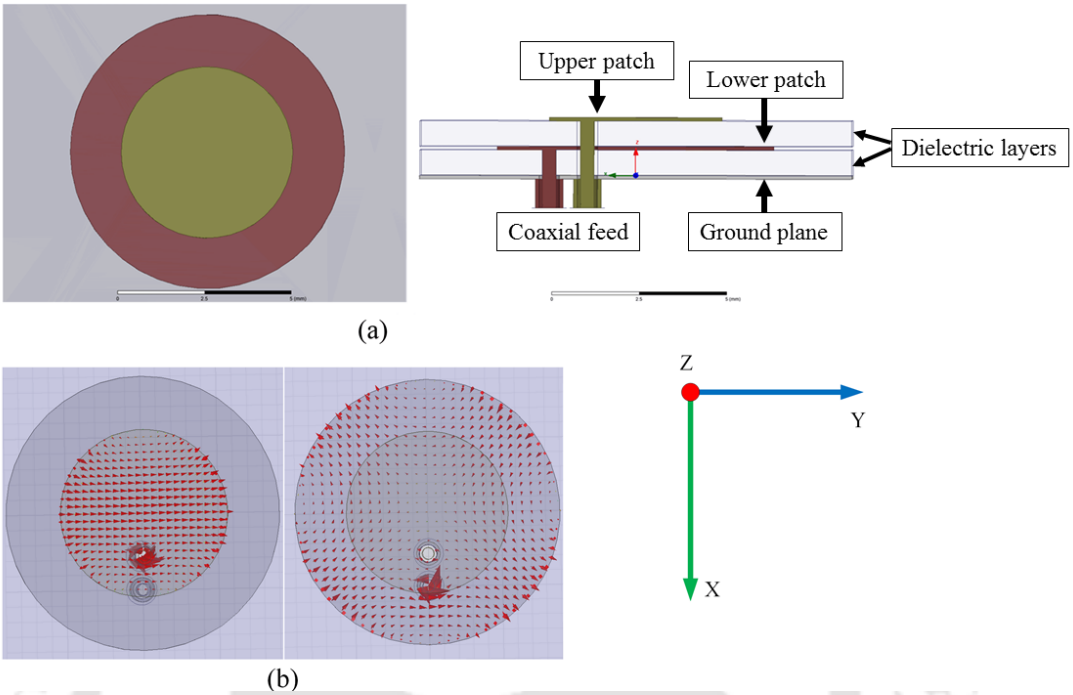

Figure 3.7: (a) Top view and side view of the dual-mode CMPA designed in HFSS and (b) Modal features of both the patch (upper patch on the left and lower at the right) when excited individually.

3.4 Investigation of Proposed Feed using CAD Simulators

3.4.1 Stacked Dual-mode CMPA

The proposed dual-mode CMPA is designed in HFSS, as shown in Fig. 3.7. The top layer consists of a CMPA generating TM_{11} mode, while the higher order TM_{21} mode is generated by the CMPA at the lower layer. Both the patch layers have a common finite ground plane. Both the substrate layers containing the CMPA patches are similar in substrate properties (Arlon DiClad 880 with $\epsilon_r = 2.2$ and height, $h = 0.762$ mm). The amplitude and phase of the modes generated at both the patches are controlled separately by individual 50Ω excitation ports (port 1 for the top layer patch and port 2 for the lower layer patch). The CMPA modal features of lower patch generating TM_{21} mode for an excitation in port 2 only, resembles the required asymmetric field component on the aperture of the proposed matched feed and is shown in 3.7(b). As shown in Fig. 3.8, the return losses obtained at both the ports using HFSS and CST are better than -17 dB.

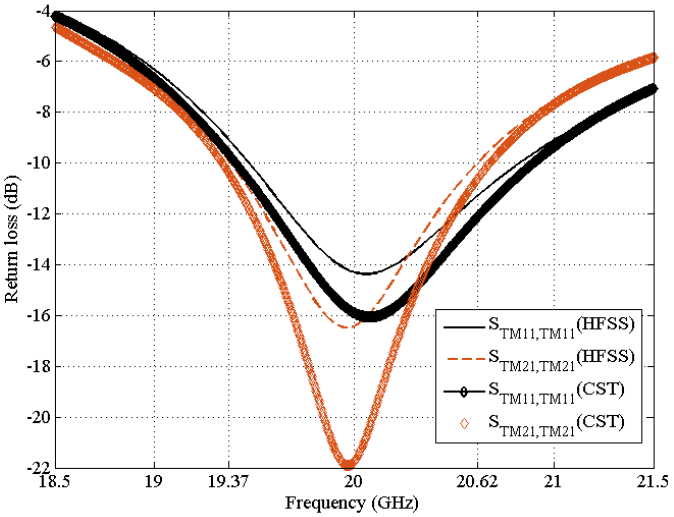

Figure 3.8: Return losses at both the ports obtained in HFSS and CST.

3.4.2 Reflector pattern using HFSS-PO

The reflector pattern of the offset reflector is obtained using the PO package of HFSS 15.0. In HFSS-PO, the reflector pattern is calculated using the surface current method. In a surface current method, current distribution on the surface of the reflector is obtained for a given feed pattern. This is followed by the fourier transform of the surface current distribution to obtain the reflector pattern. Thus, both the aperture field method and surface current method are employed to obtain the reflector pattern. Similar to the parametric study performed earlier, the excitation ratio between the two modes (TM_{11} and TM_{21} mode) is varied to obtain the optimum cross-polarization in the offset reflector field pattern. For the offset reflector specifications given earlier, the variation in the cross-polar levels obtained using both the MATLAB code and HFSS-PO are shown in Fig. 3.9. The best cross-polar performance in the reflector pattern is obtained for an excitation ratio of $C_2/C_1 = 0.55$ and $C_2/C_1 = 0.6$ using the MATLAB code and HFSS-PO, respectively for an x-polarized dual-mode CMPA feed. The secondary field pattern of the offset fed reflector for the optimum C_2/C_1 ratio is shown in Fig. 3.10. The GO code and HFSS-PO results for cross-polarization in the secondary field pattern shows some difference since HFSS takes into account the mutual coupling of stacked patches while the same was not considered in the analytical model of the feed.

The field pattern of the dual-mode CMPA with optimized mode excitation ratio evaluated using (3.8) and the CAD simulators, HFSS and CST, are depicted in Fig. 3.11. All the simulation results

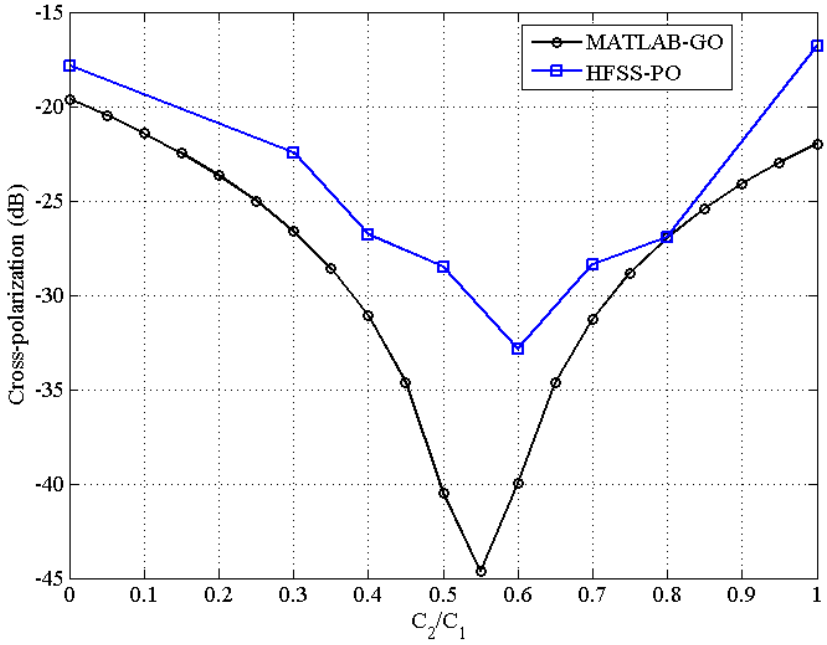

Figure 3.9: Variation in cross-polarization at the asymmetric plane with C_2/C_1 ratio.

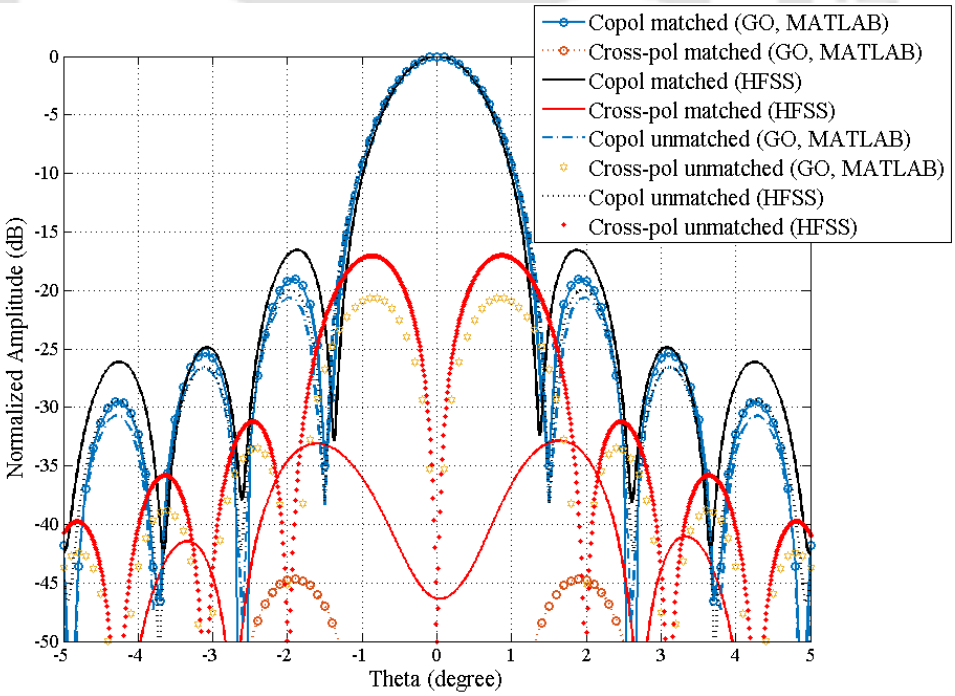

Figure 3.10: Secondary field pattern of the offset reflector at the asymmetric plane when fed by the proposed matched feed design.

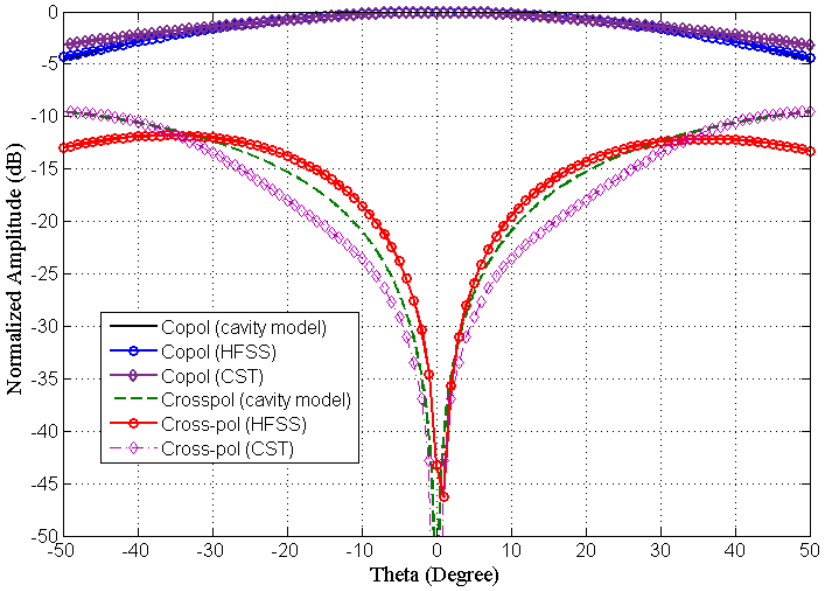

Figure 3.11: Primary feed pattern (at $\phi = 90°$) for optimized excitation ratio using both MATLAB code and HFSS-PO.

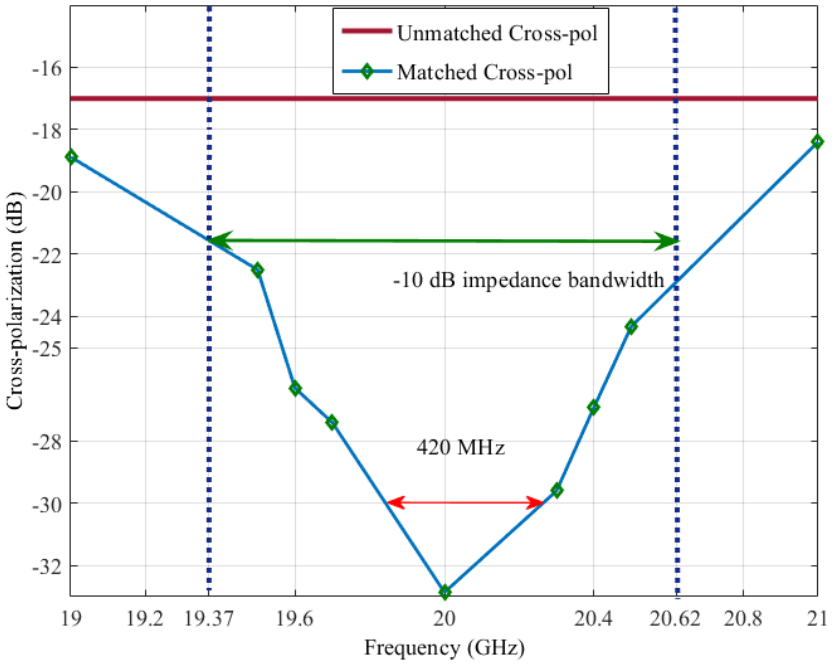

Figure 3.12: Cross-polar bandwidth in the secondary field pattern of the offset reflector with the proposed matched feed design.

show good agreement among themselves. The -30 dB cross-polar bandwidth of the dual-mode CMPA is 420 MHz as shown in Fig 3.12. The performance of offset reflector illuminated by the proposed feed

is summarized in Table 3.1. It may be noted that the -30 dB cross-polar bandwidth for the proposed dual-mode CMPA feed is narrower than a conventional matched horn feed. Hence, the proposed matched feed is more suitable for narrow band applications.

Table 3.1: Performance of ORA fed by the proposed feed

Offset reflector parameters	Value
Frequency (GHz)	20
Reflector Size	50λ
F/D	0.6
Crosspol ($\Phi = 90°$) (dB)	-32.86
First SLL (dB)	-16.86
-30 dB Xpol B.W (%)	2.1
Gain (dBi)	36

3.5 Conclusion

This chapter presents in detail the working of a dual-mode CMPA as matched feed for an offset reflector antenna. The concept of conjugate field matching is revisited for CMPA and the TM_{21} mode is selected as the asymmetric mode required for an optimum match. An extensive analysis of the dual-mode CMPA as matched feed in terms of cross-polar suppression in the reflector pattern is performed using both analytical and simulation tools for an offset reflector with $F/D = 0.6$.

4

Circular Array Matched Feeds for Offset Reflector Antenna

Contents

4.1 Introduction 44
4.2 Single Layer CCA with TM_{21} Mode operating Centre Patch 45
4.3 CCA with Dual-Mode CMPA as Central Element 51
4.4 Beam Shifting and Beam Size Control using the Dual-layer CCA Matched Feed 56
4.5 CCA Feed for Dual Band Application 62
4.6 Conclusion 74

4.1 Introduction

The investigation of dual-mode CMPA as matched feed for offset reflector antenna in the previous chapter shows that by exciting an appropriate ratio of TM_{11} mode and TM_{21} mode in the dual-mode CMPA, the reflector cross-polarization can be improved. However, the overall antenna efficiency of such offset reflectors fed by a single dual-mode CMPA may be less due to broader feed beamwidth leading to higher spillover losses. In order to reduce this spillover loss, the feed beamwidth is required to be almost equal to $2\theta^*$ (boresight angle of the reflector antenna). Achieving such beamwidth is difficult using a single dual-mode CMPA feed. Arrangement of the antenna elements in an array for feed design may help in improving the overall antenna efficiency. Further, generating both the fundamental and the higher order modes at an appropriate ratio using the array elements can provide better performance in terms of both the reflector cross-polarization and the overall antenna efficiency. From the studies conducted in chapter 2 and due to certain structural advantage offered by circular array configurations as discussed latter, centered array is the preferred array configuration in the current investigation.

In this chapter, three offset reflector feeds using centered circular array (CCA) configuration of CMPA elements are discussed in detail. All the three array designs work on the principle of conjugate field matching discussed in the previous chapter. In all the proposed CCA feeds, a central TM_{21} mode operating CMPA element is used, either at the same layer or at a lower layer. This central CMPA element suppresses the cross-polarization in the reflector pattern of the offset reflector. The CCA configuration is preferred over other array configurations, as the TM_{21} mode generating patch can be easily incorporated into the design at the centre. The proposed matched feeds in this chapter are investigated using both analytical methods and CAD simulators. The first CCA matched feed designed on a single layer with all the radiating antenna elements having a shared aperture. The second CCA matched feed design is a dual-layered structure with the TM_{21} mode operating patch at the lower layer and the dominant mode operating patch at the top. The second design is also investigated for beam shifting and beamwidth control properties along with low cross-polarization attributes. The third and final CCA array feed is similar to the second dual-layered CCA matched feed, with respect to its antenna element arrangement. However, the difference lies in the fact that the array structure in this reflector feed is designed to operate at two different frequency bands. The details of these three types of feed are discussed in this chapter.

4.2 Single Layer CCA with TM_{21} Mode operating Centre Patch

The first CCA matched feed proposed in this chapter consists of 9 CMPA elements, where the central element operates in TM_{21} mode and the 8 circular ring elements in the dominant TM_{11} mode. The matched feed is designed to operate at 20 GHz and illuminates an offset reflector with diameter= 50λ. The substrate material considered for the matched feed is RT-Duroid 5880 with$\epsilon = 2.2$ and substrate height of 0.768 mm.

4.2.1 Analytical expressions of the far-field pattern of the proposed feed

The field pattern of the matched feed design, using cavity model for the antenna elements, can be expressed as

$$\begin{bmatrix} E_\theta(\theta,\phi) \\ E_\phi(\theta,\phi) \end{bmatrix} = C_1 \begin{bmatrix} E_{\theta 11}(\theta,\phi) \\ E_{\phi 11}(\theta,\phi) \end{bmatrix} AF + (-j)C_2 \begin{bmatrix} E_{\theta 21}(\theta,\phi) \\ E_{\phi 21}(\theta,\phi) \end{bmatrix} \tag{4.1}$$

where,

$$AF = \sum_{n=1}^{N} I(n) \exp jk_0 r \sin\theta \cos(n\xi - \phi),$$

$$\begin{bmatrix} E_{\theta mn}(\theta,\phi) \\ E_{\phi mn}(\theta,\phi) \end{bmatrix} = \begin{bmatrix} -j^m \cos m\phi (J_{m-1}(u_{mn}) - J_{m+1}(u_{mn})) \\ j^m \cos\theta \sin m\phi (J_{m-1}(u_{mn}) + J_{m+1}(u_{mn})) \end{bmatrix}$$

and

$$u_{mn} = k_0 a_{mn} \sin\theta.$$

N is the number of elements, r is the radius of the circular array and ξ is the angular separation given by $\frac{2\pi}{N}$. The number of array element considered in the current work excluding the central element is 8 and are separated by an equal angular separation of 45°. A parametric study is performed to investigate the effect of excitation ratio between the two modes (TM_{21} and TM_{11}) on the cross-polar performance in the reflector pattern for different F/D and array radius, using the MATLAB code developed in chapter 2. Fig. 4.1, shows that as the array radius increases for a fixed F/D (0.6 in this case), the cross-polar suppression deteriorates. For an array radius of 0.6λ, the best cross-polar performance

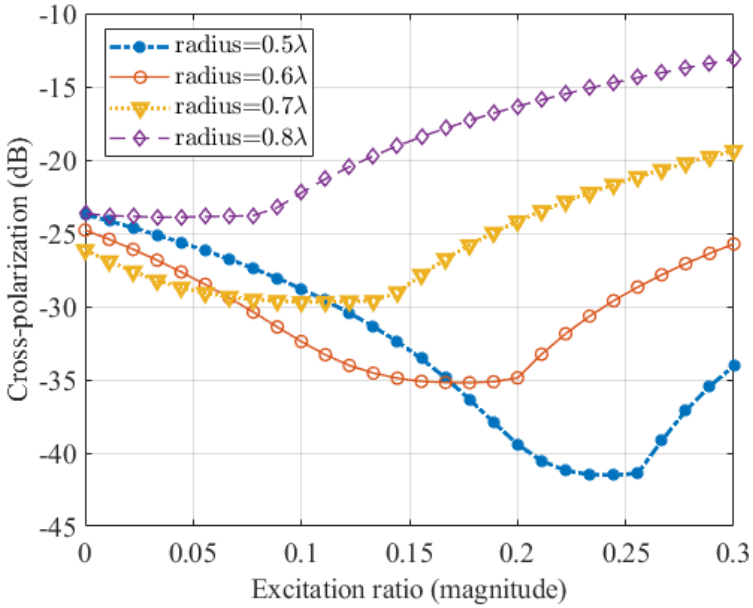

Figure 4.1: Effect of variation in the excitation ratio between TM_{11} and TM_{21} modes on the cross-polar levels for different values of circular array radius. This study is performed using the MATLAB code for $F/D = 0.6$.

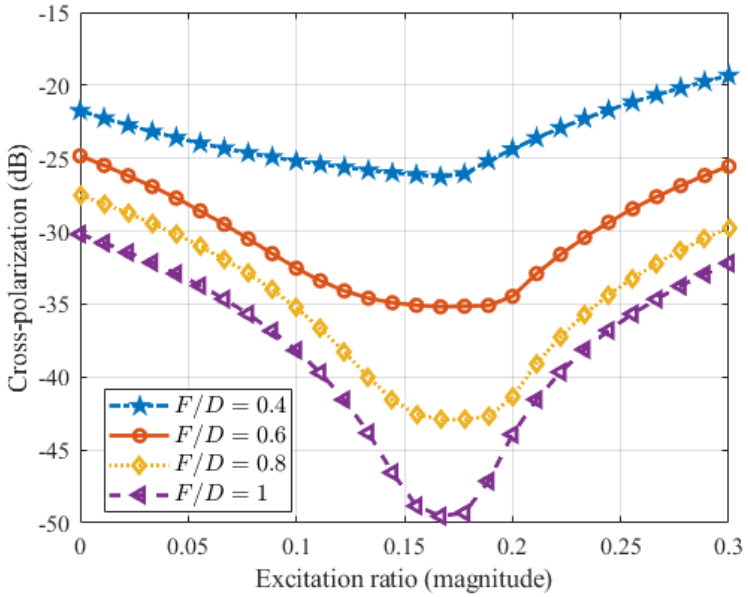

Figure 4.2: Effect of variation in the excitation ratio between the TM_{11} and TM_{21} mode on the cross-polar levels for different values of circular array radius. This study is performed using the MATLAB code for an array radius of 0.6λ.

is obtained for an excitation ratio of 0.16. As shown in Fig. 4.2, the cross-polar performance in the reflector pattern decreases as the F/D ratio decreases for a fixed array radius. The minimum cross-polarization value for different F/D ratios are attained for almost similar values of excitation

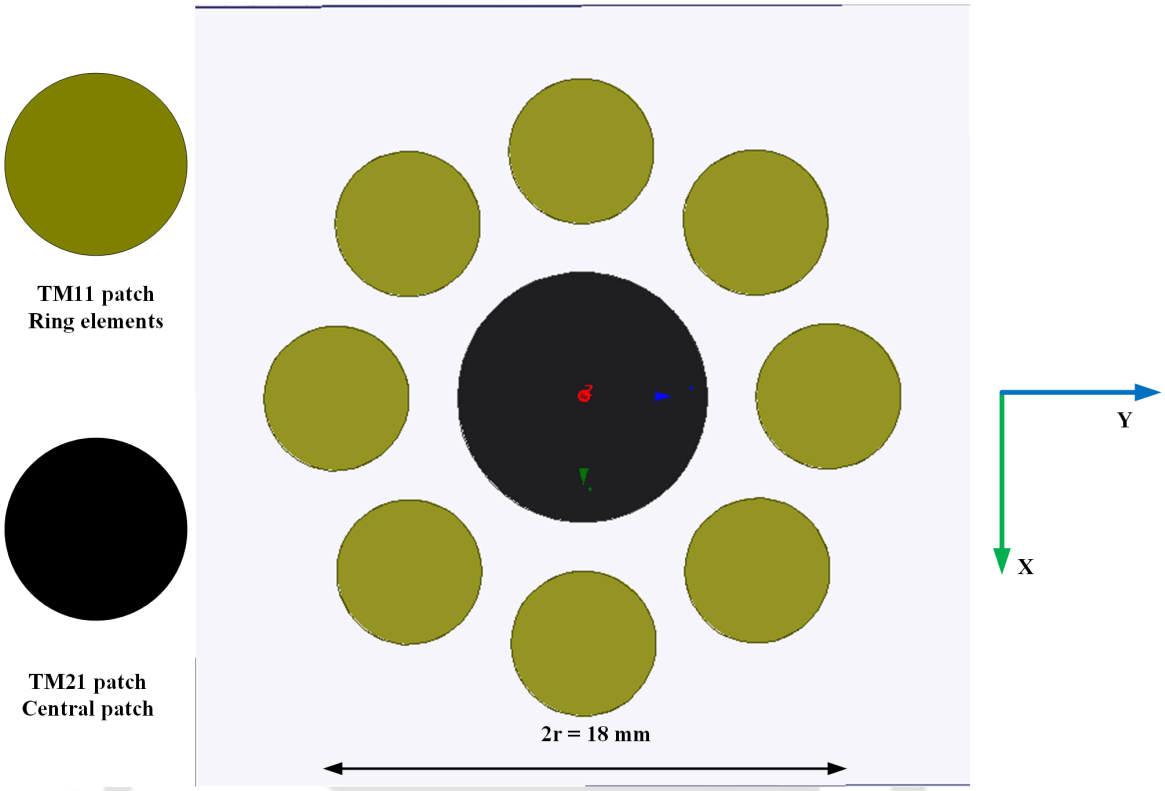

Figure 4.3: CCA with TM_{21} operating central patch.

ratios and therefore the same excitation ratio can be used even when F/D ratio is changed.

4.2.2 Proposed feed design in CAD simulator

The proposed CCA matched feed designed in HFSS, on a single layer of RT-Duroid 5880 with substrate properties ($\epsilon_r = 2.2$ and substrate heght=0.767 mm) is shown in Fig.4.3. The array radius of the CCA matched feed is considered as 9 mm (0.6λ at 20 GHz) from the parametric study performed using the analytical model previously. All the CMPA elements including the TM_{21} generating central patch are fed separately using 50 Ω wave ports.

A parametric study is performed to obtain the optimum excitation ratio between the two modes (TM_{21} mode and TM_{11} mode). The variation in cross-polar levels with the variation in the excitation ratio is shown in Fig. 4.4. It is observed that the best cross-polar performance is obtained for an excitation ratio of 0.14 using HFSS-PO. The secondary field pattern for the offset reflector for the proposed feed when TM_{21} mode is not excited, is shown in Fig. 4.5. Fig. 4.6 shows the reflector pattern when the excitation ratio between the two modes is optimum at the CCA matched feed. For an optimum excitation ratio, the proposed CCA matched feed has suppressed the cross-polarization

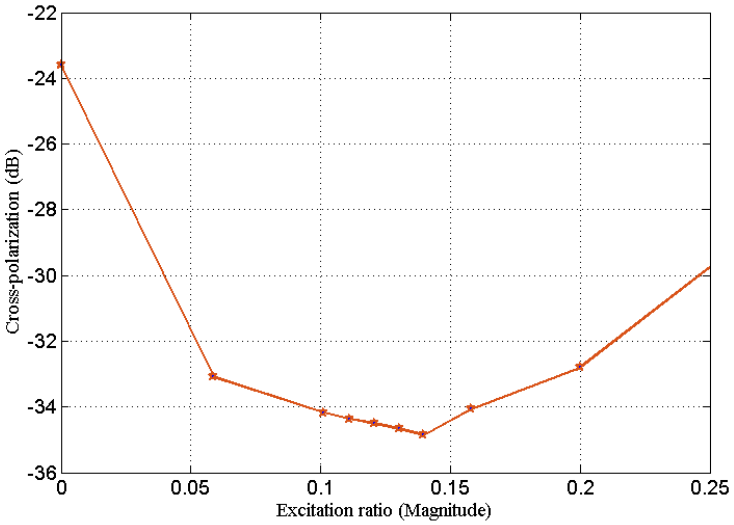

Figure 4.4: Parametric study of the effect of excitation ratio between the two modes on the cross-polarization at the asymmetric plane of the reflector pattern.

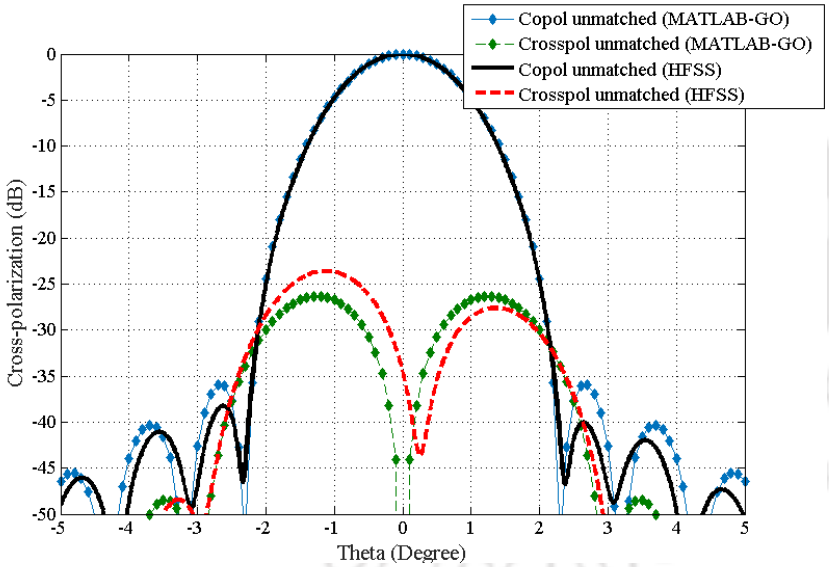

Figure 4.5: Secondary field pattern of the offset reflector at the asymmetric plane for the single layer CCA unmatched feed.

by almost 11 dB. The reflector patterns obtained for both the matched and the un-matched feed in HFSS-PO has good agreement with the results obtained using the MATLAB code. The feed pattern obtained using (4.1) and the CAD simulators namely HFSS and CST are shown in Fig. 4.7 and are in good agreement within the region of interest.

The -30 dB cross-polar bandwidth of the proposed CCA matched feed is 1.7 GHz as shown in Fig. 4.8. However, the narrow impedance bandwidth of the CCA feed limits the actual cross-polar

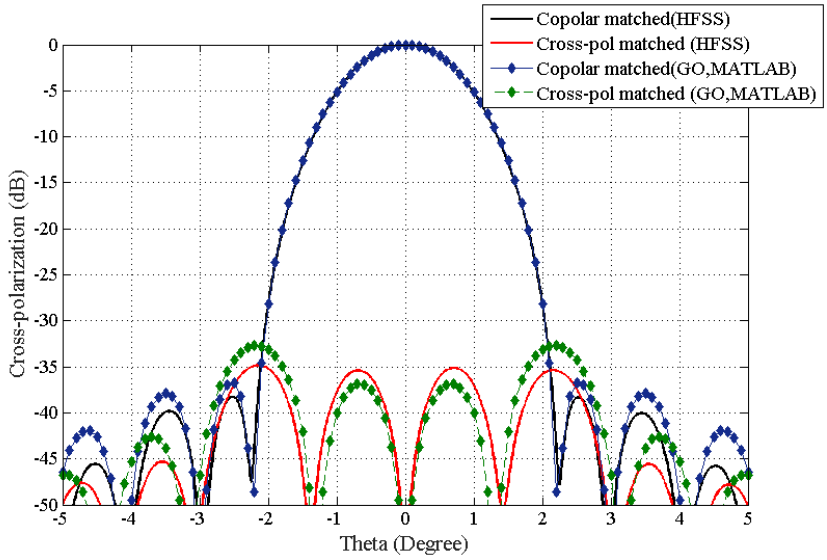

Figure 4.6: Secondary field pattern of the offset reflector at the asymmetric plane for the single layer CCA matched feed.

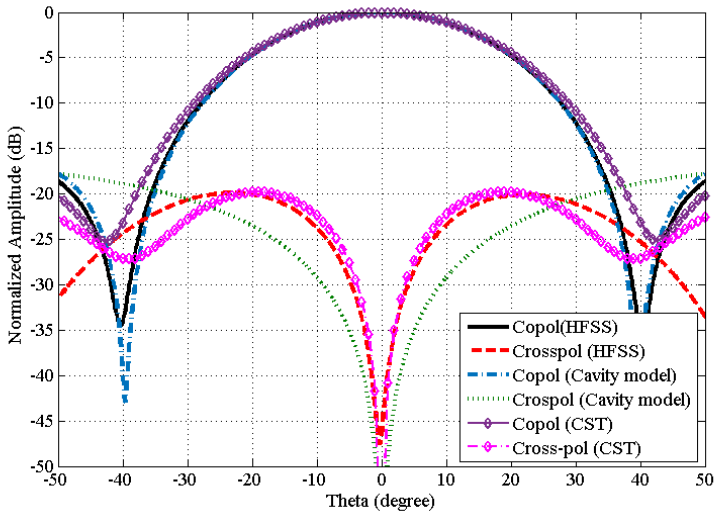

Figure 4.7: Field pattern (at $\phi = 90°$) of the proposed CCA feed using (4.1 and the two CAD simulators with optimized excitations.

bandwidth.

The gain of the offset reflector fed by the proposed CCA matched feed for normalized input power is shown in Fig. 4.9 and Fig. 4.10. The total gain of offset reflector at $\Phi = 90°$ is more than 41 dBi which is adequate for modern day applications. There is an increase of almost 5 dBi in the reflector gain when fed by the CCA matched feed as compared to the dual-mode CMPA feed of chapter 3. It may be noted the gain for a parabolic reflector is obtained for the same size of reflector. Therefore, the

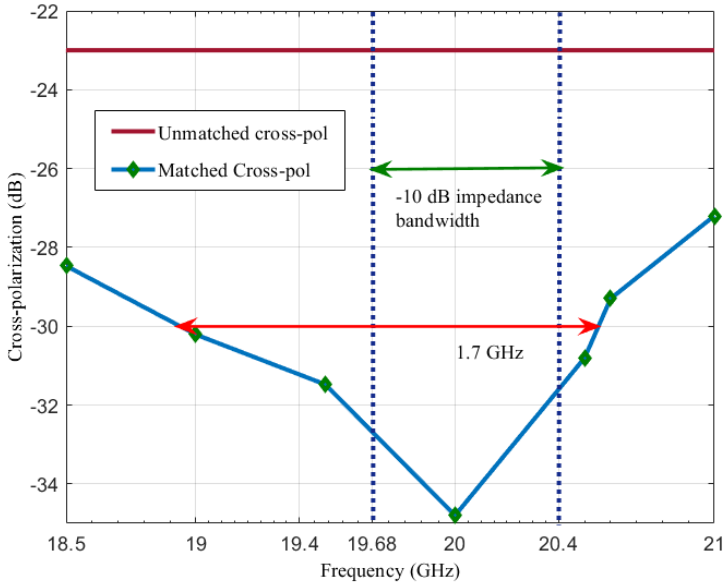

Figure 4.8: Cross-polar bandwidth in the secondary field pattern of the offset reflector with the single layer CCA matched feed.

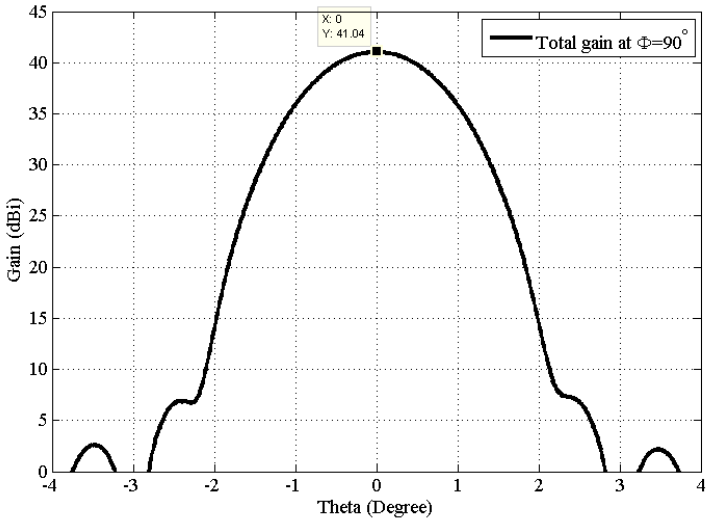

Figure 4.9: Gain pattern at $\Phi = 90°$ for the CCA feed design.

different aperture efficiencies when fed by both the matched feeds may have resulted in the difference of gain. As shown in Table 4.1, the single layer CCA matched feed shows better reflector performance in terms of gain and sidelobe over the dual-mode CMPA feed discussed in chapter 3. However, the cross-polar performance of the reflector in case of the dual-mode CMPA matched feed is marginally better than that of the single layer array feed.

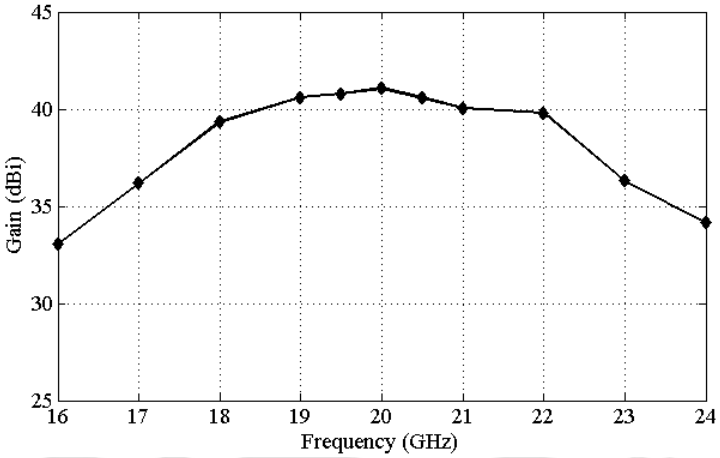

Figure 4.10: Gain versus frequency plot.

Table 4.1: Performance analysis of the matched feed designs for an offset reflector with $F/D = 0.6$ and operating at 20 GHz

Parameters	Dual-mode CMPA	Single layer CCA
Cross-polar level	-32.86 dB	-34.8 dB
First side-lobe level	-16.86 dB	-38.08 dB
Gain (dBi)	36.06	41.04

4.3 CCA with Dual-Mode CMPA as Central Element

The addition of a central dominant mode CMPA will balance the asymmetric field of the TM_{21} mode operating patch. Such CCA with dual-mode CMPA as the central element may be useful for applications such as beamwidth control and beamshift applications. In this section, a dual-layered centered circular array (CCA) of 10 CMPA elements as matched feed for an offset reflector configuration given in Table 4.2 is investigated.

Table 4.2: Offset reflector dimensions

Parameters	Diameter of projected aperture (D)	Focal length (F)	Offset height (H)	Offset angle (α)	Boresight angle (θ^*)
Value	2.5 m	1.75 m	0.25 m	42.24°	34.07°

The proposed array matched feed is shown in Fig. 4.11. The proposed matched feed is a two-layer stacked patch and consists of 9 TM_{11} mode operating CMPA elements arranged in the CCA configuration at the top layer. The lower layer consists of a single TM_{21} mode operating CMPA placed

inline with the central element of the upper CCA arrangement. The substrate used for simulation is RT Duroid 5880 with $\epsilon_r = 2.2$ and substrate height= 0.786 mm. The excitation ratio between the CMPA operating dominant mode and CMPA operating in TM_{21} mode is chosen in such a way that conjugate matching (CFM) is achieved and the cross polarization in the reflector pattern gets reduced. The radius of the array is decided by the reflector geometry and the same is obtained through parametric studies.

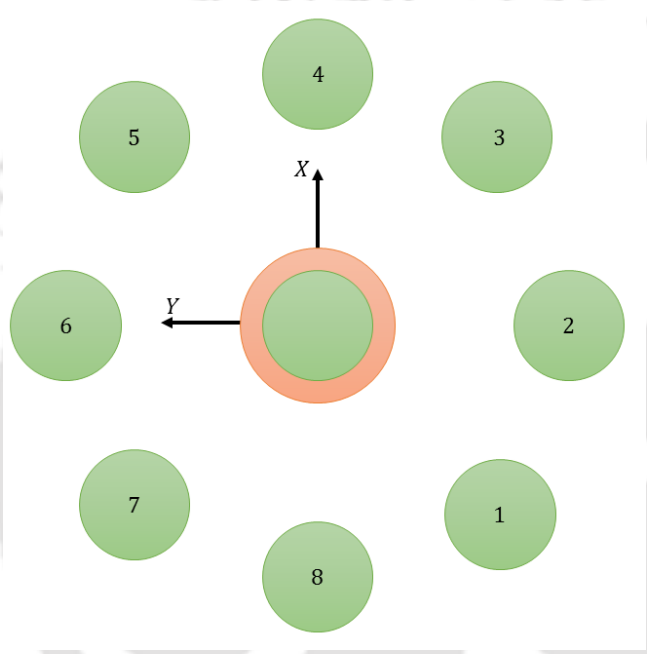

Figure 4.11: Proposed matched feed array dual-layered structure. The proposed structure consists of 10 CMPA elements.

4.3.1 Analytical model of the proposed dual-layer CCA matched feed

The field pattern of the proposed matched feed array can be expressed using basic cavity model as

$$\begin{bmatrix} E_\theta(\theta,\phi) \\ E_\phi(\theta,\phi) \end{bmatrix} = C1 \begin{bmatrix} E_{\theta 11}(\theta,\phi) \\ E_{\phi 11}(\theta,\phi) \end{bmatrix} (AF+1) + (-j)C2 \begin{bmatrix} E_{\theta 21}(\theta,\phi) \\ E_{\phi 21}(\theta,\phi) \end{bmatrix} \tag{4.2}$$

where,

$$\begin{bmatrix} E_{\theta mn}(\theta,\phi) \\ E_{\phi mn}(\theta,\phi) \end{bmatrix} = \begin{bmatrix} -j^m \cos m\phi (J_{m-1}(u_{mn}) - J_{m+1}(u_{mn})) \\ j^m \cos\theta \sin m\phi (J_{m-1}(u_{mn}) + J_{m+1}(u_{mn})) \end{bmatrix},$$

and

$$AF = \sum_{n=1}^{N} I(n) \exp jk_0 r sin\theta cos(n\xi - \phi).$$

and N is the number of elements, r is the radius of the circular array and ξ is the angular separation given by $\frac{2\pi}{N}$. The number of array element considered in the current work excluding the central element is 8 and are separated by an equal angular separation of 45°. To perform an initial investigation on the functioning of the proposed matched feed array, equal excitation is given to all the CMPA elements working in the dominant mode. The reflector pattern of the offset reflector fed by the proposed matched feed array is obtained using the MATLAB codes developed based on the geometrical optics (GO) method.

4.3.1.1 Effect of array radius on cross-polarization

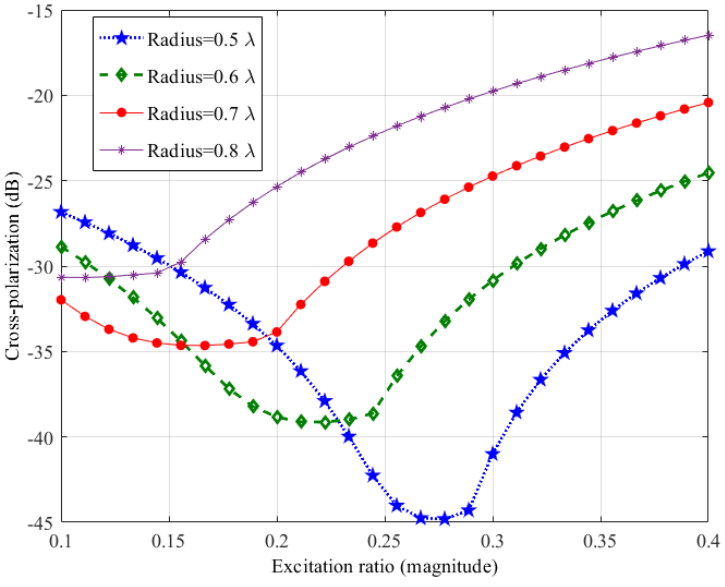

Figure 4.12: Effect of variation in excitation ratio between the TM_{11} and TM_{21} mode for different values of circular array radius on cross-polarization. The F/D of the reflector is kept as 0.7 for this study.

Further, a parametric study is performed to investigate the effect of the array radius of the circular array on the cross-polar performance. As shown in Fig. 4.12, the cross-polarization in the reflector pattern deteriorates with an increase in the array radius for an offset reflector with $F/D = 0.7$. The best cross-polar performance is obtained at an array radius of 0.5λ. However, as a compromise, to reduce the effect of mutual coupling, which was not considered in the analytical modeling, the radius of the circular array has been taken as 0.6λ. Another parametric study is performed to obtain the

optimum excitation ratio between the TM_{21} and TM_{11} modes for different F/D ratios for an array radius of 0.6λ and is shown in Fig. 4.13. The cross-polar performance of the reflector improves with increase in the F/D ratio. The variation in cross-polarization for different values of F/D is different from the single layer CCA matched feed and is more similar in nature to the variation in the single dual-mode CMPA matched feed.

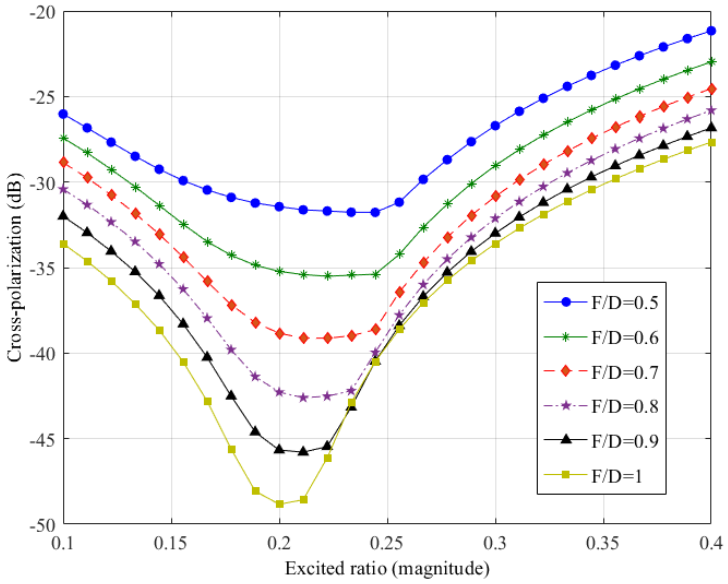

Figure 4.13: Effect of variation in excitation ratio between the TM_{11} and TM_{21} mode for different values of $\frac{F}{D}$ ratio on cross-polarization. The array radius is kept as 0.6λ in this study.

4.3.1.2 Offset reflector pattern for $F/D = 0.7$

The cross-polarization in the reflector pattern when the offset reflector is illuminated by unmatched and matched feed for an F/D ratio of 0.7 are shown in Fig. 4.14 and Fig. 4.15, respectively. The excitation ratio of the TM_{21} and TM_{11} modes in the proposed feed structure is varied to obtain CFM. By illuminating the offset reflector with the dual layer CCA matched feed, an improvement of 17 dB in the reflector cross-polar performance is achieved.

Table 4.3: Variation of the simulated reflector gain with frequency

Frequency (GHz)	4	5	5.5	6	6.5	7	8
Gain (dBi)	25.38	30.54	36.57	41.81	37.91	34.8	30.67

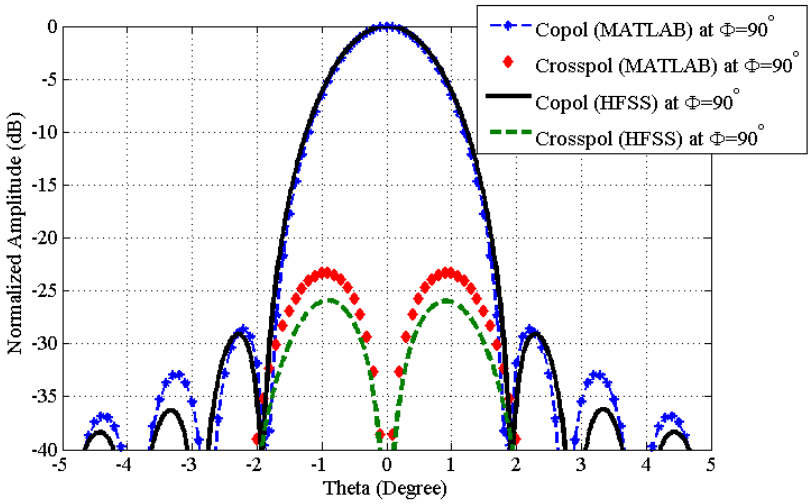

Figure 4.14: Offset reflector pattern for $\frac{F}{D} = 0.7$ with unmatched CCA feed.

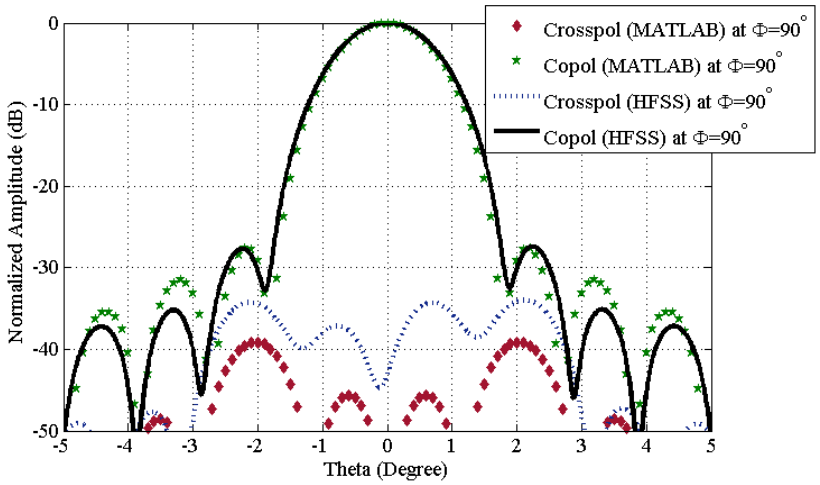

Figure 4.15: Offset reflector pattern for $\frac{F}{D} = 0.7$ with matched CCA feed.

Table 4.3 shows the variation in the gain of the overall reflector antenna system over the frequency band of 4-8 GHz. The gain of the reflector is 41.81 dBi at 6 GHz. In the next section, the pattern reconfigurability in terms of beamwidth variation and beamshift control in the reflector pattern with the proposed CCA structure as the reflector feed is investigated.

4.4 Beam Shifting and Beam Size Control using the Dual-layer CCA Matched Feed

Pattern reconfigurability in terms of beamwidth variation and beamshift control are requirements of some modern communication systems [71–74]. By selectively exciting either a single element or a group of elements of the circular array of the dual layer CCA matched feed proposed in the previous section, in this section, the beam size and beam shifting reconfigurability of the reflector pattern is studied. The cross-polar performance in the reflector pattern is also improved by having a proper excitation ratio between the TM_{11} and TM_{21} mode.

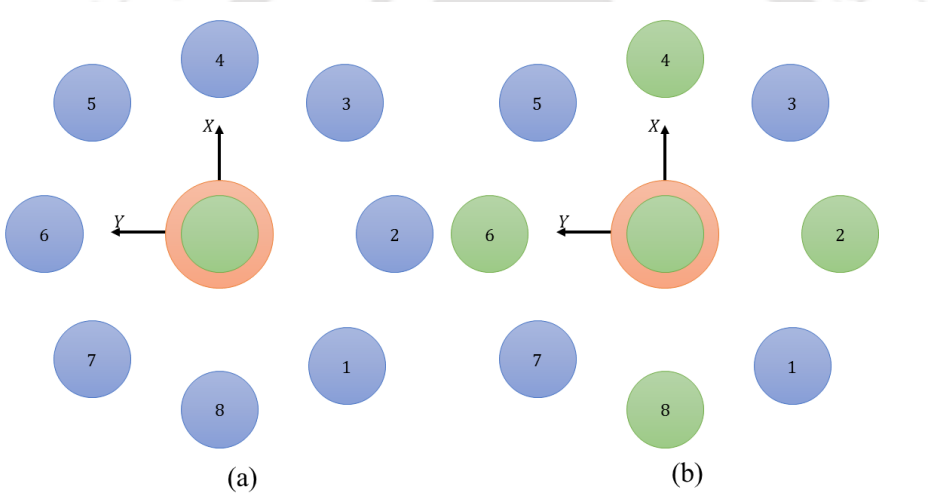

Figure 4.16: Combinations of array elements for beamwidth control (a) only the central dominant and higher mode operating patches are excited (b) antenna element 2,4,6 and 8 along with the central dominant and higher mode operating patches are excited.

4.4.1 Beamwidth control

By controlling the ring CMPA element excitations electronically, the beamwidth of the reflector pattern can be varied. As shown in Fig. 4.16, two different combinations of elements of the array structure can be excited. In the first combination, only the central TM_{11} and TM_{21} mode operating patches are excited whereas CMPA 2, 4, 6 and 8 are excited along with the central TM_{11} and TM_{21} mode operating patches in the second case. Fig. 4.17 shows the variation of beamwidth in reflector pattern at $\Phi = 0°$ and $\Phi = 90°$ for the two combinations.

Excitation of ring elements along with the central CMPA leads to broadening of the reflector beam

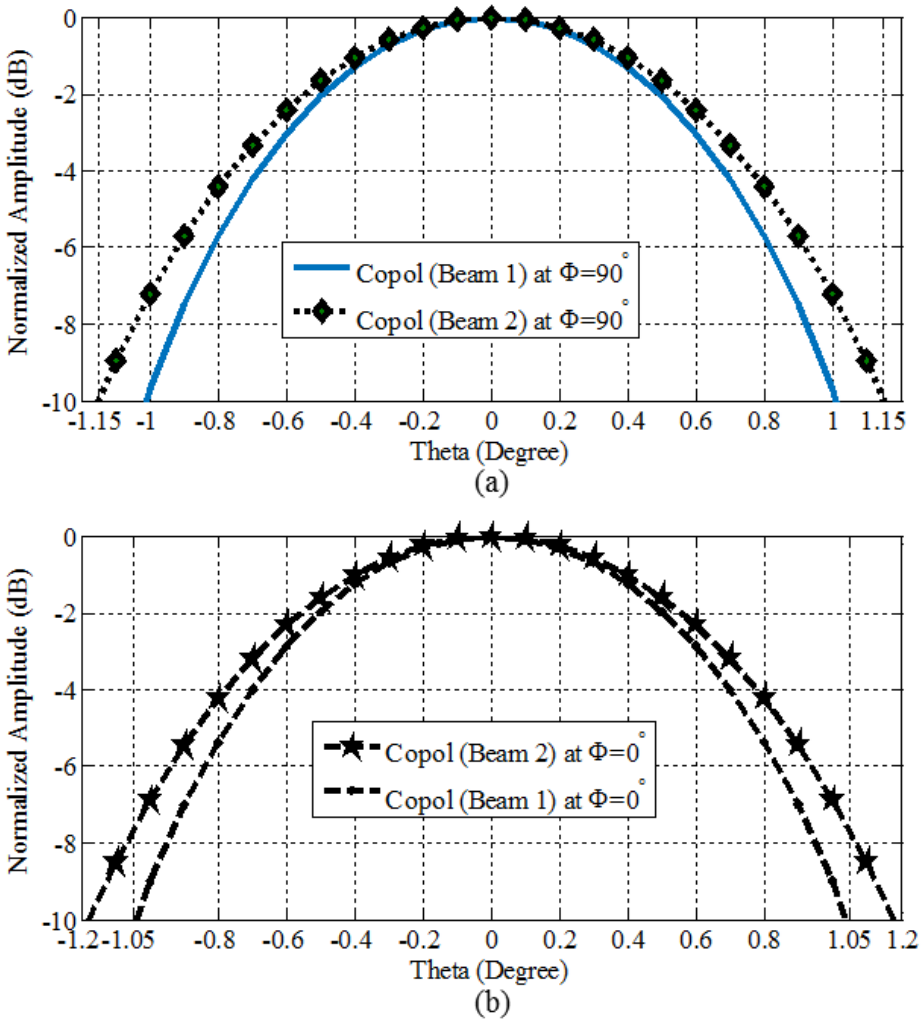

Figure 4.17: Beamwidth variation in reflector pattern (a) at $\Phi = 90°$ (b) at $\Phi = 0°$.

as compared to excitation of only the central CMPA elements. Broadening of the beamwidth only in either of the planes (0° or 90°) is also possible by exciting only the elements along either of the principal axes. It is worth noting that an increase in the array radius increases the beamwidth of the reflector pattern. However, there is a tradeoff between the cross-polar performance and the beamwidth of the reflector, when excited by the matched feed array.

Similar to the study performed in earlier section, here also the array radius is considered to be 0.6λ. Fig. 4.18 shows the beamwidth reconfigurability of the reflector fed by the proposed structure when the higher order TM_{21} mode patch is not excited. The cross-polar performance in the reflector pattern is improved by having proper excitation ratio between the two modes. The optimum excitation ratio of TM_{21} by TM_{11} mode for best cross-polar performance is found to be 0.23 in the second case and

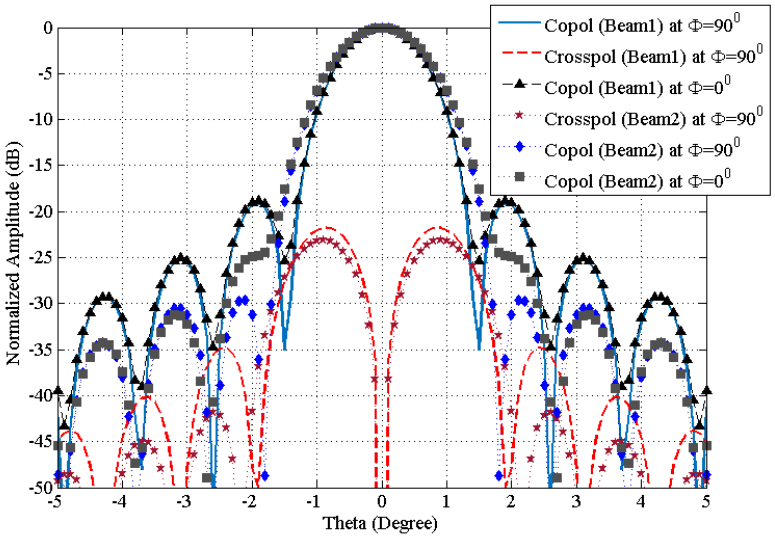

Figure 4.18: Reflector pattern at $\Phi = 0°$ (symmetric plane) for unmatched feed array.

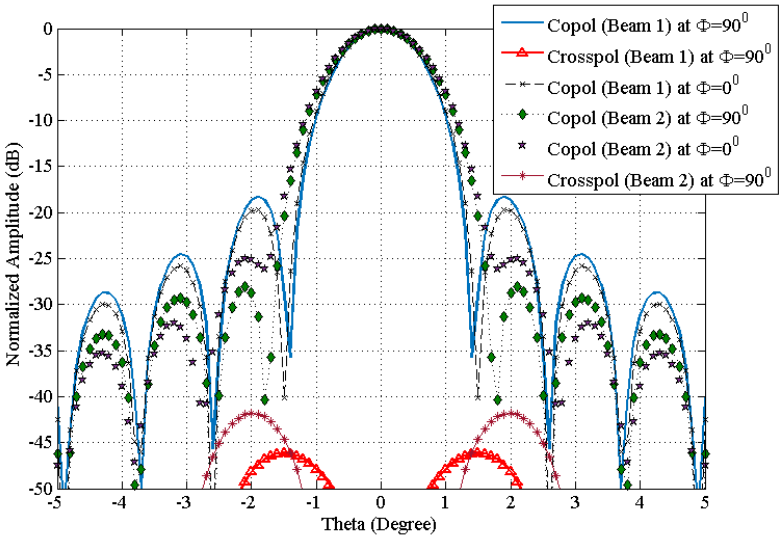

Figure 4.19: Reflector pattern at $\Phi = 90°$ (asymmetric plane) for matched feed array with proper excitation ratio between the two modes.

0.4 in case of the first combination. As shown in Fig. 4.19, the cross-polarization performance in the reflector pattern for an array radius of 0.6λ is found to be better than -42 dB in both the cases. Though, uniform excitation of all the CMPAs operating in TM_{11} mode and only the four such CMPA ring elements along the axes lead to same beamwidth, the cross polarization is found to be better in the latter case.

4.4.2 Beam-shifting in the reflector pattern

4.4.2.1 Large beam shift case: 0.4° beam shift

The main beam of the reflector pattern can be shifted in both the planes or in either of the planes by selectively exciting a single CMPA element of the circular array along with the central dual-mode CMPA element and is shown in Fig. 4.20. However, selective excitation of single CMPA element except those aligned along X-axis will have poor cross-polar performance in both the plane or either of the planes due to the asymmetry of the offset reflector along the X-axis. Thus, the offset reflector excited by only those CMPA elements aligned along X-axis are shown in Fig. 4.21 and are being investigated here. As shown in Fig. 4.22, the main beam of the reflector pattern gets shifted by 0.4° (approximately 31% of 3 dB beamwidth) from the principal axis whenever either of CMPA element 4 or CMPA element 8 is excited along with the central TM_{11} and TM_{21} mode operating patches. The amount of beamshift depends on the radius of the circular array and has a tradeoff with the sidelobe and cross-polar levels in the reflector pattern. For an array radius of 0.6λ, the best cross-polar performance is achieved when the overall excitation ratio between the TM_{21} and TM_{11} modes generated is 0.18. The reflector pattern at the asymmetric plane for the matched condition and unmatched condition are shown in Fig. 4.23 and Fig. 4.24, respectively. The cross-polarization in the reflector pattern for the matched feed is found to be better than -38 dB for an F/D = 0.7. The offset reflector has sidelobe levels at the asymmetric plane of the reflector pattern better than -17 dB.

4.4.2.2 Small beam shift case: 0.1° beam shift

The proposed feed structure can also be used to obtain a smaller beam shift with a broader main beam in the reflector pattern by exciting a group of three ring CMPA elements along with the central dual-mode CMPA element. Such combination of three ring elements when aligned along Y-axis shifts the main beam in the asymmetric plane but deteriorates the overall cross-polar performance of the reflector. Hence, two different combinations along X-axis as shown in Fig. 4.25 are studied here which can be used for reflector beam shifting.

A beam shift of 0.1° (approximately 7.2% of 3 dB beamwidth) is obtained in the reflector pattern when the offset reflector is fed by the proposed matched feed with such excitation combination along the X-axis. The beam shift in the reflector pattern at the symmetric plane is shown in Fig. 4.26. The cross-polarization in the reflector pattern is reduced by having proper excitation ratio between the

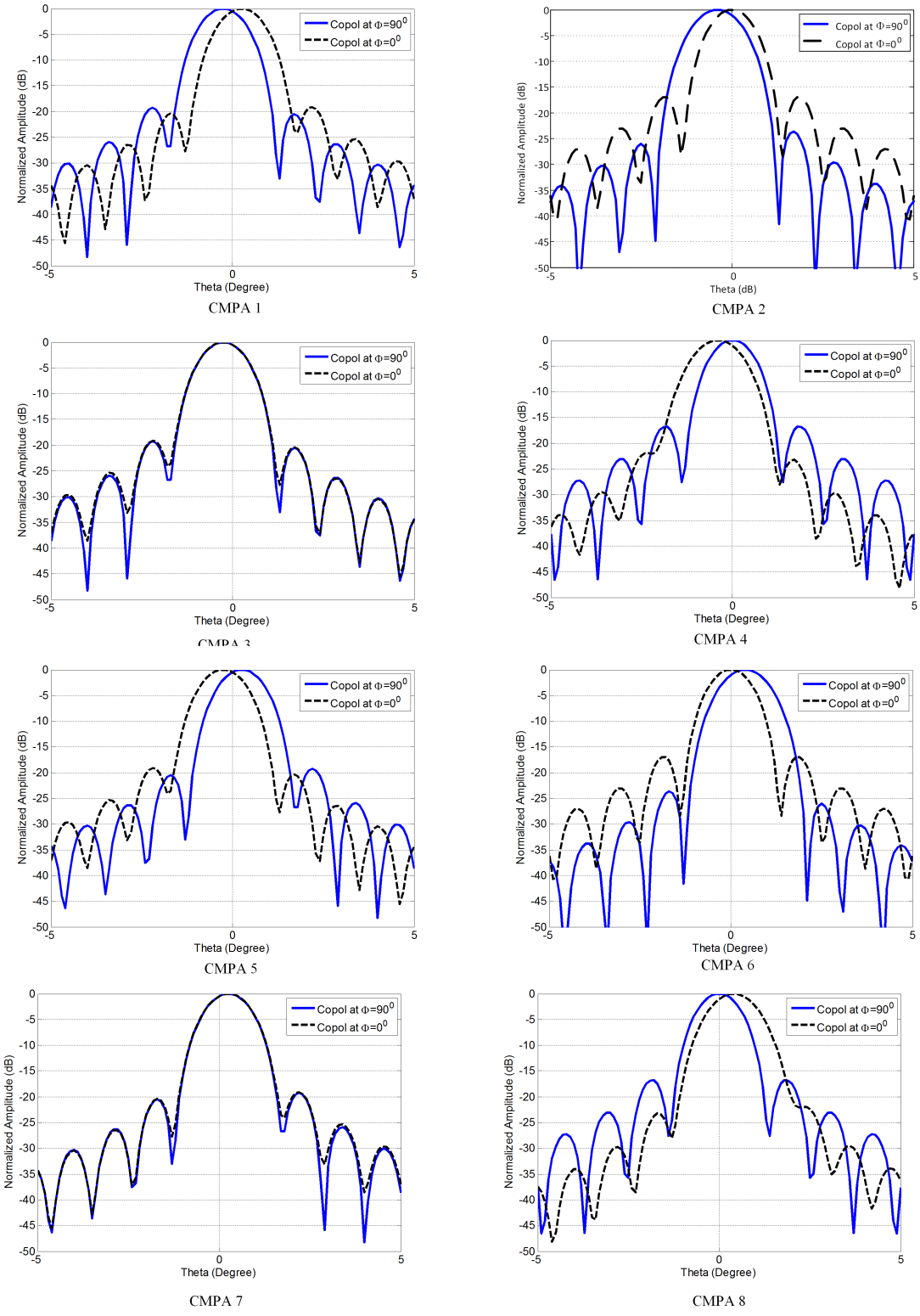

Figure 4.20: Reflector pattern beam shift in different direction on selective excitation of only a single CMPA array element.

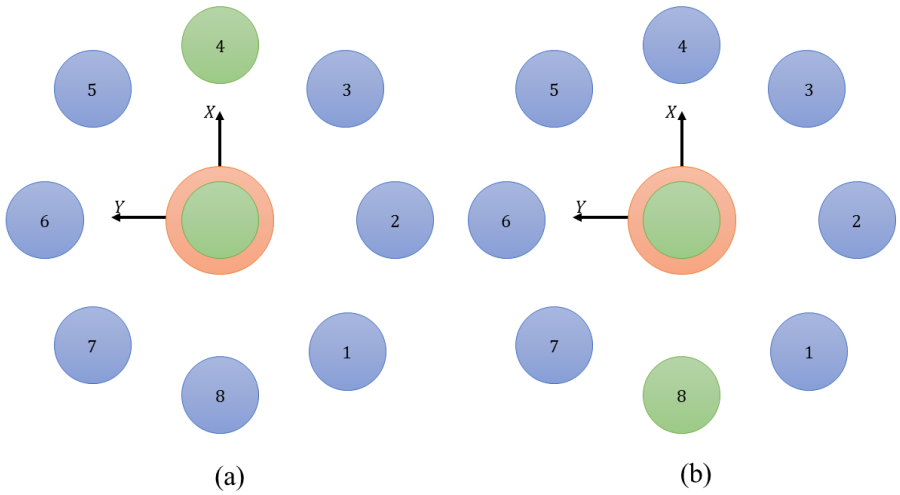

Figure 4.21: Matched feed array (a) only CMPA 4 is excited along with the central TM_{11} and TM_{21} mode operating patches (b) only CMPA 8 is excited along with the central TM_{11} and TM_{21} mode operating patches.

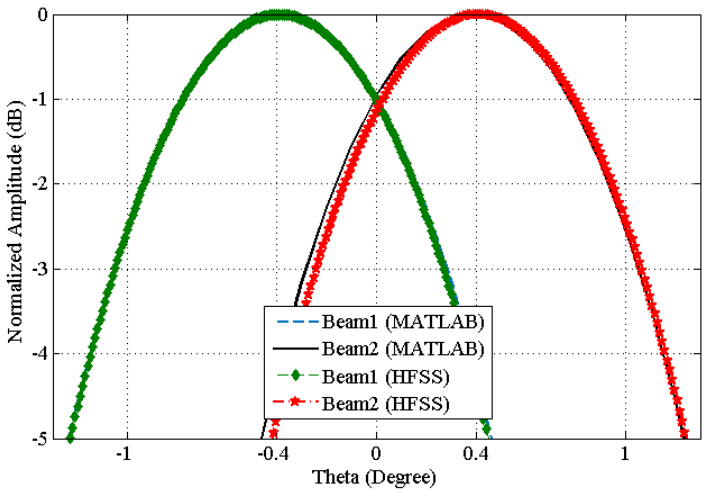

Figure 4.22: Beam shift of 0.4° from the principal axis in the reflector pattern at $\Phi = 0°$ (symmetric plane).

two modes. The best cross-polarization is obtained at the asymmetric plane of the reflector pattern for an excitation ratio of 0.2. The unmatched and the matched reflector pattern at the asymmetric plane for both the excitation combination is shown in Fig. 4.27 and Fig. 4.28, respectively. The cross-polarization is better than -45 dB at the asymmetric plane of the reflector pattern in both the cases.

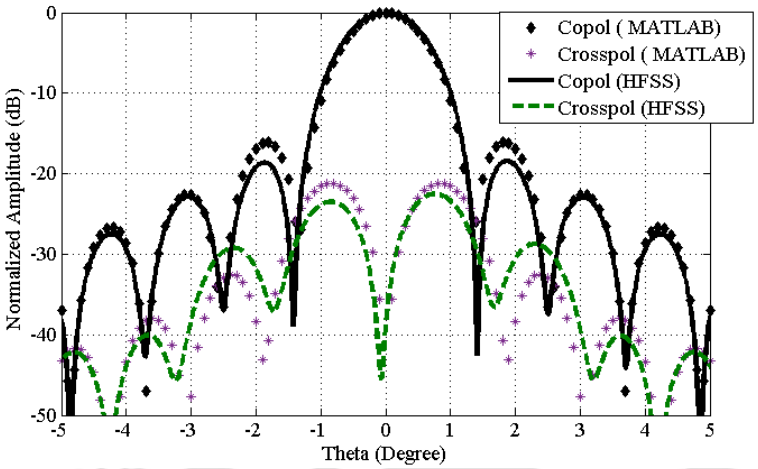

Figure 4.23: Reflector pattern for unmatched feed at $\Phi = 90°$ (asymmetric plane).

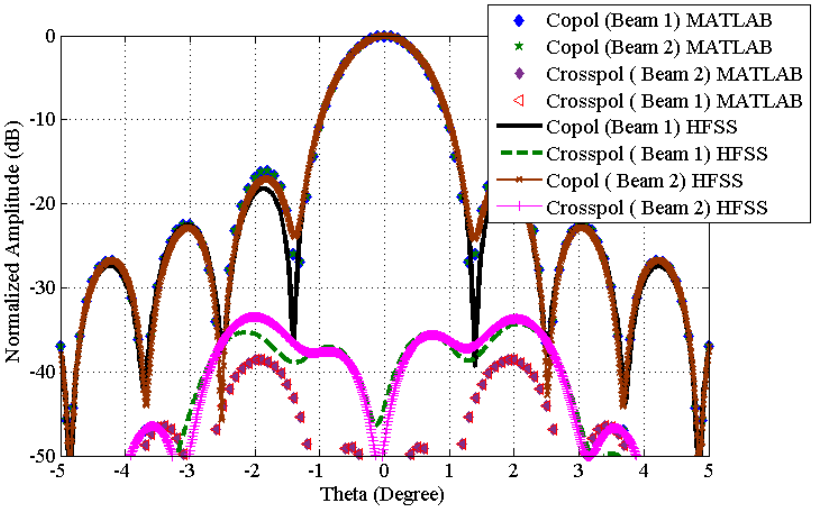

Figure 4.24: Reflector pattern for matched feed at $\Phi = 90°$ (asymmetric plane).

4.5 CCA Feed for Dual Band Application

All the microstrip based feeds discussed till now in this thesis are designed to operate at a single frequency band. However, some of the emergent scenarios require a single antenna structure to operate in multiple bands as evident in [41, 75–78]. Although, a dual band microstrip patch antenna (MPA) array feed is reported in the literature [41] operating at Ka / Ku band, the number of MPA array elements (4×166 at Ka band) used in the feed is very large which may not be suitable at frequencies lower than 10 GHz. This has motivated us to design a dual frequency microstrip feed with small aperture size. This investigation aims at designing a dual band circular array feed using CMPA

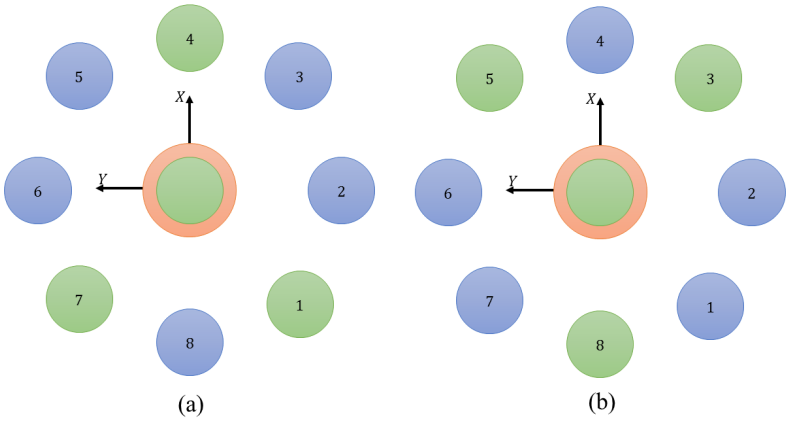

Figure 4.25: Matched feed array excitation (a) combination 1 (b) combination 2.

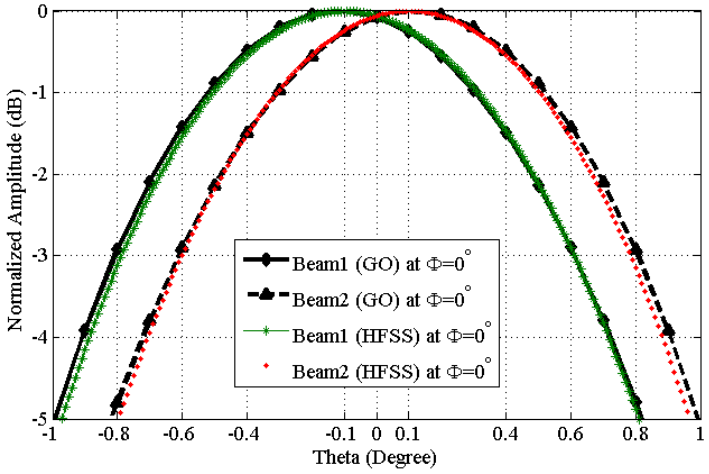

Figure 4.26: Beam shifting at $\Phi = 0°$(symmetric plane) of the reflector pattern. Beam 1 corresponds to combination 1 and beam 2 corresponds to combination 2.

elements for offset reflectors which can provide cross-polarization lower than -30 dB. In this section, the design insights gained while working with circular array as feed for ORA in the previous section is used to propose a dual band microstrip circular array feed for an ORA which can operate at 4 GHz and 6 GHz. The proposed dual band feed is a centered circular array with two groups of antenna elements: a circular ring of 8 CMPA elements radiating at 4 GHz and a dual-mode CMPA (DCMPA) radiating at 6 GHz. A parametric study is performed to obtain the optimum array radius of the proposed structure for which the reflector cross-polarization is better than -30 dB at both the operating frequency.

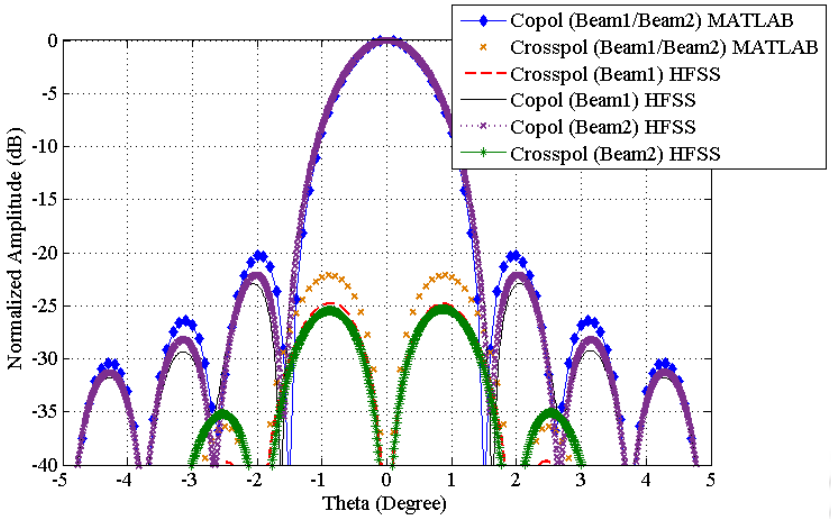

Figure 4.27: Reflector pattern for unmatched feed at $\Phi = 90°$ (asymmetric plane).

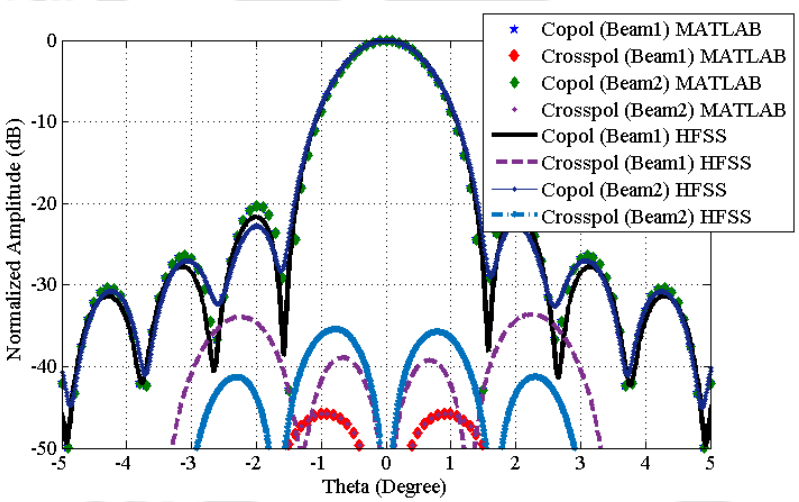

Figure 4.28: Reflector pattern for matched feed at $\Phi = 90°$ (asymmetric plane).

Table 4.4: Offset reflector dimensions

Parameters	Diameter of projected aperture (D)	Focal length (F)	Offset height (H)	Offset angle (α)	Boresight angle (θ^*)
Value	2.5 m	2 m	0.25 m	38.08°	30.56°

4.5.1 Design issues

A dual band CCA feed for an ORA with the specifications given in Table 4.4 is designed for 4/6 GHz dual-band applications using the dual layer CCA structure. The CCA considered for the

proposed dual band feed design has an outer ring of 8 CMPA elements and a central patch which operates in dual mode (TM_{11} and TM_{21}). The CCA configuration, because of its structural symmetry has the same phase center for both the bands. In the proposed structure, the outer ring elements contribute to radiation at 4 GHz while the dual mode central patch element is the main radiator for 6 GHz. Since, in this design, radiation at one of the operating frequencies is contributed by a selected subset of antennas, the effect of other antenna elements at this operating frequency is required to be considered appropriately and antenna dimensions and their positions are optimized accordingly. Through a parametric study in HFSS, array radius and excitation ratio between the two modes of the central element are found out for obtaining good cross-polar performance at both the operating frequencies. The number of circular rings and elements in each ring of the CCA configuration is decided by θ^* shown in Fig. 1.1. For the present offset reflector dimensions, a single ring of 8 CMPA element is found to be sufficient. It may be noted that for simulation of the proposed structure, the array elements are fed equally and total excitation power of the array is same as that of the dual mode CMPA. Further, the feed network that would be needed for feeding the proposed structure from a single source is not detailed here.

4.5.2 Proposed dual-band microstrip patch antenna feed

Based on the discussions in the previous subsection, the proposed structure for the dual band feed is shown in Fig. 4.29, which consists of two groups of radiating antennas: (a) a circular array of 8 CMPA elements operating at the lower frequency of 4 GHz and (b) a dual mode CMPA (DCMPA) operating at the higher frequency of 6 GHz. The dual band CCA feed is designed using a stacked layer configuration. Patches operating in dominant mode are placed at the top of upper substrate layer while the TM_{21} mode operating patch is located on the top of the lower substrate layer.

Ground plane for the structure is situated at the bottom of the lower substrate layer. It may be noted that both the upper and the lower substrate are of the same thickness and material properties (i.e. dielectric constant and loss tangent). The size of the ground plane considered in simulation is 200 mm×200 mm. After some parametric study of the excitation ratio of the two modes (TM_{21} and TM_{11}) generated in the DCMPA part, the best cross-polar suppression is found when TM_{21} is excited at a ratio of 0.08 and in quadrature phase with TM_{11} mode. The variation in array radius plays an important role in controlling the cross-polarization at the asymmetric plane of the reflector pattern at both the frequencies. As shown in Fig. 4.30, the cross-polar levels at 6 GHz decreases gradually from

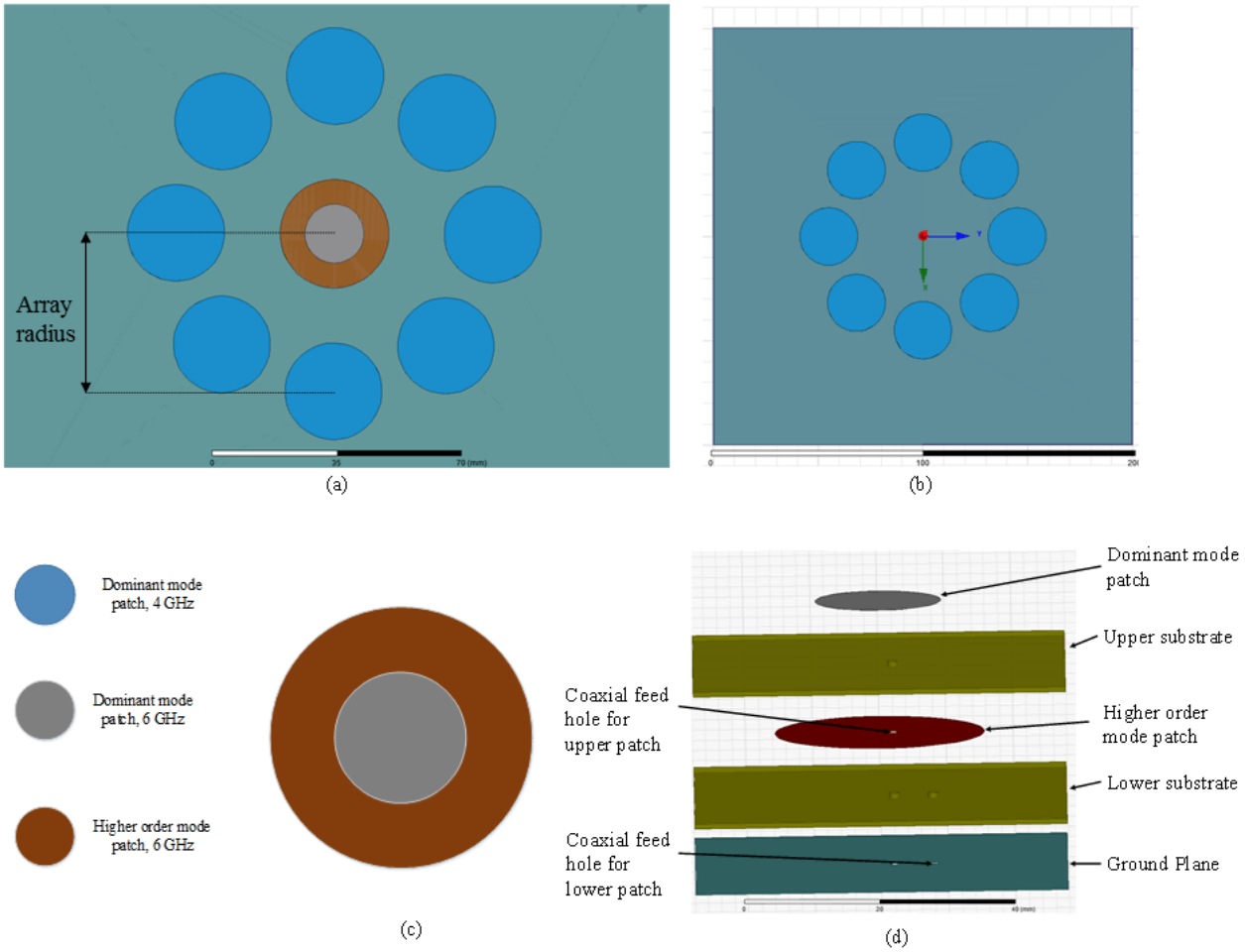

Figure 4.29: Proposed dual band dual-layer CCA reflector feed antenna

-27 dB to -37.17 dB as the array radius increases. While, the cross-polarization at 4 GHz is -31.2 dB for 40 mm radius and -30.83 dB for 50 mm radius of the circular array. The better cross-polar levels at 4 GHz for an array radius of 40 mm is due to the field coupling from the DCMPA part. However, due to the same reason the cross-pol performance at 6 GHz deteriorates for an array radius of 40 mm. A smaller array radius will lead to higher field coupling between the two groups of antenna radiators and thus influence the feed performance. Hence, the CCA radius of 50 mm is chosen where cross-polar levels are below -30 dB at both the frequencies.

The return losses at all the coaxial ports of the proposed structure using HFSS and CST are shown in Fig. 4.31 and Fig. 4.32, respectively. The two coaxial ports corresponding to the DCMPA show return losses better than -12 dB while the 8 circular array ports show better than -19 dB. The dimension details of the dual band CCA feed for an array radius of 50 mm is given in Table 4.5.

Table 4.5: Dual band feed parameters

Parameters	Diameter of projected aperture (D)
Substrate material	RT/ Duroid 5870
Substrate height, h	0.762 mm
ϵ_r	2.33
Radius of CMPA, 4 GHz	14 mm
Radius of CMPA, 6 GHz	9.2 mm
Position of coaxial feed for upper patch, 4 GHz	3.5 mm
Position of coaxial feed for upper patch, 6 GHz	2 mm
Position of coaxial feed for lower patch, 6 GHz	7.5 mm
Array radius	50 mm

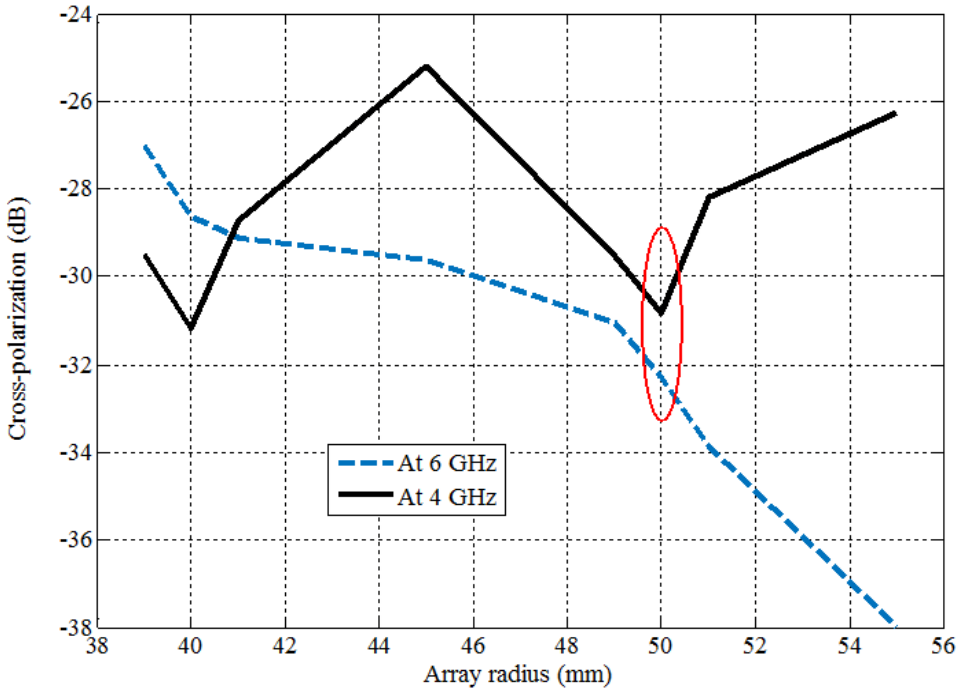

Figure 4.30: Cross-polar variation with the array radius for dual band antenna

4.5.2.1 Feed and reflector pattern at 6 GHz

The reflector pattern of the dual band MPA feed at 6 GHz in shown in Fig. 4.33.

As mentioned previously, the central DCMPA radiating element is primarily responsible for the reflector pattern at 6 GHz. Therefore, in the proposed design, the feed pattern at 6 GHz has a very broad main lobe as shown in Fig. 4.33. Addition of the TM_{21} mode in quadrature phase to the dominant mode increases the cross-pol levels of the feed pattern by an appropriate amount, which in

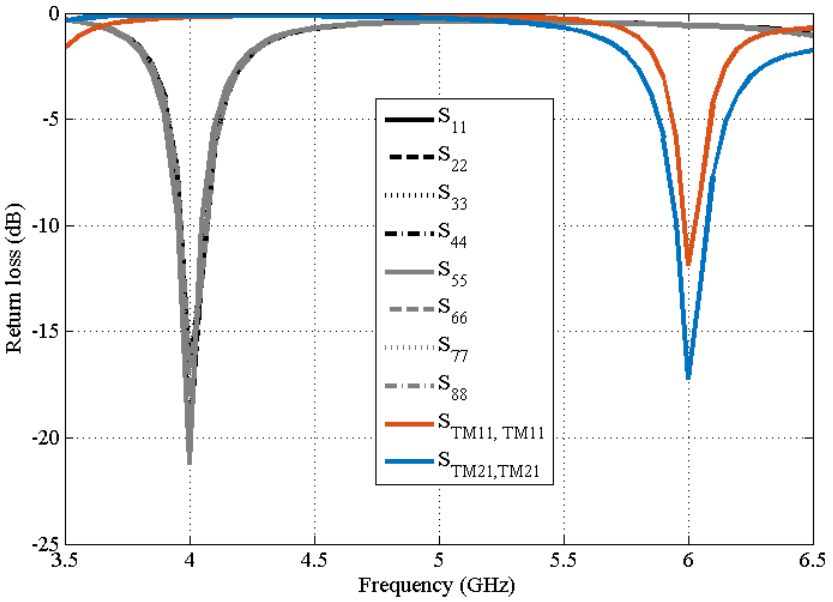

Figure 4.31: Return losses of the proposed dual band antenna feed at both the operating frequencies

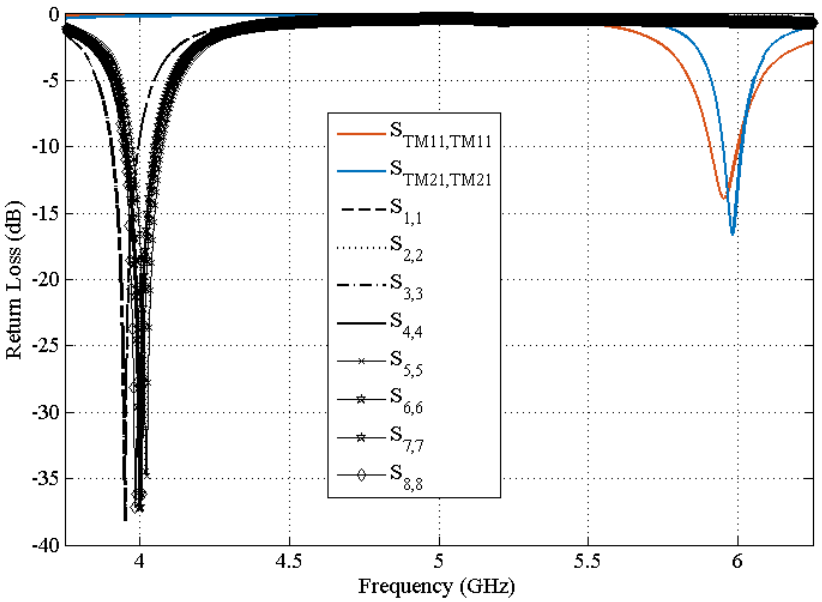

Figure 4.32: Return losses of the proposed dual band antenna feed at both the operating frequencies using CST.

turn reduces the cross-polarization at the asymmetric plane of reflector pattern as shown in Fig. 4.34. ORA performance when fed by the proposed structure at 6 GHz is summarized in Table 4.6.

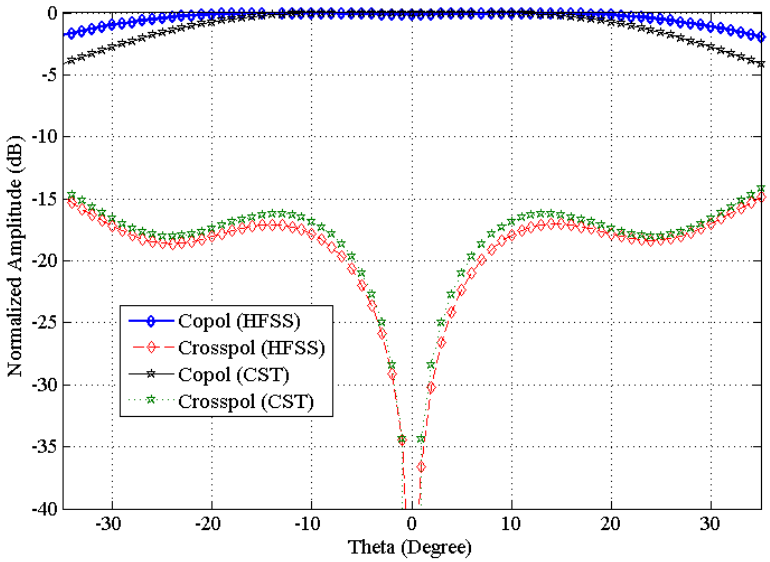

Figure 4.33: Primary feed pattern of the proposed dual band antenna feed at 6 GHz obtained using both HFSS and CST.

Table 4.6: Offset reflector performance at 6 GHz

Parameters	Reflector gain	Cross-polarization in the reflector pattern		-30 dB cross-polar bandwidth	First-null beamwidth
		At array radius= 55 mm	At array radius= 50 mm		
Value	38.46 dBi	-37.17 dB	-32.28 dB	150 MHz	2.92°

4.5.2.2 Feed and reflector pattern at 4 GHz

The SCA configuration of 8 CMPA elements in the proposed structure illuminates the reflector at the lower frequency of 4 GHz. The best cross-polar performance is achieved at an array radius of 50 mm. The feed pattern of the dual band feed is shown in Fig. 4.35 and the corresponding reflector pattern of the reflector is shown in Fig. 4.36. The first null beamwidth of the feed (60°) is almost equal to the boresight angle of the reflector. The change in radius of the circular array changes the cross-polar levels in the feed pattern which in turn is responsible for the reflector pattern at 4 GHz. The reflector pattern obtained at 4 GHz when illuminated by the SCA feed has a broader main beam due to the smaller electrical size of the reflector at the particular frequency. The cross-polarization in the reflector pattern at the asymmetric plane will be relatively poor as shown in Fig. 4.36. Summarized ORA performance is given in Table 4.7.

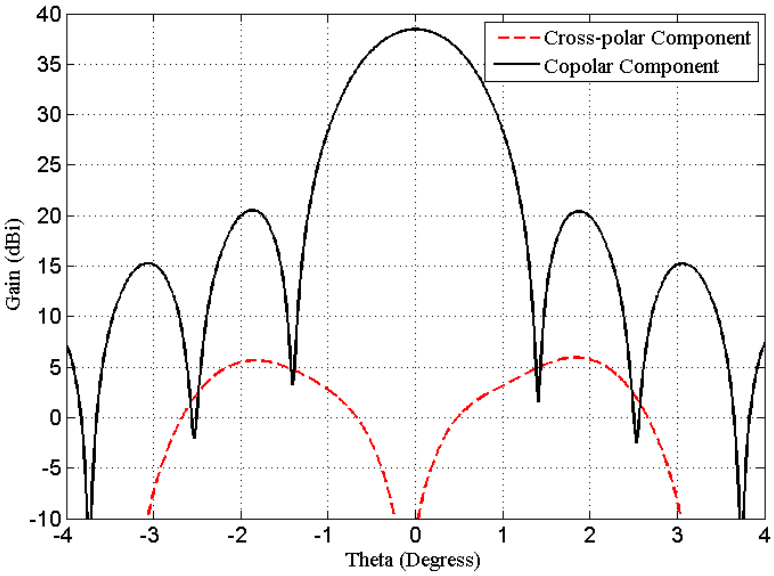

Figure 4.34: Reflector pattern obtained using HFSS-PO at 6 GHz.

Performance of the reflector illuminated by the proposed feed structure is shown in Table 5.3. The -30 dB cross-polar bandwidth is slightly narrow and can be used for narrow band applications at both 4 GHz and 6 GHz. The overall efficiency of the reflector fed by the proposed dual-band feed at 4 GHz and 6 GHz as calculated from the simulated gain is found to be 54% and 29%, respectively. The difference in the overall efficiency at both the frequencies is mainly due to the fact that at 6 GHz,

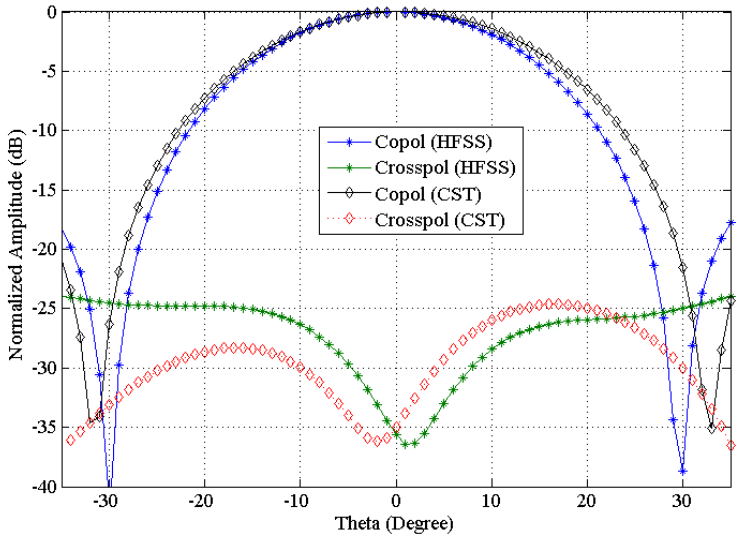

Figure 4.35: Feed pattern of the dual band CCA at 4 GHz obtained using HFSS and CST.

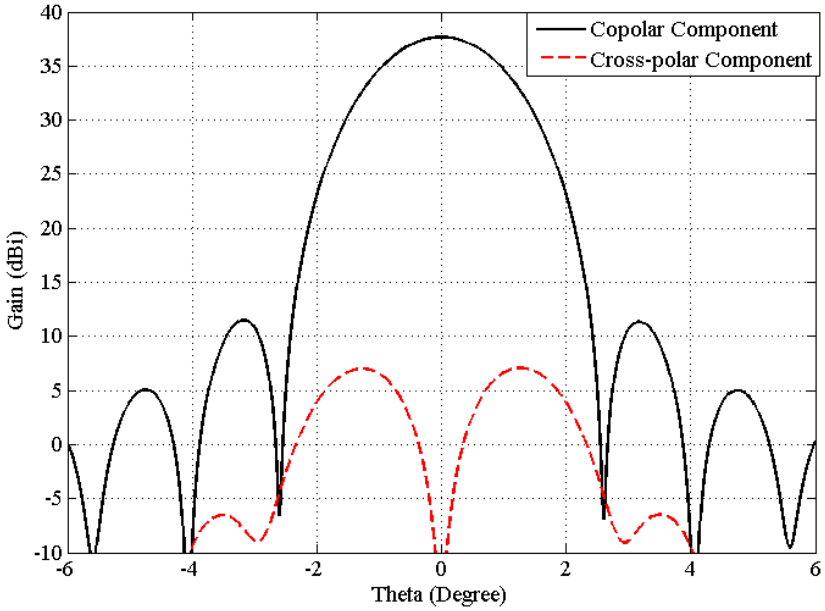

Figure 4.36: Reflector pattern of the offset reflector at 4 GHz.

Table 4.7: Offset reflector performance at 4 GHz

Parameters	Reflector gain	Cross-polarization in the reflector pattern		-30 dB cross-polar bandwidth	First-null beamwidth
		At array radius= 40 mm	At array radius= 50 mm		
Value	37.6 dBi	-31.2 dB	-30.83 dB	160 MHz	5.2°

the central dual-mode MPA part is a single element feed and at 4 GHz, the feed is the circular array. Thus, at 6 GHz band, the spillover becomes higher and the efficiency is reduced.

Table 4.8: Performance analysis of the dual layer CCA matched feed

Parameters	At 4 GHz	At 6 GHz
Cross-polar level	-30.83 dB	-32.78 dB
First side-lobe level	-26.25 dB	-18.93 dB
Cross-polar B.W(-30 dB)	4%	2%
Gain	37.6 dBi	38.46 dBi

4.5.3 Experimental validation

The central element (dual-mode CMPA) of the dual-band CCA feed mainly contributes to the feed pattern at the 6 GHz. A prototype of the dual-mode CMPA is fabricated on a 40mm×40mm ground plane.

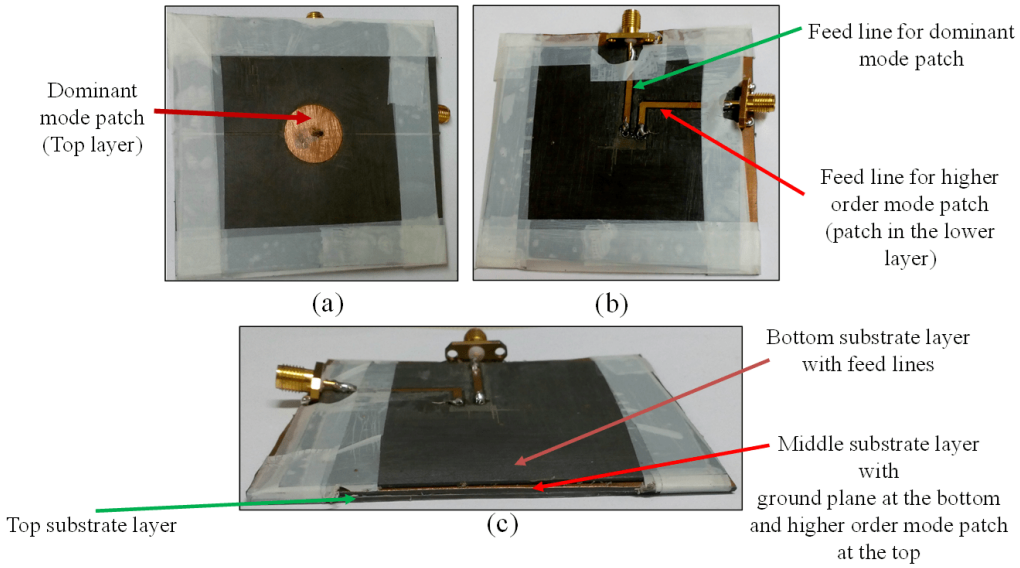

Figure 4.37: Fabricated prototype of the central part of the dual band feed operating at 6 GHz.

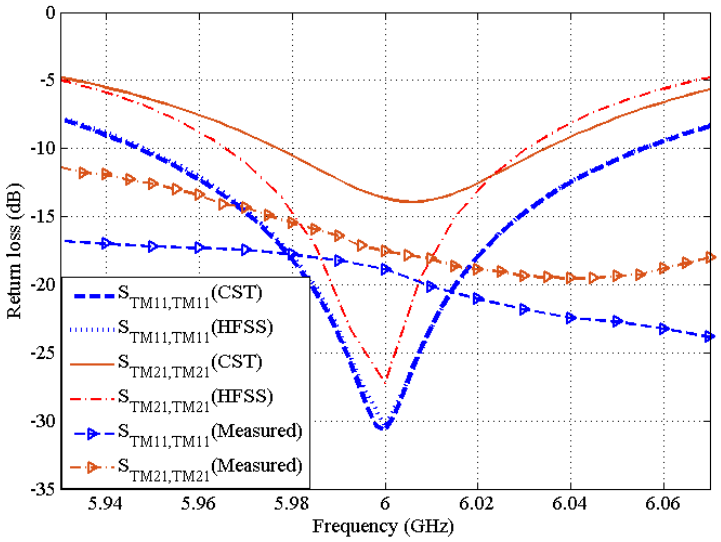

Figure 4.38: Return losses of the proposed dual band antenna feed at both the operating frequencies.

Fig. 4.37, shows the fabricated prototype antenna. The return loss and the radiation pattern

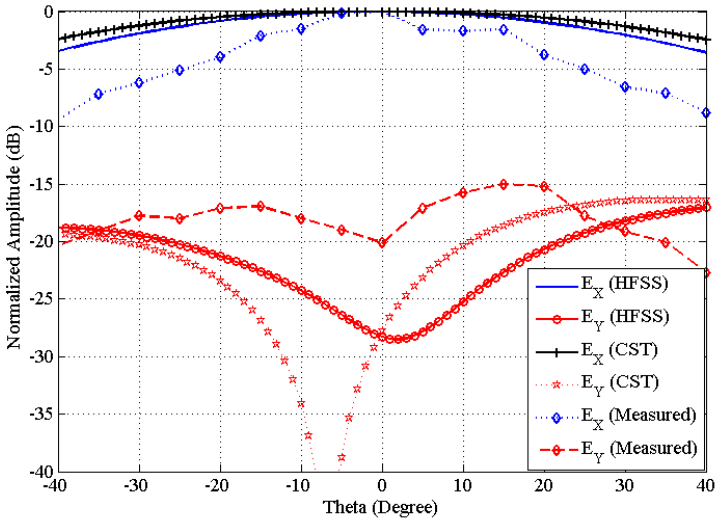

Figure 4.39: Field pattern of the prototype when only port 1 is excited.

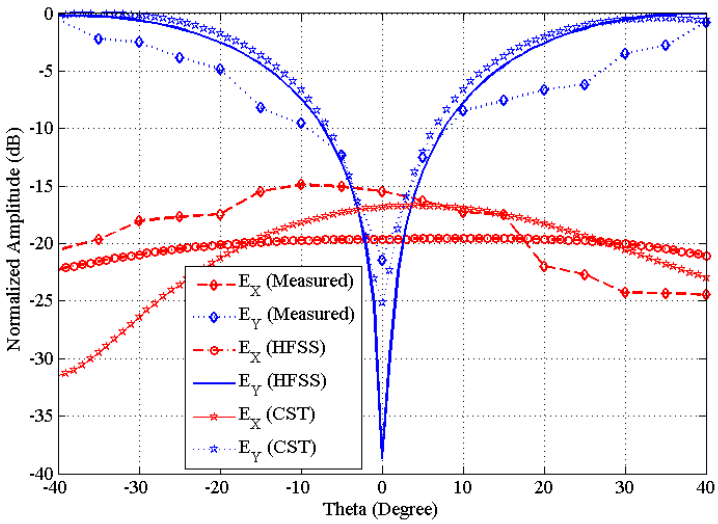

Figure 4.40: Field pattern of the prototype when only port 2 is excited.

of the prototype is measured. As shown in Fig. 4.38, the measured return loss in both the ports are comparable with the simulated results obtained from HFSS and CST. A slight increase in the impedance bandwidth is observed, which may be due to the presence of air gap between the substrate layers while stacking them. The radiation pattern of the dual-mode antenna is measured by exciting one port at a time and terminating the other port by 50Ω matched termination. The comparison of the measured radiation pattern of the prototype with the simulation results from HFSS and CST is shown in Fig. 4.39 and Fig. 4.40. Fig. 4.39 shows the radiation pattern of the prototype when only

port 1 is excited whereas Fig. 4.40 shows the far field pattern of the same when only port 2 is excited. The measured radiation pattern in both the cases are in close agreement with the simulation results.

4.6 Conclusion

This chapter discusses three circular array designs as feed for offset reflector antenna. The first circular array is a single layer matched feed designed to operate at 20 GHz of Ka-band. The TM_{21} mode operating patch is placed at the centre of the array and is excited at an appropriate ratio. The cross-polar performance of the single layer CCA matched feed is better than -33 dB for an offset reflector with $F/D = 0.6$.

The second design is double layer CCA matched feed similar to the first matched feed in this chapter. The difference here is the placement of the TM_{21} mode operating patch which is kept at the lower layer. Moreover, the dual layer CCA feed has an extra dominant operating patch at the centre of the array at the top layer. The double layer CCA matched feed provides cross-polarization better than -38 dB for a reflector with $F/D = 0.7$. Further, investigation has been done to show that by exciting selective array antenna elements, beamwidth and beam shift reconfigurability in the reflector pattern can be achieved, while maintaining the cross-polar level below -38 dB. A maximum beam shift of 0.4° (approximately 31% of 3 dB beamwidth) from the principal axis has been achieved in the reflector pattern.

The third CCA feed is also similar in array configuration to the dual-layer CCA matched feed. However, the reflector feed is designed such that the same reflector can be used for dual-band applications. This is achieved by operating the central dual-mode CMPA and the surrounding ring elements at two different frequencies. The array radius is optimized such that the cross-polarization in the reflector pattern is above -30 dB at both the frequency bands.

5

Matched MPA Feeds for Small Offset Reflector Antenna

Contents

5.1 Introduction 76
5.2 Design and Analysis of First Matched Feed 76
5.3 Design and Analysis of Second Matched Feed 89
5.4 Conclusion 94

5.1 Introduction

In the previous chapters, the reported matched feeds are designed using CMPA elements generating both the dominant mode and the required higher order mode at an appropriate ratio. Further, the size (diameter) of the offset reflectors in the earlier chapters are of the order of 50λ. While, the reflectors used in satellite communication are considerably large (diameter $\geq 50\lambda$), in some modern day applications such as cellular communication, the reflectors used at the base stations [79–81], are considerably smaller (diameter$<$ 1m). Moreover, as the frequency of operation for base station antenna is usually in the sub-6 GHz band for 4G and 5G systems, the electrical length of the reflector is typically small ($\leq 10\lambda$) in order to meet the physical size constraint.

This chapter presents investigation of the cross-polar performance in the offset reflector pattern when the reflector size is $\leq 10\lambda$. It is challenging to design matched feed for small reflectors maintaining proper reflector illumination and avoiding large spillover. Two matched feeds are analyzed for smaller reflectors operating at the 5G sub-6GHz band of 3.5 GHz. The first matched feed design has an annular ring patch at the lower layer for TM_{21} mode generation. In the second matched feed design, a rectangular patch is used to generate the fundamental mode (TM_{10} mode) while the higher order mode is generated by a CMPA.

5.2 Design and Analysis of First Matched Feed

In the dual-mode CMPA matched feeds reported in chapter 3, the asymmetric field component at the feed aperture is contributed by the generation of TM_{21} mode using conventional CMPAs. However, it is reported in [82, 83], that fields similar to the TM_{21} mode can also be generated by annular ring (AR) antennas with different combinations of inner and outer radius. In a stacked patch configuration it is found that, the AR patch at the lower layer induces a coupled field on the upper layer which is different from the one induced in the stacked patches proposed in the previous chapters. The nature of the coupled field is mainly a dependant of the inner radius of the AR patch and is found to have a notable influence on the overall cross-polar performance, which is studied in detail in the subsequent subsections.

5.2.1 Working principle

5.2.1.1 Analytical model

The analytical model of the proposed feed is a combination of the TM_{11} mode in CMPA and the TM_{21} mode in AR patch. This model does not take into account the coupling between the two patches. Further, an infinite ground plane is assumed here. The analytical model of the proposed matched feed is derived from the basic cavity model analysis of CMPA and AR patches, as follows:

The far-field pattern of a CMPA operating in TM_{mn} mode is given by:

$$\begin{bmatrix} E_{\theta mn}(\theta,\phi) \\ E_{\phi mn}(\theta,\phi) \end{bmatrix} = \begin{bmatrix} -j^m \cos 2\phi (J_{m-1}(u_{21}) - J_{m+1}(u_{21})) \\ j^m \cos\theta \sin 2\phi (J_{m-1}(u_{21}) + J_{m+1}(u_{21})) \end{bmatrix} \tag{5.1}$$

where,

$$u_{mn} = k_0 a \sin\theta,$$

a is the radius of CMPA operating in TM_{mn} mode and k_0 is the free-space wave number. Similarly, the far-field pattern of an AR patch operating in TM_{21} mode can be expressed as:

$$\begin{bmatrix} E^{ar}_{\theta 21}(\theta,\phi) \\ E^{ar}_{\phi 21}(\theta,\phi) \end{bmatrix} = \begin{bmatrix} \cos 2\phi L^{ar}_{\theta 21}(\theta,\phi) \\ -\cos\theta \sin 2\phi L^{ar}_{\phi 21}(\theta,\phi) \end{bmatrix} \tag{5.2}$$

where,

$$\begin{bmatrix} L^{ar}_{\theta 21}(\theta,\phi) \\ L^{ar}_{\phi 21}(\theta,\phi) \end{bmatrix} = \begin{bmatrix} b_1 f_{21}(b_1) g'_{21}(b_1) - a_1 f_{21}(a_1) g'_{21}(a_1) \\ b_1 f_{21}(b_1) g_{21}(b_1) - a_1 f_{21}(a_1) g_{21}(a_1) \end{bmatrix}$$

$$f_{mn}(r) = Y'_m(k_{mn}a_1) J_m(k_{mn}r) - J'_m(k_{mn}a_1) Y_m(k_{mn}r),$$
$$g'_{mn}(r) = J_{m-1}(k_0 r \sin\theta) - J_{m+1}(k_0 r \sin\theta),$$
$$g_{mn}(r) = J_{m-1}(k_0 r \sin\theta) + J_{m+1}(k_0 r \sin\theta)$$

and

$$k_{mn} = \frac{2(m)}{a_1 + b_1}.$$

a_1 and b_1 are the inner and outer radius of the AR patch, respectively. J_m and Y_m represent Bessel functions of first and second kind, respectively. Further, the value of k_{mn} depends on the operating frequency of the AR patch as given by

$$f_0 = \frac{ck_{mn}}{2\pi\sqrt{\epsilon_r}} \tag{5.3}$$

where, c is the speed of light in vacuum and ϵ_r is the dielectric constant of the substrate. The analytical model of the proposed matched feed is obtained by combining (5.1) and (5.2), and is expressed as:

$$\begin{bmatrix} E_\theta(\theta,\phi) \\ E_\phi(\theta,\phi) \end{bmatrix} = \begin{bmatrix} E_{\theta 11}(\theta,\phi) \\ E_{\phi 11}(\theta,\phi) \end{bmatrix} + \frac{C_2}{C_1} \begin{bmatrix} E^{ar}_{\theta 21}(\theta,\phi) \\ E^{ar}_{\phi 21}(\theta,\phi) \end{bmatrix} \tag{5.4}$$

Here, the unprimed field components correspond to CMPA. C_2/C_1 is a complex number which represents the excitation ratio between the TM_{11} and TM_{21} mode. An optimum value of C_2/C_1 in the analytical feed model is required to achieve CFM, and cross-polar suppression.

5.2.1.2 HFSS model

In this work, the AR patch considered for the lower layer is investigated for four different values of inner radius (3 mm, 4 mm, 5 mm, 6 mm and 7 mm). When these two radiating patches are arranged in a stacked configuration and designed to operate at 5G sub-6 GHz band of 3.5 GHz, the variation in the inner radius will also effect the dimensions of the upper patch and will be discussed later in the section. A pictorial representation of the proposed stacked matched feed geometry is shown in Fig. 5.1. A TM_{11} mode generating circular disk of radius a is placed at the top layer, while the lower layer consists of an AR patch with an appropriate inner radius (a_1) and outer radius (b_1). Both the radiating patches are designed on FR4 substrate ($\epsilon_r = 4.4$) with 1.6 mm substrate thickness. Both the upper and the lower patch are fed by individual 50Ω coaxial feed at 4 mm and 12 mm from the center, respectively. The feed position of both the patches is chosen such that the return loss obtained

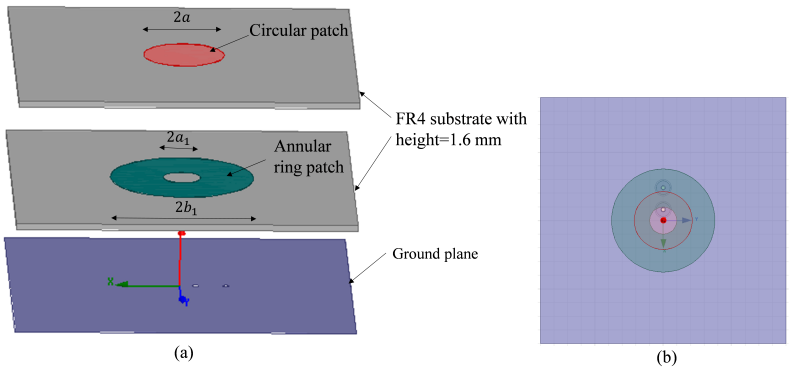

Figure 5.1: Geometry of the proposed feed design (a) side view along X-axis and (b) top view.

Table 5.1: Different stacked patch dimensions with varying a_1 resonating at 3.5 GHz

a_1 in mm	b_1 in mm	a in mm
3	19	11.2
4	19	10.9
5	18.9	10.6
6	18.8	10.2
7	18.7	10.2

at both the ports is better than 15 dB. The variation in dimensions (a and b_1) of the proposed stacked patch at the operating frequency of 3.5 GHz for a variation in a_1 is obtained through a parametric study and is shown in Table 5.1. The transverse H-fields in the AR patch for all the combinations listed in Table 5.1 for an excitation in port 2 only is shown in Fig. 5.2.

The strength and nature of the TM_{21} mode field distribution is similar for all variations of a_1. Thus, ideally the cross-polar performance obtained in the reflector pattern for all the variations of a_1 at optimum matching is expected to remain same.

5.2.2 Reflector pattern analysis

The geometry of the ORA system is same as in Fig. 1.1 and is shown in Fig 5.3 for ready reference. The ORA has a diameter of the projected aperture (D) equal to be 0.85 m (roughly 10λ) and the reflector positioned at an offset height (H) of 0.085 m. The offset reflector is illuminated by the matched feed placed at the focus of the parent paraboloid. The focal length to diameter (F/D) of the ORA is considered to be 0.6 for performance evaluation of the matched feed.

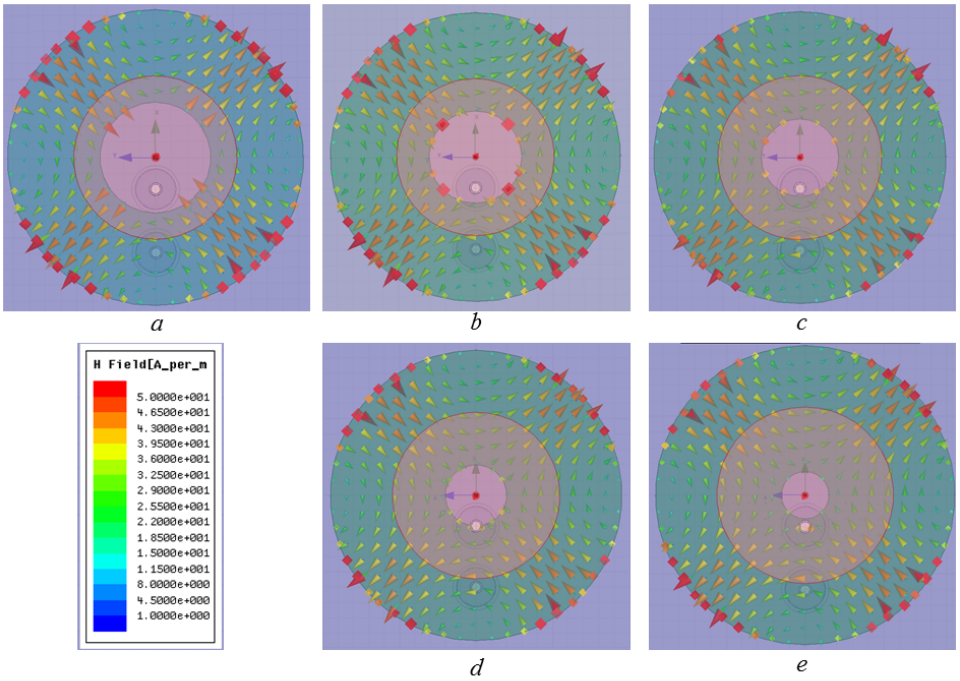

Figure 5.2: Nature of field distribution in AR for different values of a_1 given by (a) 3 mm (b) 4 mm (c) 5 mm (d) 6 mm and (e) 7 mm.

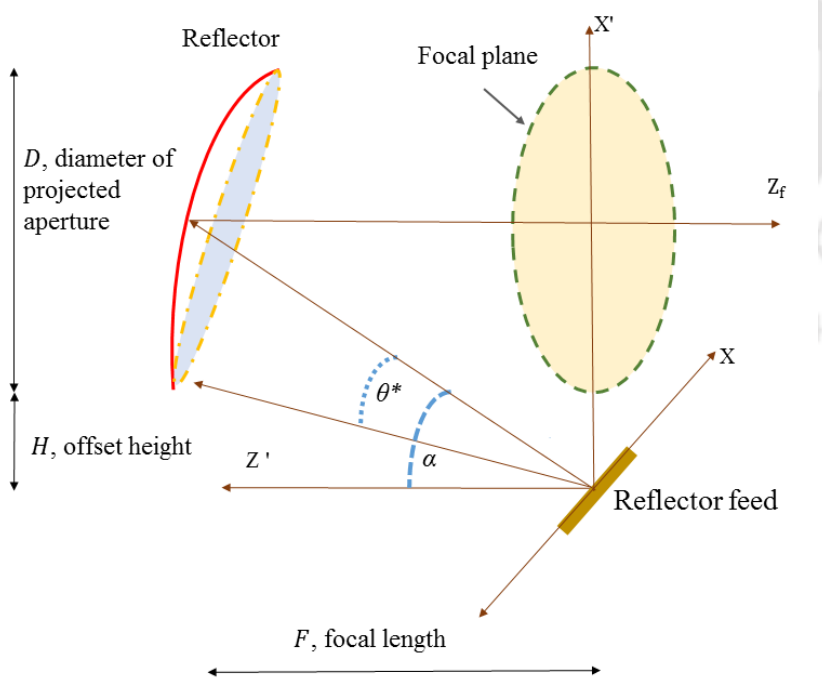

Figure 5.3: Offset reflector antenna configuration.

5.2.2.1 Using GO technique

Reflector pattern of the ORA specified earlier is obtained from the analytical feed model given by (5.4) using geometrical optics (GO) technique. The value of C_2/C_1 is crucial for achieving CFM. An

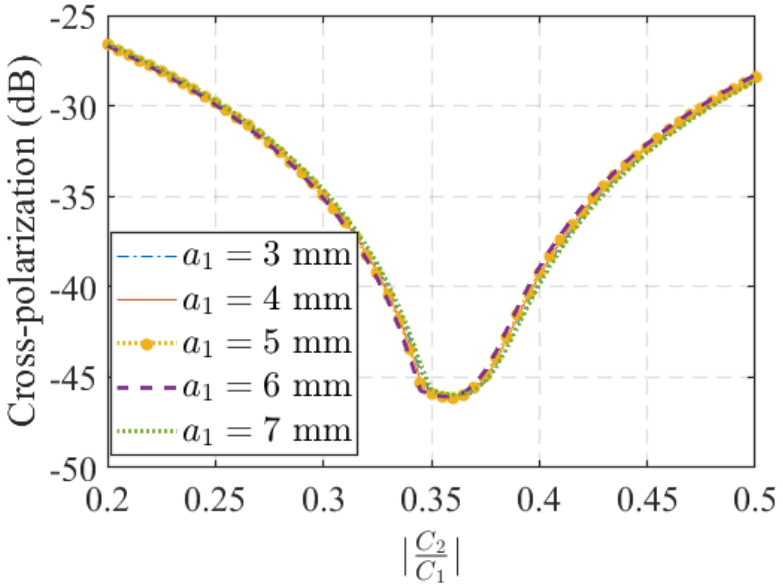

Figure 5.4: Optimum excitation ratio (magnitude) for different a_1

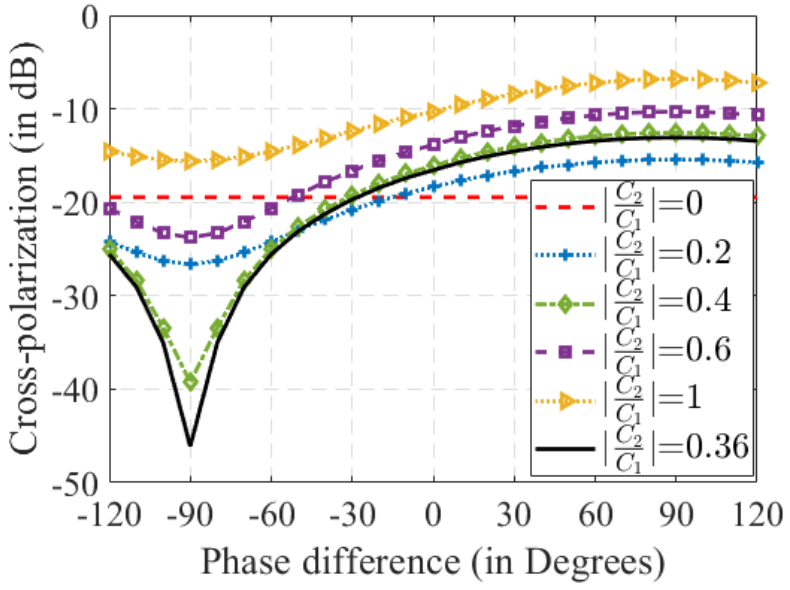

Figure 5.5: Variation in reflector cross-polarization for different excitation ratios for $a_1 = 5$ mm

investigation on the effect of C_2/C_1 on the reflector cross-polar levels for different combinations of a,

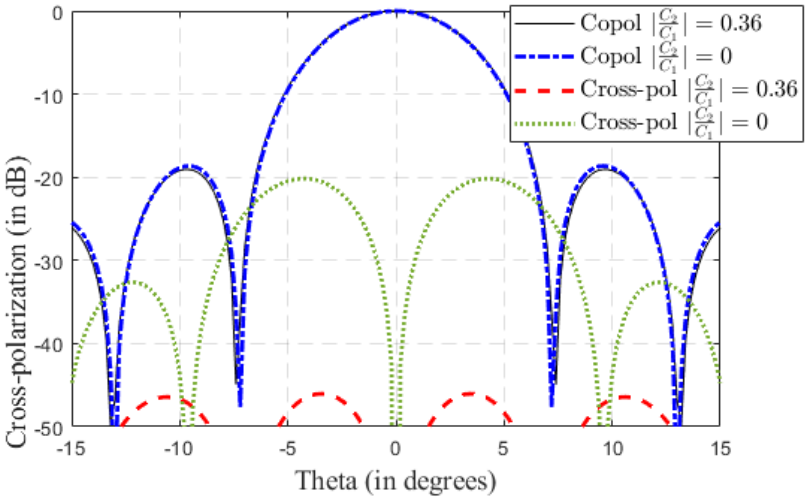

Figure 5.6: Simulated reflector pattern obtained using the analytical feed model (for $a_1 = 5$ mm)

a_1 and b_1 of the proposed matched feed is performed. The optimum values of C_2/C_1 for the proposed feed structure with different combinations of a_1, b_1 and a listed in Table 5.1 is shown in Fig. 5.4 a. The cross-polar performance in the reflector pattern is found to optimum when $|C_2/C_1| = 0.36$ and the phase difference between the two modes is $-90°$ as shown in Fig. 5.5. The nature of variation in cross-polarization is also found to be similar for all a_1 variations. Thus, in the analytical modelling, variation in the a_1 of the AR patch have very limited effect on cross-polarization in the reflector pattern.

A cross-polar suppression of more than 25 dB is observed in the ORA pattern shown in Fig. 5.6, when optimum matching is obtained. It is worth noting that the coupling between the patches is not considered in the analytical feed model. The effect of the coupled field between the patches on the reflector cross-polarization is later studied by using the HFSS feed model.

5.2.2.2 Using HFSS-PO

The reflector pattern of the ORA with the proposed matched feed is also obtained using HFSS-PO. A parametric study is performed to obtain the appropriate port excitation ratio required for CFM in case of all five a_1 combinations.

As shown in Fig. 5.7, the overall cross-polarization is better than -37 dB at the optimized excitation ratio for the proposed feed with 3 mm $\leq a_1 \leq$ 6 mm. Table 5.2 shows the best cross-polarization in the reflector pattern of the ORA illuminated by the proposed stacked feed with different dimensions

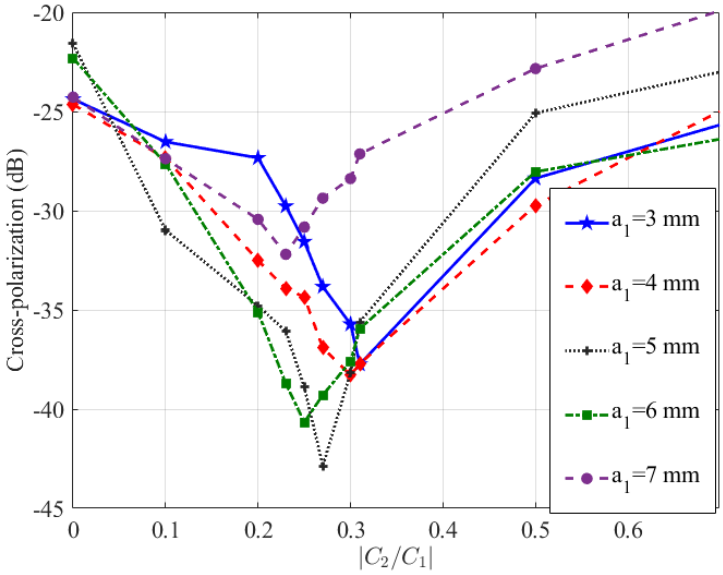

Figure 5.7: Reflector cross-polar performance with variation in excitation ratio for different feed dimensions.

Table 5.2: Cross-polarization in the reflector pattern at 3.5 GHz for different values of a_1

a_1 (mm)	Crosspol (dB)	Optimum excitation ratio, $\frac{C_2}{C_1}$
3	-37.76	0.31
4	-38.29	0.30
5	-42.86	0.27
6	-40.32	0.25
7	-32.20	0.23

of upper and lower patch obtained in Table 5.1. For $a_1 > 6$ mm, the cross-polar performance degrades in the reflector pattern. A gradual decrease in the required excitation ratio (magnitude) between the two ports for an increase in a_1 is also observed. Improved cross-polar performance for certain matched feed dimension can be attributed to the variation in the a_1. Since, both the CMPA and AR patches are co-located, an increase in a_1 changes the nature and strength of coupled fields on the CMPA placed at the top. Thus, variation in a_1 is also effecting the reflector cross-polarization. In order to understand this behaviour, an investigation is performed over the nature and strength of the coupled fields generated on the upper circular patch from the lower AR patch.

Fig. 5.8 shows the nature and strength of the coupled fields for different values of a_1. It may be noted that the coupled fields are observed by excitation of port 2 only. An increase in the coupled field strength is observed as the inner radius (a_1) is increased. Further, the nature of this coupled field distribution changes for $a_1 \geq 4$ mm. In the proposed matched feed with $a_1 = 5$ mm, three types

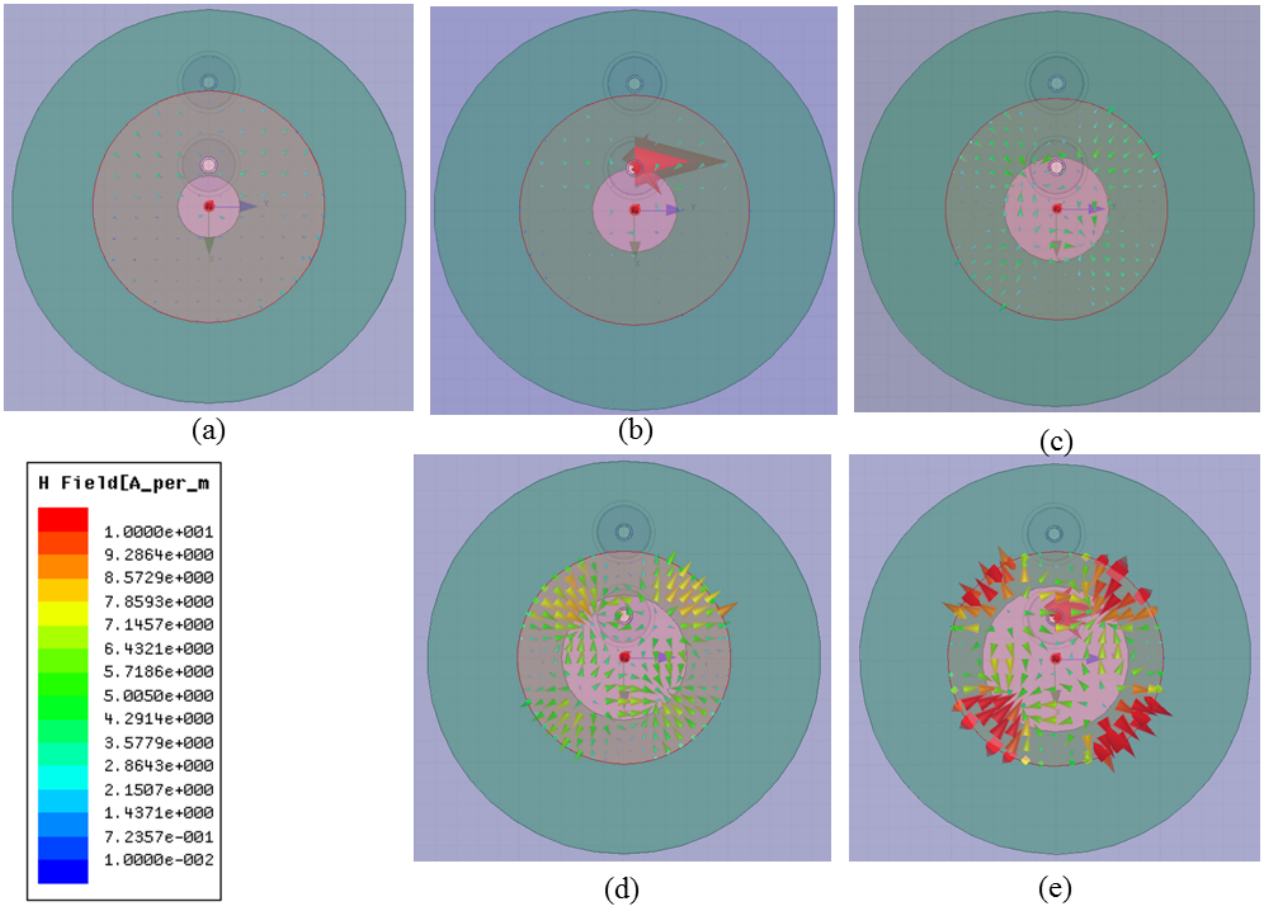

Figure 5.8: Aperture H-fields generated at the upper circular patch due to the AR with inner radius given by(a) $a_1 = 3$ mm (b) $a_1 = 4$ mm (c) $a_1 = 5$ mm (d) $a_1 = 6$ mm and (e) $a_1 = 7$ mm.

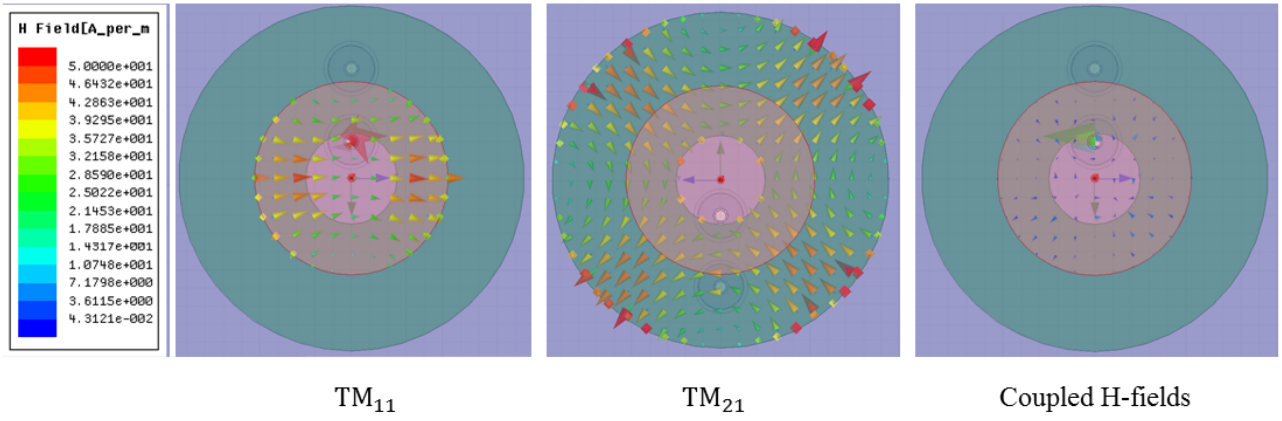

Figure 5.9: Nature of transverse H-field distribution in the proposed matched feed for $a_1 = 5$ mm.

of field distributions as shown in Fig. 5.9 are generated by the two 50 Ω ports. Further, the best cross-polar suppression is achieved when $a_1 = 5$ mm and the excitation ratio between the two ports is $0.27\angle -90°$. The excitation ratio of both TM_{21} mode and the coupled field with respect to the TM_{11}

mode in the proposed matched feed is optimum in this case.

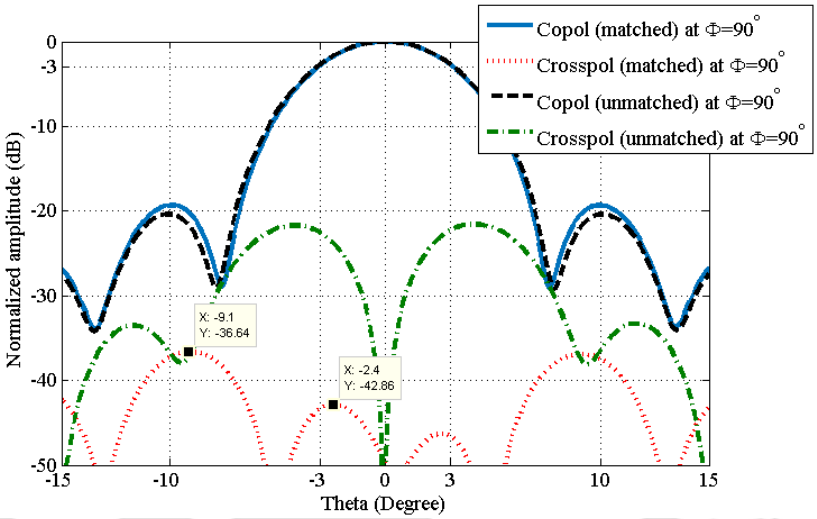

Figure 5.10: Normalized offset reflector pattern at $\Phi = 90°$ obtained using HFSS-PO.

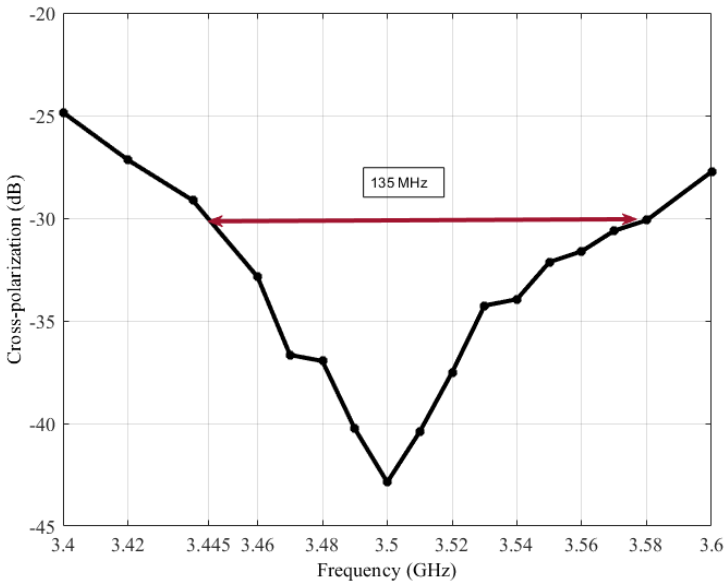

Figure 5.11: -30 dB cross-polar bandwidth of the ORA illuminated by the proposed matched feed.

Normalised reflector pattern of the ORA when illuminated by the proposed stacked feed with $a_1 = 5$ mm at optimum port excitation ratio is given in Fig. 5.10. Co-pol and cross-pol patterns for both $C_2/C_1 = 0$ and $C_2/C_1 = 0.27$ are shown. Further, for $C_2/C_1 = 0.27$, the cross-polarization within the 3-dB beamwidth is better than -42 dB at the asymmetric plane of the reflector. Hence, a cross-polar suppression of more than 20 dB is achieved by the matched feed proposed with the optimized

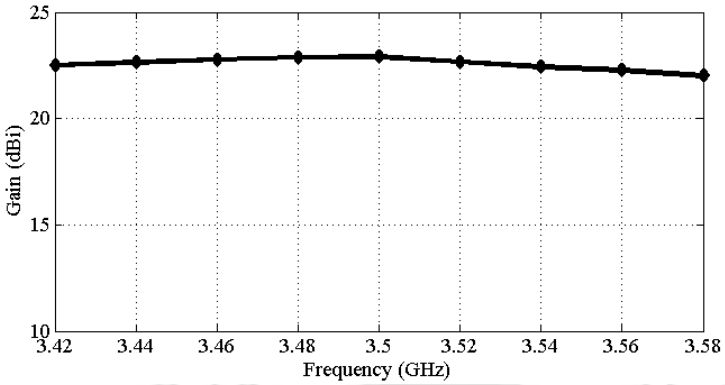

Figure 5.12: Gain v/s frequency plot.

Table 5.3: Performance of ORA fed by the proposed feed

Offset reflector parameters	[Proposed matched feed]
F/D	0.6
Crosspol ($\Phi = 90°$) (dB)	-42.86
First SLL (dB)	-18.75
-30 dB Xpol B.W (%)	3.857%
Gain (dBi)	22.91

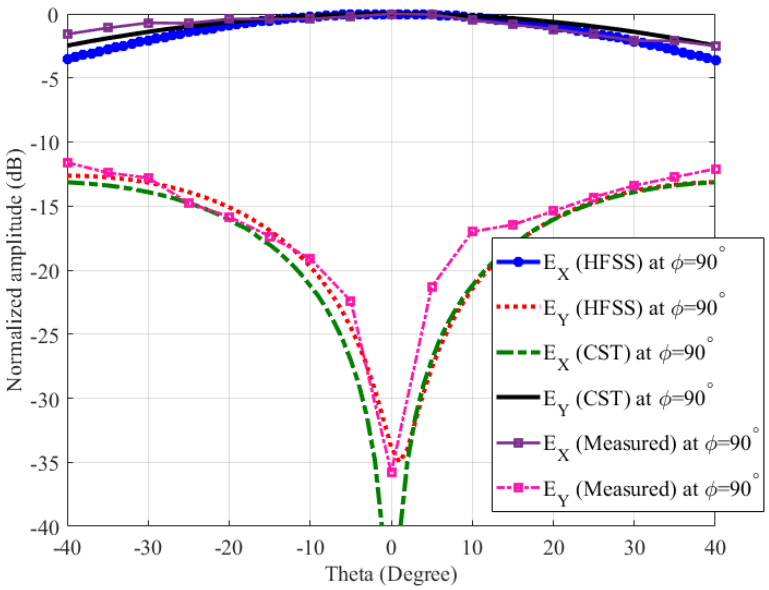

Figure 5.13: Radiation pattern of the proposed feed with the optimized excitation ratio and $a_1 = 5$ mm.

dimension at the reflector pattern when compared with the cross-pol performance of an unmatched feed (feed with TM_{11} mode only). The primary pattern of the matched feed with $a_1 = 5$mm and $C_2/C_1 = 0.27$ is shown in Fig. 5.13.

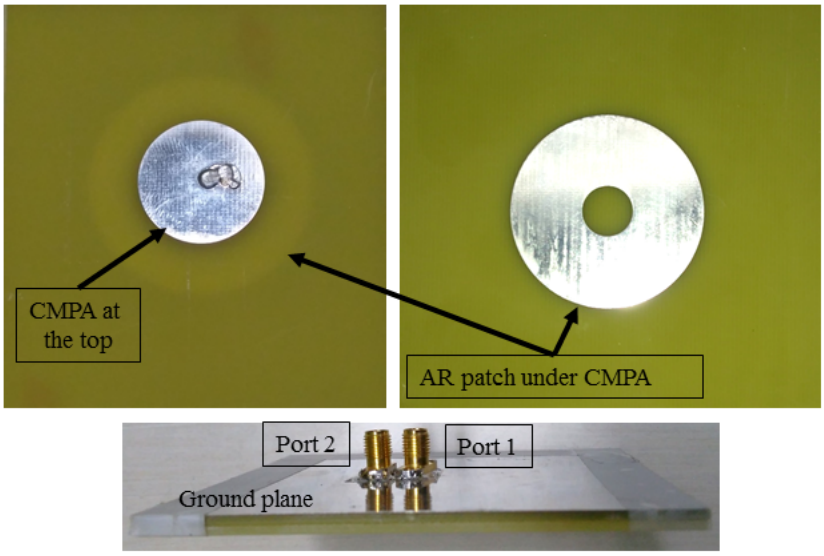

Figure 5.14: Fabricated prototype of the proposed feed.

The -30 dB cross-polar bandwidth of the ORA fed by our proposed matched feed is given in Fig. 5.11 and is 135 MHz. Gain of the reflector shown in Fig. 5.12 is found to be better than 22 dBi over the entire -30 dB cross-polar bandwidth. Performance of the ORA illuminated by this matched feed is summarized in Table 5.3. The normalized radiation pattern of the matched feed with $a_1 = 5$ mm, is obtained using two commercially available CAD tools, HFSS and CST and is shown in Fig. 5.13. Radiation pattern of the matched feed for -50° $\leq \theta \leq$ 50° is considered as the illumination angle of the reflector is $\theta^{\star} \leq 76°$. Both simulation results show good agreement with each other.

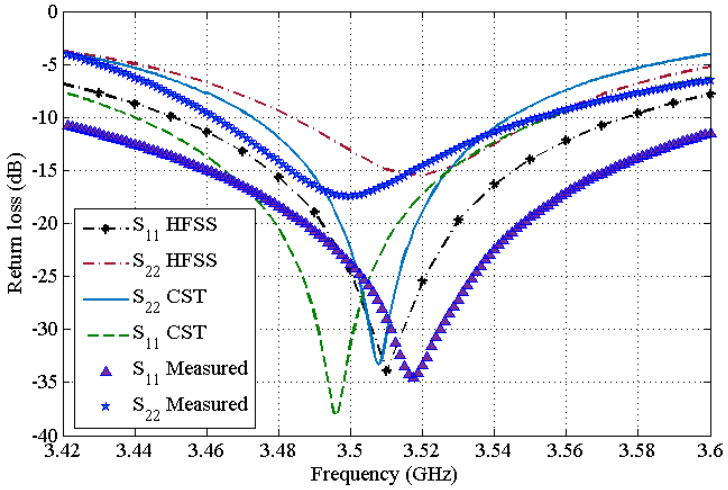

Figure 5.15: Comparison of the measured return losses of the proposed feed with the simulated results obtained in both HFSS and CST.

5.2.3 Experimental Validation

A prototype of the matched feed is fabricated on a FR4 substrate as shown in Fig. 5.14 and experimental validation of the same has been performed.

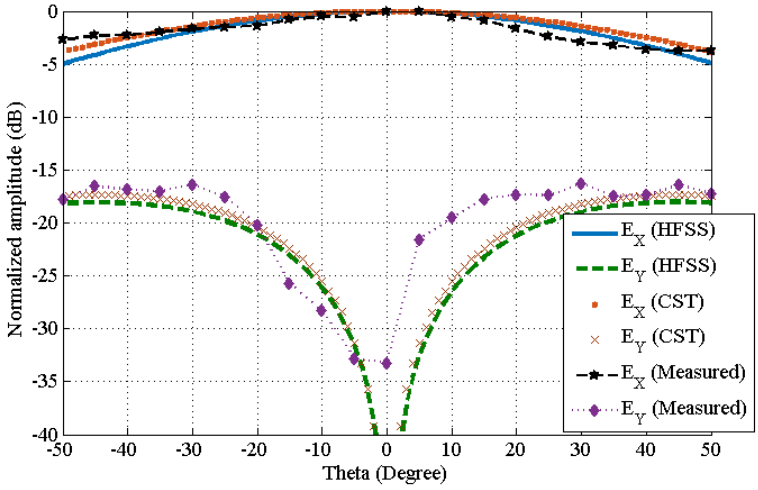

Figure 5.16: Feed pattern of the proposed structure when only port 1 is excited.

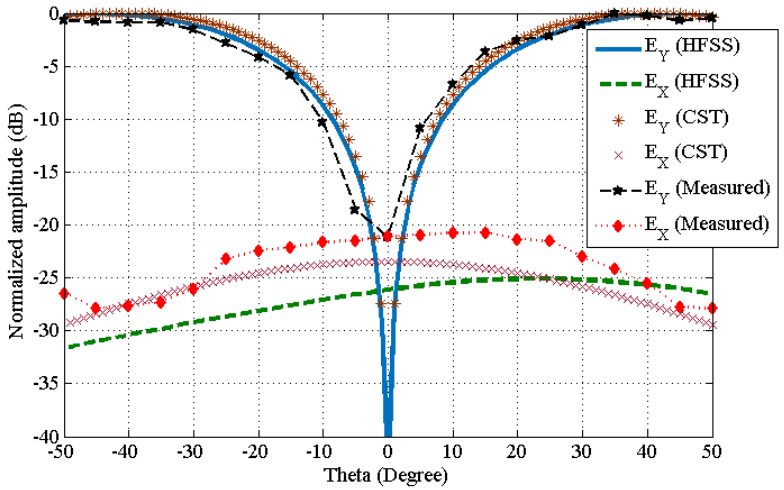

Figure 5.17: Feed pattern of the proposed structure when only port 2 is excited.

Fig. 5.15 shows the return losses at both the ports of the proposed feed. The measured return losses at both the ports have good agreement with both the simulation results. The feed pattern of the proposed structure when only port 1 is excited is shown in Fig. 5.16. It may be noted that the proposed matched feed shows behaviour similar to a CMPA operating in TM_{11} mode. The measured and the simulation results are in good agreement. Fig. 5.17 shows the feed pattern when port 2 is

excited. In this case, the feed pattern is similar to a CMPA operating in TM_{21} mode. Closeness of the measured results of the feed patterns with simulation results (using HFSS and CST) suggests that the proposed feed would be able to achieve the CFM for reflector patterns when the ports are excited at the desired ratio.

5.3 Design and Analysis of Second Matched Feed

A dual-mode matched feed using the dominant mode of a RMPA and a higher order mode of a CMPA at an appropriate excitation ratio is investigated in this section. The broadside pattern and the conical patterns are generated in the proposed feed using two different geometry, RMPA for broadside pattern and the circular microstrip patch antenna (CMPA) for conical pattern. The matched feed is used to illuminate an ORA as depicted in Fig. 5.3 with $D = 10\lambda$ at the operating frequency of 3.5 GHz (5G mid-band) for 5G base stations. The cross-polar performance of the ORA fed by the proposed matched is investigated for $F/D = 0.4, 0.6$ and 0.8.

5.3.1 Working principle

Matched feeds are designed to suppress the cross-polarization in the asymmetric plane by adding suitable higher order modes at an appropriate excitation ratio. When an ORA is illuminated with only dominant mode operating RMPA, high cross-polarization is obtained at the asymmetric plane of the reflector pattern. To suppress this cross-polarization, the proposed structure in this section, generates two modes (dominant mode of RMPA and the TM_{21} mode of CMPA) at an appropriate ratio. The TM_{21} mode in the CMPA is excited at an orthogonal phase relation with the dominant mode in RMPA patch. Assuming an infinite ground plane, the field pattern for the proposed feed can be expressed using basic cavity model as;

$$\begin{bmatrix} E_\theta(\theta,\phi) \\ E_\phi(\theta,\phi) \end{bmatrix} = \begin{bmatrix} E_{\theta 10}(\theta,\phi) \\ E_{\phi 10}(\theta,\phi) \end{bmatrix} + (-j)\frac{C_{21}}{C_{10}} \begin{bmatrix} E'_{\theta 21}(\theta,\phi) \\ E'_{\phi 21}(\theta,\phi) \end{bmatrix} \tag{5.5}$$

where,

$$\begin{bmatrix} E_{\theta 10}(\theta,\phi) \\ E_{\phi 10}(\theta,\phi) \end{bmatrix} = \begin{bmatrix} -j\cos\phi(\frac{\sin w}{w}\cos v) \\ j\cos\theta\sin\phi(\frac{\sin w}{w}\cos v) \end{bmatrix},$$

$$w = \frac{Wk_0}{2}\sin\theta\sin\phi,$$

$$v = \frac{L_{eff}k_0}{2}\sin\theta\cos\phi,$$

$$\begin{bmatrix} E'_{\theta 21}(\theta,\phi) \\ E'_{\phi 21}(\theta,\phi) \end{bmatrix} = \begin{bmatrix} \cos 2\phi(J_1(u_{21}) - J_3(u_{21})) \\ -\cos\theta\sin 2\phi(J_1(u_{21}) + J_3(u_{21})) \end{bmatrix},$$

and

$$u_{mn} = k_0 a_{mn}\sin\theta.$$

Here, the primed and unprimed field components corresponds to CMPA and RMPA, respectively. It may be noted that the analytical model discussed in this section assumes zero coupling between the two patch layers. The analytical expression obtained is then used to calculate the reflector pattern of the ORA using geometrical optics (GO) method using a code developed in MATLAB in chapter 2. While, the analytical model of the proposed feed clearly depicts its working, the CAD model designs of the feed obtained in HFSS is further used to obtain the coupling between the two ports and the aperture field distribution of the feed. The proposed matched feed structure is designed in HFSS as shown in Fig. 5.18. It is a two layer structure with both the patch layers being excited by two individual 50Ω wave ports. The substrate material selected for both the dielectric layers is FR4 (dielectric constant of 4.4 and dielectric height of 1.6 mm). The length (L) and width (W) of the rectangular patch at the top layer is 19.5 mm and 23.5 mm, respectively. The radius of the TM_{21} mode generating lower CMPA is 19.1 mm. The aperture field distribution of the structure obtained in HFSS is shown in Fig. 5.19. It can be observed that the aperture field distribution is similar to the

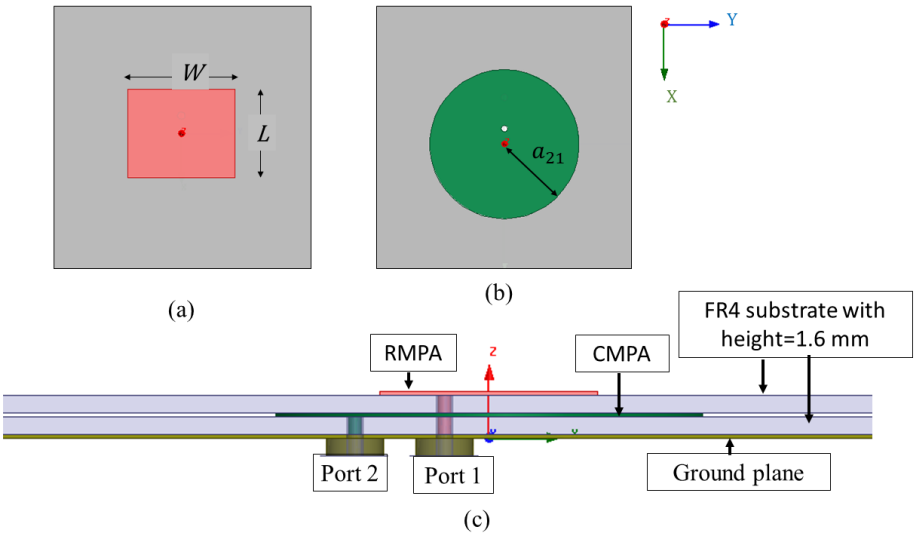

Figure 5.18: Proposed matched feed in HFSS.

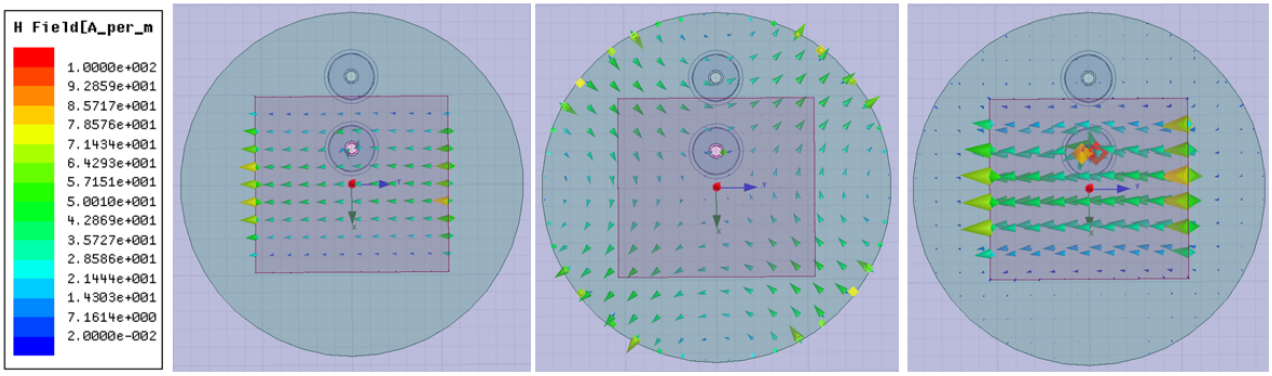

Figure 5.19: Aperture field distribution of the proposed feed when (a) only port 1 is excited, (b) only port 2 is excited and (c) both the ports are excited.

dominant mode of RMPA when port 1 is excited. Similarly, TM_{21} mode of CMPA is obtained when port 2 is excited. While, in case of simultaneous excitation of both the ports at an appropriate ratio, will result in the aperture field depicted in Fig. 5.19(c), which will be discussed in further details in the next section.

5.3.2 Simulation results and discussions

The $\frac{C_{21}}{C_{11}}$ value plays a crucial role in the design of a matched feed. At an optimum value of the $\frac{C_{21}}{C_{11}}$, the aperture field distribution of the proposed structure will provide an optimal field matching required to achieve minimum cross-polarization and is obtained through a parametric study. The optimum value

Table 5.4: Cross-polarization at $\Phi = 90°$ in the reflector pattern when the F/D of the ORA is varied

$\frac{F}{D}$	$\frac{C_{21}}{C_{10}}$ HFSS	Cross-pol (HFSS-PO) Unmatched	Cross-pol (HFSS-PO) Matched	$\frac{C_{21}}{C_{10}}$ analytical	Cross-pol (MATLAB-GO) Umatched	Cross-pol (MATLAB-GO) Matched
0.4	0.4	-17 dB	-34.1 dB	0.55	-18 dB	-37.14 dB
0.6	0.3	-21 dB	-40.28 dB	0.45	-21.7 dB	-42.67 dB
0.8	0.2	-24 dB	-42.05 dB	0.3	-24.86 dB	-45.71 dB

of $\frac{C_{21}}{C_{11}}$ obtained using this parametric study for three different values of F/D is tabulated in Table 5.4. It may be noted that as the F/D increases, the value of $\frac{C_{21}}{C_{11}}$ also decreases. Moreover, the cross-polar performance of the ORA with the matched feed also improves for higher values of F/D. To account for the amount of cross-polar suppression obtained by the proposed matched feed, a comparison of the cross-polar levels obtained in the reflector pattern of an ORA with $F/D = 0.6$ at the asymmetric plane is shown with matched and unmatched feed, in Fig. 5.20 and Fig. 5.21.

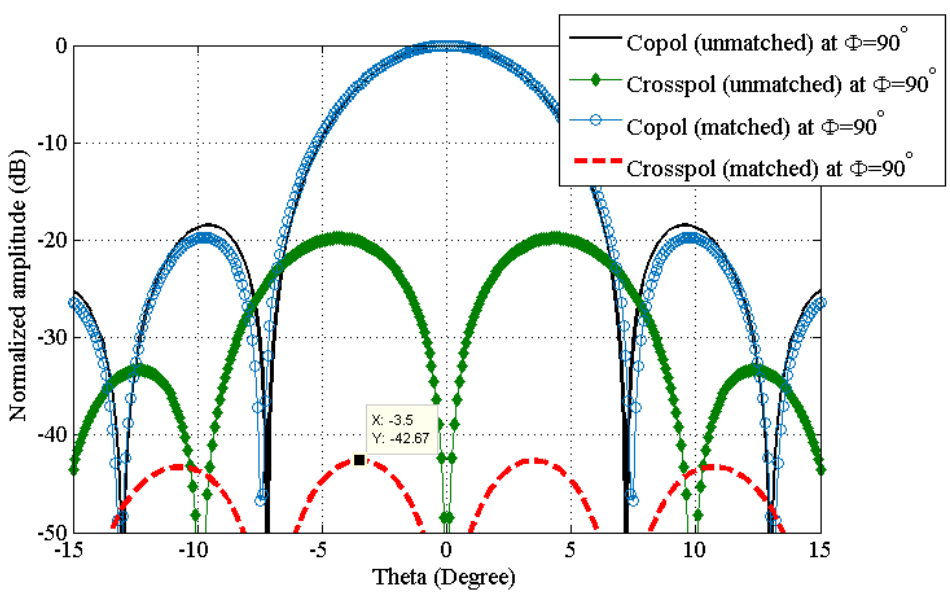

Figure 5.20: Reflector pattern at the asymmetric plane ($\Phi = 90°$) obtained for an ORA with $\frac{F}{D} = 0.6$ using GO MATLAB code

The copolar pattern obtained using both the GO code and the HFSS-PO show similar trends. While, the unmatched cross-polar levels using both the techniques is almost the same, the matched cross-polar levels within the main beamwidth differ slightly. This difference may be due to the fact that the analytical equations of the proposed model used for GO code does not consider the mutual coupling between the two patch layers which is taken into account in HFSS-PO. The feed pattern of

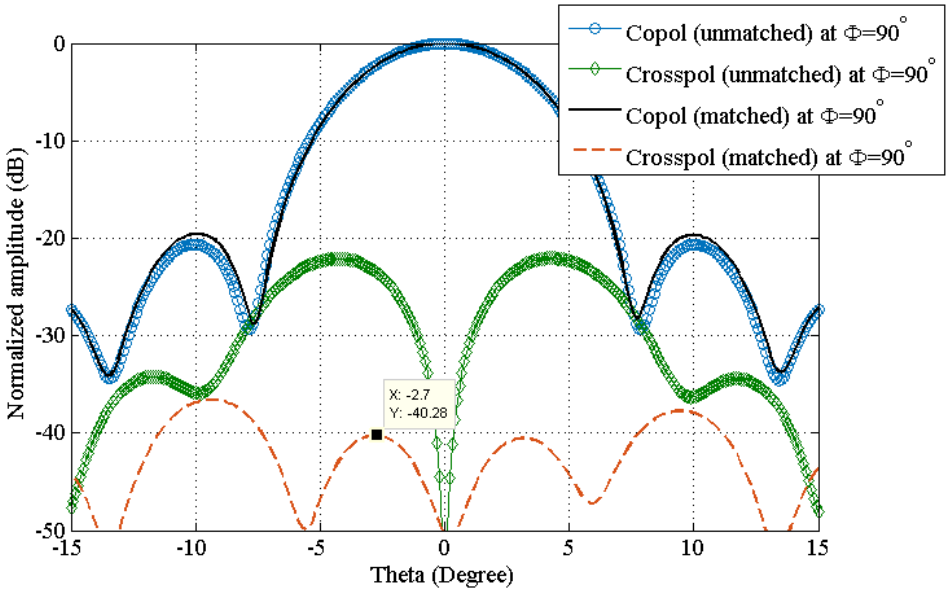

Figure 5.21: Reflector pattern at the asymmetric plane ($\Phi = 90°$) obtained for an ORA with $\frac{F}{D} = 0.6$ using HFSS-PO

the proposed structure with the optimized value of $\frac{C_{21}}{C_{11}}$ using both HFSS and CST is shown in Fig. 5.22. The feed pattern has higher cross-polarization in comparison to an unmatched feed (TM_{10} mode of RMPA). This higher cross-polarization in the matched feed is due to the TM_{21} mode generated in the CMPA and has led to the cross-polar suppression of more than 19 dB as depicted in Fig. 5.20 and Fig. 5.21.

Table 5.5: Performance of ORA fed by the proposed feed

Offset reflector parameters	[Proposed matched feed]
Frequency (GHz)	3.5
Reflector Size	10λ
Crosspol (dB)	-40.28
First SLL (dB)	-19.61
-30 dB Xpol B.W	2.28%
Gain (dBi)	22.83

5.3.3 Experimental validation

A prototype of the proposed dual-mode matched feed structure is fabricated and is shown in Fig. 5.23. As discussed earlier, the prototype is a stacked dual layer microstrip patch antenna with two ports at 4 mm and 12 mm from the centre of the prototype. The prototype has a finite ground plane of dimension 90 mm × 90 mm. The measured return losses obtained at both the ports are shown in

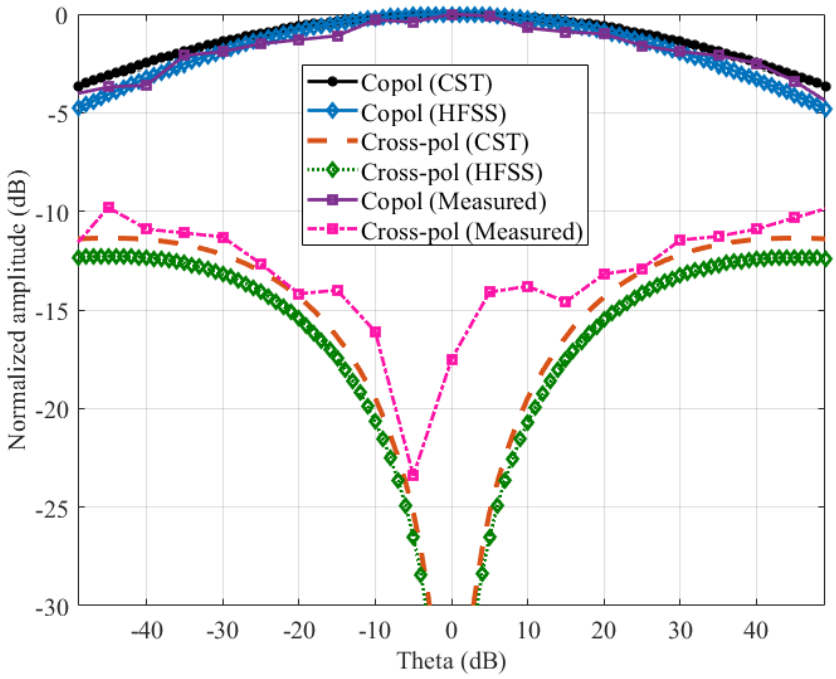

Figure 5.22: Feed pattern of the proposed dual-mode matched feed with optimized excitation ratio between the two modes (TM_{10} mode and TM_{21} mode).

Fig. 5.24, and are in good agreement with the results obtained from HFSS and CST. The radiation pattern of the prototype for two cases are measured for an X-polarized wave at $\phi = 90°$. In case 1, port 1 is excited and port 2 is terminated with a 50 Ω matched load. Similarly, in case 2, port 2 is excited and port 1 is terminated with a 50 Ω matched load. The radiation pattern measured in both the cases as shown in Fig. 5.25 and Fig. 5.26 are in good agreement with the simulation results.

The small deviation observed between the measured and the simulation results may be due to some minute fabrication errors in terms of dimensions. Further, presence of a small air gap while stacking the patches may have resulted in the slightly improved return losses in case of measured results.

5.4 Conclusion

Two matched feeds for an offset reflector with small size is presented in this chapter. The first matched feed is a stacked microstrip antenna consisting of a TM_{11} mode operating CMPA on the top and a TM_{21} generating lower AR patch. The optimum excitation ratio between the two ports is obtained using a parametric study. The effect of the inner radius of the AR patch on the overall cross-polar performance of the reflector is studied. The nature and strength of the asymmetric coupled

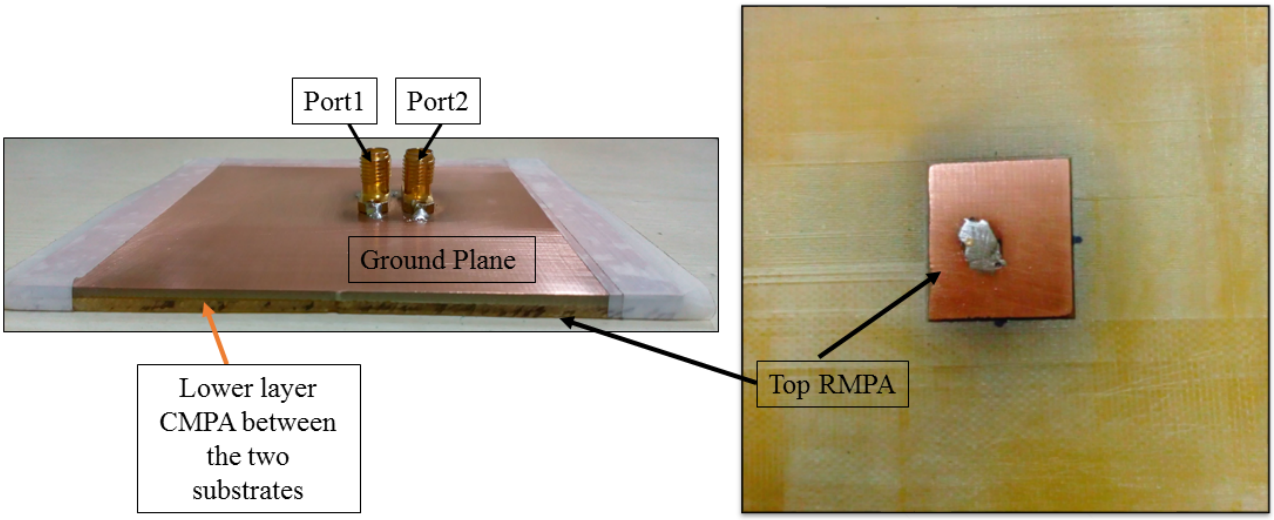

Figure 5.23: An image of the matched feed prototype fabricated on FR4.

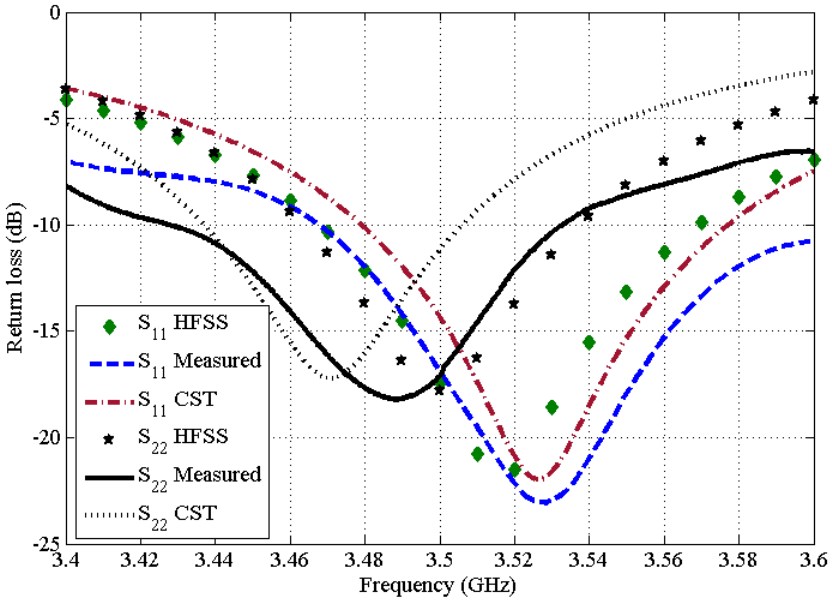

Figure 5.24: Return loss of the proposed matched obtained using HFSS, CST and measurement.

field generated on the CMPA at the top varies due to variation in the inner radius of AR patch. This asymmetric coupled field also aids in the cross-polar suppression in the reflector pattern. The cross-polar performance of the ORA illuminated by the proposed matched feed is found to be better than -42 dB at the asymmetric plane.

The second matched feed is a dual-mode stacked microstrip antenna consisting of a bottom layer TM_{21} mode generating CMPA and a dominant mode RMPA at the top has shown good performance as

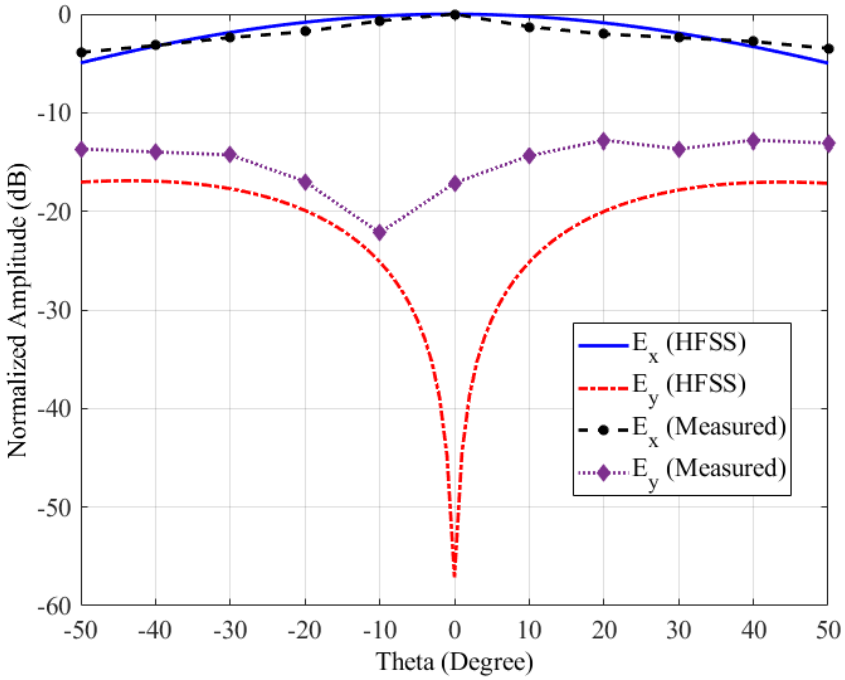

Figure 5.25: Feed pattern when only port 1 is excited and port 2 is terminated by a 50 Ω matched load.

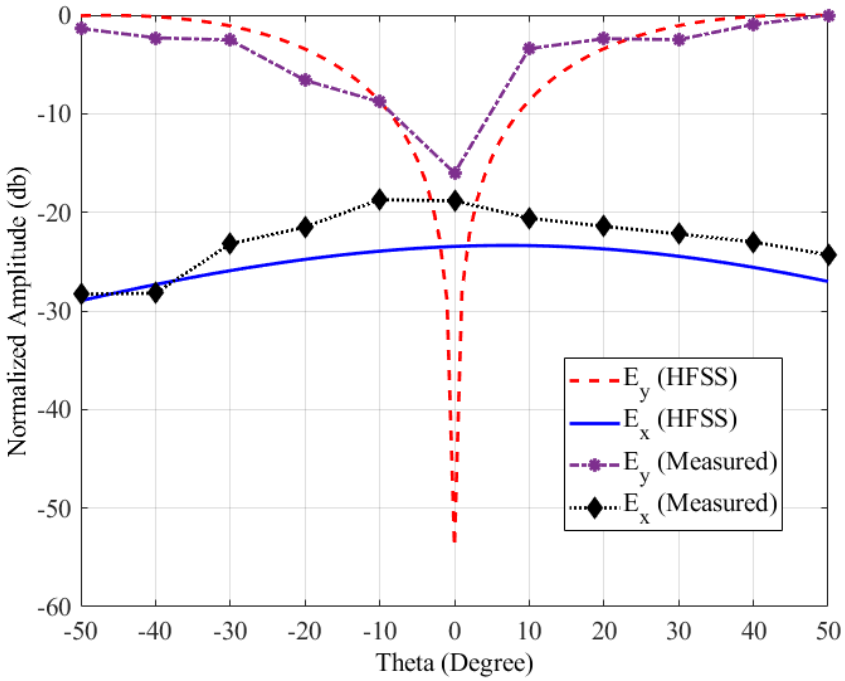

Figure 5.26: Feed pattern when only port 2 is excited and port 1 is terminated by a 50 Ω matched load.

a matched feed. Cross-polar performance in the reflector pattern for the matched feed is obtained for different values of F/D. A cross-polar performance is improved by almost 20 dB when the proposed matched feed is used to illuminate an ORA, instead of a single dominant mode operating RMPA. The ORA with the two novel matched feeds presented in this chapter has potential application as a backhaul antenna for 5G sub-6 GHz band.

6

Summary of Thesis and Future Study

Contents

6.1 Summary of Work 100
6.2 Future Scope of Investigation 101

In this thesis, matched feeds for offset reflector antennas using microstrip antenna elements and arrays are investigated. A summary of the contributions of the thesis is given in section 6.1 and an overview of the possible future scope of investigation is provided in section 6.2.

6.1 Summary of Work

The contributions of this thesis can be summarized as:

6.1.1 Dual-mode CMPA as matched feed

A dual-mode CMPA is proposed as matched feed for the offset reflector. TM_{11} and TM_{21} modes are generated at an appropriate ratio using a dual-layer stacked CMPA. An analytical model of the proposed feed is derived using the basic cavity model. The proposed matched feed has been investigated using the analytical model and two commercial CAD simulators, namely HFSS and CST. The cross-polar performance of the feed in the reflector pattern is analyzed using a GO code and HFSS-PO. The proposed matched feed has achieved cross-polarization better than -32 dB in the reflector pattern.

6.1.2 Single layer CCA matched feed

A single layer CCA matched feed is proposed and investigated as matched feed for offset reflector antenna. The CCA matched feed is analyzed using the mathematical model as well as CAD simulators. The single layer CCA matched feed also works on the same principle of conjugate field matching and provides a cross-polarization better than -34 dB in the reflector pattern. The overall gain of the reflector is also improved by this proposed matched feed.

6.1.3 Dual layer CCA matched feed

A dual layer CCA matched which works on a technique similar to the previous matched feeds is proposed.

6.1.3.1 Beam shifting and beam size control

The dual layer CCA matched feed is also investigated for beamwidth and beam size control in the reflector pattern.

6.1.3.2 Dual band application

A dual band feed using the same dual layer CCA arrangement is also proposed. In the dual band feed, the central dual-mode CMPA and the surrounding ring elements work on two different frequency bands. The dual band feed is designed to provide cross-polarization performance better than -32 dB in the reflector pattern for an offset reflector with $F/D = 0.8$

6.1.4 Matched feeds using annular ring patches

Annular ring is used to generate the required TM_{21} mode in a dual layer matched feed. For an optimum inner and outer radius of the annular ring, a coupled field similar to TE_{21} mode is generated which further aids the cross-polar suppression in the reflector pattern. This matched feed is analyzed for a smaller offset reflector with diameter of 10λ. The cross-polarization within the main beam of the reflector is better than -42 dB.

6.1.5 Matched feed using RMPA for dominant mode and CMPA for TM_{21} mode

A matched feed using RMPA for dominant mode and CMPA for TM_{21} mode is proposed for an offset reflector with diameter 10λ. The proposed matched feed is investigated for different F/D using both the GO code and the HFSS-PO. The cross-polar performance of the matched feed is better than -40 dB. The offset reflector system is designed at the sub-6 GHz frequency band.

6.2 Future Scope of Investigation

Some of future scope of investigation on matched feeds using microstrip antenna elements and arrays are given as:

6.2.1 Circularly polarized matched feeds

The matched feeds designed and investigated in this thesis are linearly polarized feeds. However, some of the emergent applications require the reflector feed to be circularly polarized. It may be noted that for a circularly polarized feed, beam squint occurs in the reflector pattern. This beam squint can be rectified by using circularly polarized matched feed. Thus, investigation of such circularly polarized matched feed can be an attractive option for future studies based on microstrip matched feeds.

6.2.2 Multibeam offset reflectors

The matched feeds designed in this thesis mostly produce single beam in the reflector pattern. Although, chapter 5 discusses the beam shifting and beam size control in the reflector pattern by using dual-layer CCA matched feeds, use of such matched feeds for multibeam application presents an exciting prospect for future studies.

6.2.3 Investigation of other higher order modes for conjugate field matching

The higher order asymmetric mode used for conjugate matching in the entire thesis is primarily TM_{21} mode. From the literature review discussed in chapter 1, it is observed that certain other asymmetric field configurations can also be used for cross-polar reduction in the reflector pattern. A similar investigation can be performed for microstrip antenna modes for different mode combinations.

A

Experimental Setup for Measuring Feed Antenna Pattern

A. Experimental Setup for Measuring Feed Antenna Pattern

The measurement of the feed pattern is performed under normal laboratory condition. An illustrative diagram and photograph of the experimental setup is shown in Fig. A.1. The transmitter block consists of a broadband horn antenna which is fed by Rohde & Schwarz RF signal generator (SMBV100A). The receiver block consists of the proposed matched feed antenna which is mounted on a rotary mechanism. The strength of the receiving RF signal is measured using Agilent spectrum analyzer (N1996A). The radiation pattern at principle plane is measured by rotating the test antenna by 5°.

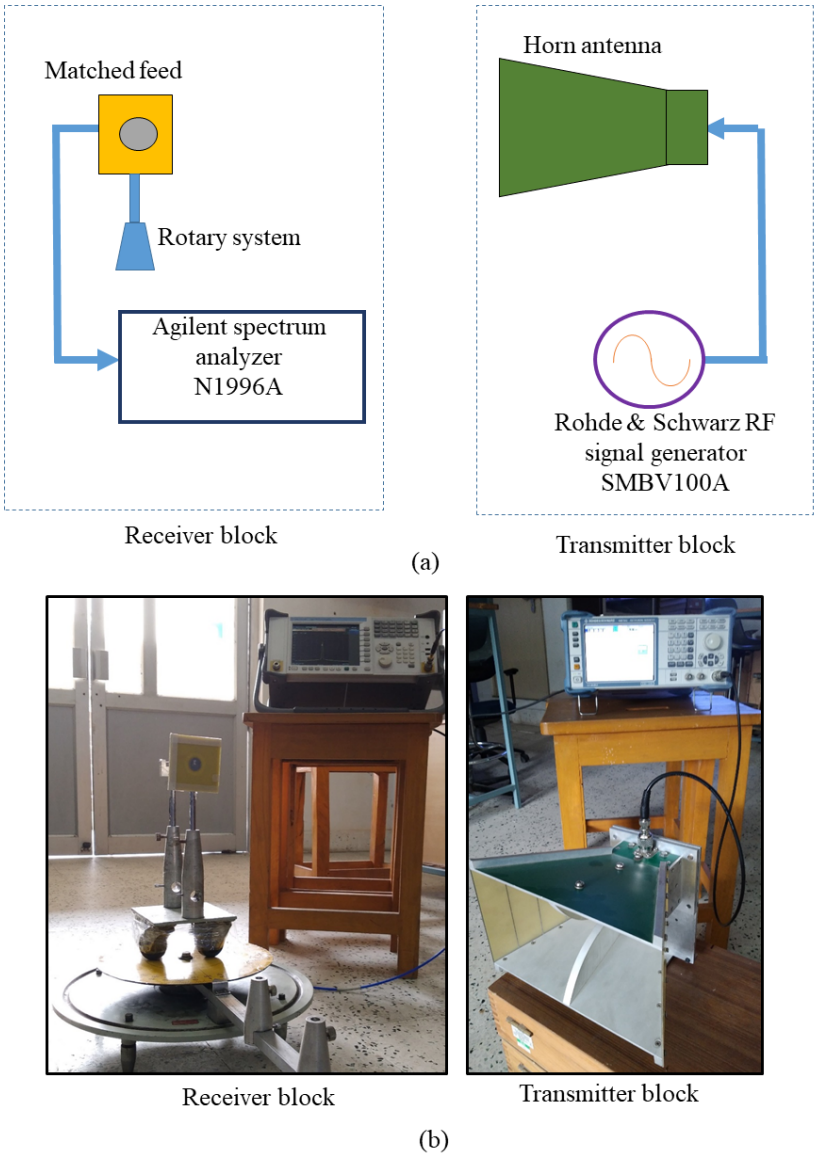

Figure A.1: (a) Illustrative diagram of the experimental setup (b) Photograph of the experimental setup for pattern measurement of the proposed feed with annular ring patch at the bottom.

Bibliography

[1] Y. Rahmat-Samii and R. Haupt, "Reflector antenna developments: A perspective on the past, present and future," *IEEE Antennas and Propagation Magazine*, vol. 57, no. 2, pp. 85–95, April 2015.

[2] A. W. Rudge and N. A. Adatia, "Offset-parabolic-reflector antennas: A review," *Proceedings of the IEEE*, vol. 66, no. 12, pp. 1592–1618, Dec 1978.

[3] M. Terada, N. Bludworth, J. Moore, and J. Sullivan, "A new deployment mechanism for reflector antennas," in *2005 IEEE Antennas and Propagation Society International Symposium*, vol. 2B, July 2005, pp. 490–493 vol. 2B.

[4] S. K. Rao, "Advanced antenna technologies for satellite communications payloads," *IEEE Transactions on Antennas and Propagation*, vol. 63, no. 4, pp. 1205–1217, April 2015.

[5] S. B. Sharma, D. A. Pujara, S. B. Chakrabarty, and V. K. Singh, "Improving the cross-polar performance of an offset parabolic reflector antenna using a rectangular matched feed," *IEEE Antennas and Wireless Propagation Letters*, vol. 8, pp. 513–516, 2009.

[6] S. Futatsumori, K. Morioka, A. Kohmura, M. Shioji, and N. Yonemoto, "Evaluation of fan beam carbon fiber reinforce plastics offset parabolic reflector antenna for w-band millimeter-wave radar systems," in *2014 International Symposium on Antennas and Propagation Conference Proceedings*, Dec 2014, pp. 307–308.

[7] R. C. Gupta, K. K. Sood, and R. Jyoti, "Investigation of factors contributing depolarization in offset reflector antenna and trimmed-reflector offset parabolic antenna with lower cross-polarization," *International Journal of RF and Microwave Computer-Aided Engineering*, vol. 22, no. 3, pp. 411–420, 2012. [Online]. Available: https://onlinelibrary.wiley.com/doi/abs/10.1002/mmce.20615

[8] Z. A. Pour and L. Shafai, "Beam squint correction in offset reflector antennas with circularly-polarized tapered primary feeds," in *2015 IEEE International Symposium on Antennas and Propagation USNC/URSI National Radio Science Meeting*, July 2015, pp. 2189–2190.

[9] C. Granet, "Designing classical offset cassegrain or gregorian dual-reflector antennas from combinations of prescribed geometric parameters. part 2: feed-horn blockage conditions," *IEEE Antennas and Propagation Magazine*, vol. 45, no. 6, pp. 86–89, Dec 2003.

[10] W. S. Gregorwich, "Polarization selective reflectors for spacecraft applications," in *IEEE Conference on Aerospace Applications*, Feb 1990, pp. 61–71.

[11] K. Nakamura and M. Ando, "A full-wave analysis of offset reflector antennas with polarization grids," *IEEE Transactions on Antennas and Propagation*, vol. 36, no. 2, pp. 164–170, Feb 1988.

[12] C. C. Cruz, J. R. Costa, C. A. Fernandes, and S. A. Matos, "Focal-plane multibeam dual-band dielectric lens for ka-band," *IEEE Antennas and Wireless Propagation Letters*, vol. 16, pp. 432–436, 2017.

[13] A. W. Rudge and N. A. Adatia, "Matched-feeds for offset parabolic reflector antennas," in *1976 6th European Microwave Conference*, Sep. 1976, pp. 143–147.

[14] ——, "New class of primary-feed antennas for use with offset parabolic-reflector antennas," *Electronics Letters*, vol. 11, no. 24, pp. 597–599, November 1975.

[15] Ta-Shing Chu and R. Turrin, "Depolarization properties of offset reflector antennas," *IEEE Transactions on Antennas and Propagation*, vol. 21, no. 3, pp. 339–345, May 1973.

[16] *Reflector Antennas*. John Wiley and Sons, Ltd, 2015, ch. 6, pp. 149–217. [Online]. Available: https://onlinelibrary.wiley.com/doi/abs/10.1002/9781119127451.ch6

[17] P. Meincke, M. Palvig, N. Vesterdal, and E. Jrgensen, "Direct optimization of electrically large reflectors and feed chains," in *2019 IEEE MTT-S International Microwave Symposium (IMS)*, 2019, pp. 897–900.

[18] R. Jana and R. Bhattacharjee, "A novel matched feed structure for achieving wide ieeehowto:kopkacross-polar bandwidth for an offset parabolic reflector antenna system," *IEEE Antennas and Wireless Propagation Letters*, vol. 14, pp. 1590–1593, 2015.

[19] K. M. Prasad and L. Shafai, "Improving the symmetry of radiation patterns for offset reflectors illuminated by matched feeds," *IEEE Transactions on Antennas and Propagation*, vol. 36, no. 1, pp. 141–144, Jan 1988.

[20] O. A. Aboul-Atta and L. Shafai, "Performance of offset parabolic reflectors illuminated by matched feeds," *Canadian Electrical Engineering Journal*, vol. 4, no. 3, pp. 26–32, July 1979.

[21] Z. A. Pour and L. Shafai, "Analytical models of dual-polarized primary matched feeds for offset reflector antennas with low cross-polarization properties at both asymmetry and diagonal planes," *IEEE Transactions on Antennas and Propagation*, vol. 64, no. 5, pp. 1627–1633, May 2016.

[22] K. Bahadori and Y. Rahmat-Samii, "Tri-mode horn feeds revisited: Cross-pol reduction in compact offset reflector antennas," *IEEE Transactions on Antennas and Propagation*, vol. 57, no. 9, pp. 2771–2775, Sept 2009.

[23] S. B. Sharma, D. Pujara, S. B. Chakrabarty, and R. Dey, "Cross-polarization cancellation in an offset parabolic reflector antenna using a corrugated matched feed," *IEEE Antennas and Wireless Propagation Letters*, vol. 8, pp. 861–864, 2009.

[24] A. Bayat and A. Khaleqi, "Design and implementation of an x-band corrugated feed horn for offset reflector antenna," in *6th International SYmposium on Antennas, Propagation and EM Theory, 2003. Proceedings. 2003*, Oct 2003, pp. 157–160.

[25] S. K. Sharma, L. Shafai, B. Balaji, A. Damini, and G. Haslam, "Multimode feed horn providing multi-phase centres with offset reflector antenna," in *2005 IEEE Antennas and Propagation Society International Symposium*, vol. 3A, July 2005, pp. 355–358 vol. 3A.

[26] M. N. M. Kehn and L. Shafai, "Characterization of dense focal plane array feeds for parabolic reflectors in achieving closely overlapping or widely separated multiple beams," *Radio Science*, vol. 44, no. 3, pp. 1–25, June 2009.

[27] Z. Allahgholi Pour and L. Shafai, "A ring choke excited compact dual-mode circular waveguide feed for offset reflector antennas," *IEEE Transactions on Antennas and Propagation*, vol. 60, no. 6, pp. 3011–3015, June 2012.

[28] R. Dey, "Wideband corrugated conjugate matched feed horn," *Electromagnetics*, vol. 37, no. 3, pp. 150–161, 2017. [Online]. Available: https://doi.org/10.1080/02726343.2017.1301187

[29] Z. Allahgholi Pour and L. Shafai, "A novel impedance matched mode generator for excitation of the te_{21} mode in compact dual-mode circular waveguide feeds," *IEEE Antennas and Wireless Propagation Letters*, vol. 10, pp. 427–430, 2011.

[30] D. Pujara and S. B. Chakrabarty, "Cancellation of high cross-polarization of an offset parabolic reflector antenna using a rectangular matched feed," *IETE Journal of Research*, vol. 58, no. 4, pp. 317–321, 2012. [Online]. Available: https://www.tandfonline.com/doi/abs/10.4103/0377-2063.102312

[31] S. B. Sharma, D. Pujara, and S. B. Chakrabarty, "Design and development of a dual-mode corrugated horn for an offset reflector antenna," *Microwave and Optical Technology Letters*, vol. 52, no. 1, pp. 113–116, 2010. [Online]. Available: https://onlinelibrary.wiley.com/doi/abs/10.1002/mop.24852

[32] R. Jana and R. Bhattacharjee, "Matched feed design employing te01 and tm11 modes in a smooth walled rectangular waveguide for cross-polar reduction in offset reflector antenna systems," *AEU - International Journal of Electronics and Communications*, vol. 69, no. 6, pp. 873 – 877, 2015. [Online]. Available: http://www.sciencedirect.com/science/article/pii/S1434841115000217

[33] Z. A. Pour and L. Shafai, "A simplified feed model for investigating the cross polarization reduction in circular- and elliptical-rim offset reflector antennas," *IEEE Transactions on Antennas and Propagation*, vol. 60, no. 3, pp. 1261–1268, March 2012.

[34] M. F. Palvig, E. Jrgensen, P. Meincke, and O. Breinbjerg, "Optimization procedure for wideband matched feed design," in *2016 10th European Conference on Antennas and Propagation (EuCAP)*, 2016, pp. 1–4.

[35] M. F. Palvig, O. Breinbjerg, P. Meincke, and E. Jrgensen, "Demonstration of tm01 circular waveguide mode in matched feeds for single offset reflectors," in *2018 IEEE International Symposium on Antennas and Propagation USNC/URSI National Radio Science Meeting*, July 2018, pp. 723–724.

[36] M. F. Palvig, P. Meincke, E. Jrgensen, and O. Breinbjerg, "A design method for mode-selective waveguide couplers in dual-polarized wideband matched-feed antennas," *IEEE Transactions on Antennas and Propagation*, vol. 66, no. 2, pp. 990–995, 2018.

[37] Songnan Yang, Sungwoo Lee, and A. E. Fathy, "Patch antennas: an alternative feed to reflectors," in *2005 IEEE Antennas and Propagation Society International Symposium*, vol. 3A, July 2005, pp. 642–645 vol. 3A.

[38] Y. L. Luo and K. M. Luk, "Characteristics of a ku-band parabolic cylindrical reflector antenna with a linear microstrip array offset feed," in *1995 Ninth International Conference on Antennas and Propagation, ICAP '95 (Conf. Publ. No. 407)*, vol. 1, April 1995, pp. 336–339 vol.1.

[39] K. S. Kona, K. Bahadori, and Y. Rahmat-Samii, "Stacked microstrip-patch arrays as alternative feeds for spaceborne reflector antennas," *IEEE Antennas and Propagation Magazine*, vol. 49, no. 6, pp. 13–23, Dec 2007.

[40] K. S. Kona, K. Bahadori, and Y. Rahmat-Samii, "Parametric study of stacked patch array configurations as alternative feeds for offset reflectors," in *2006 IEEE Antennas and Propagation Society International Symposium*, July 2006, pp. 4331–4334.

[41] Y. Rahmat-Samii, J. Huang, B. Lopez, M. Lou, E. Im, S. L. Durden, and K. Bahadori, "Advanced precipitation radar antenna: array-fed offset membrane cylindrical reflector antenna," *IEEE Transactions on Antennas and Propagation*, vol. 53, no. 8, pp. 2503–2515, Aug 2005.

[42] T. Chen and H. Wu, "Dual-polarized planar reflector feed for direct broadcast satellite systems," *IEEE Antennas and Wireless Propagation Letters*, vol. 9, pp. 693–696, 2010.

[43] Gardelli, L. Cono, and Albani, "A low-cost suspended patch antenna for wlan access points and point-to-point links," *IEEE Antennas and Wireless Propagation Letters*, vol. 3, pp. 90–93, 2004.

[44] R. Mizzoni, G. Orlando, and P. Valle, "Unfurlable reflector sar antenna at p-band," in *2009 3rd European Conference on Antennas and Propagation*, March 2009, pp. 589–593.

[45] P. Valle, G. Orlando, R. Mizzoni, F. Hlire, and K. van't Klooster, "P-band feedarray for biomass," in *2012 6th European Conference on Antennas and Propagation (EUCAP)*, March 2012, pp. 3426–3430.

[46] C. Cappellin, S. Pivnenko, K. Pontoppidan, E. Jrgensen, and P. Meincke, "Diagnostics of the biomass feed array prototype," in *2013 7th European Conference on Antennas and Propagation (EuCAP)*, April 2013, pp. 4072–4073.

[47] c. Cappellin and s. Pivnenko, "Field reconstruction and estimation of the antenna support structure effect on the measurement uncertainty of the bts1940 antenna," in *The 8th European Conference on Antennas and Propagation (EuCAP 2014)*, April 2014, pp. 2491–2494.

[48] S. Huber, F. Q. de Almeida, M. Villano, M. Younis, G. Krieger, and A. Moreira, "Tandem-l: A technical perspective on future spaceborne sar sensors for earth observation," *IEEE Transactions on Geoscience and Remote Sensing*, vol. 56, no. 8, pp. 4792–4807, Aug 2018.

[49] R. Chantalat, C. Menudier, M. Thevenot, T. Monediere, E. Arnaud, and P. Dumon, "Enhanced ebg resonator antenna as feed of a reflector antenna in the ka band," *IEEE Antennas and Wireless Propagation Letters*, vol. 7, pp. 349–353, 2008.

[50] A. Kanso, R. Chantalat, M. Thevenot, E. Arnaud, and T. Monediere, "Offset parabolic reflector antenna fed by ebg dual-band focal feed for space application," *IEEE Antennas and Wireless Propagation Letters*, vol. 9, pp. 854–858, 2010.

[51] Z. Yang, K. C. Browning, and K. F. Warnick, "High-efficiency stacked shorted annular patch antenna feed for ku-band satellite communications," *IEEE Transactions on Antennas and Propagation*, vol. 64, no. 6, pp. 2568–2572, June 2016.

[52] Z. Yang, K. F. Warnick, and C. L. Holloway, "A high radiation efficiency microstrip array feed for ku band satellite communication," in *2013 IEEE Antennas and Propagation Society International Symposium (APSURSI)*, July 2013, pp. 1576–1577.

[53] Y. Jung and S. Park, "Ka-band shaped reflector hybrid antenna illuminated by microstrip-fed horn array," *IEEE Transactions on Antennas and Propagation*, vol. 56, no. 12, pp. 3863–3867, Dec 2008.

[54] M. Nagasaka, S. Nakazawa, and S. Tanaka, "Prototype of a dual-circularly polarized parabolic reflector antenna with microstrip antenna array for 12-ghz band satellite broadcasting reception," in *2016 10th European Conference on Antennas and Propagation (EuCAP)*, April 2016, pp. 1–5.

[55] Y. L. Luo and K. M. Luk, "Radiation characteristics of a ku-band parabolic cylindrical reflector antenna fed by an offset linear array of microstrip patches," *Microwave and Optical Technology Letters*, vol. 13, no. 1, pp. 19–21, 1996. [Online]. Available: https://onlinelibrary.wiley.com/doi/abs/10.1002/%28SICI%291098-2760%28199609%2913%3A1%3C19%3A%3AAID-MOP7%3E3.0.CO%3B2-Q

[56] A. Zamanifekri and A. B. Smolders, "Beam squint compensation in circularly polarized offset reflector antennas using a sequentially rotated focal-plane array," *IEEE Antennas and Wireless Propagation Letters*, vol. 14, pp. 815–818, 2015.

[57] A. Kanso, R. Chantalat, M. Thevenot, U. Naeem, S. Bila, and T. Monediere, "Multifeed ebg dual band antenna to feed a reflector antenna," in *2011 41st European Microwave Conference*, Oct 2011, pp. 866–869.

[58] C. Menudier, R. Chantalat, M. Thevenot, T. Monediere, P. Dumon, and B. Jecko, "Phase center study of the electromagnetic band gap antenna: Application to reflector antennas," *IEEE Antennas and Wireless Propagation Letters*, vol. 6, pp. 227–231, 2007.

[59] P. Juyal and L. Shafai, "A high-gain single-feed dual-mode microstrip disc radiator," *IEEE Transactions on Antennas and Propagation*, vol. 64, no. 6, pp. 2115–2126, June 2016.

[60] N. Herscovici, C. Christodoulou, E. Rajo-Iglesias, O. Quevedo-Teruel, and M. Sanchez-Fernandez, "Compact multimode patch antennas for mimo applications [wireless corner]," *IEEE Antennas and Propagation Magazine*, vol. 50, no. 2, pp. 197–205, April 2008.

[61] T. Q. Tran and S. K. Sharma, "Radiation characteristics of a multimode concentric circular microstrip patch antenna by controlling amplitude and phase of modes," *IEEE Transactions on Antennas and Propagation*, vol. 60, no. 3, pp. 1601–1605, March 2012.

[62] C. Chiu, F. Xu, S. Shen, and R. D. Murch, "Mutual coupling reduction of rotationally symmetric multiport antennas," *IEEE Transactions on Antennas and Propagation*, vol. 66, no. 10, pp. 5013–5021, Oct 2018.

[63] S. Dumanli, "On-body antenna with reconfigurable radiation pattern," in *2014 IEEE MTT-S International Microwave Workshop Series on RF and Wireless Technologies for Biomedical and Healthcare Applications (IMWS-Bio2014)*, Dec 2014, pp. 1–3.

[64] Deqiang Yang, Yubo Wen, Mengfei Chen, and Huiling Zeng, "A multimode annular ring patch antenna for mimo applications," in *2015 IEEE 6th International Symposium on Microwave, Antenna, Propagation, and EMC Technologies (MAPE)*, Oct 2015, pp. 197–200.

[65] P. Juyal and L. Shafai, "Gain enhancement in circular microstrip antenna via linear superposition of higher zeros," *IEEE Antennas and Wireless Propagation Letters*, vol. 16, pp. 896–899, 2017.

[66] W. T. Smith and W. L. Stutzman, "A comparison of physical optics and geometrical optics methods for computation of reflector surface error effects," in *Proceedings. IEEE Energy and Information Technologies in the Southeast'*, April 1989, pp. 214–219 vol.1.

[67] S. Mercader-Pellicer, G. M. Meder, and G. Goussetis, "Comparison of geometrical and physical optics for cross-polarisation prediction in reflector antennas," in *Active and Passive RF Devices (2017)*, May 2017, pp. 1–5.

[68] C. A. Balanis, *Antenna Theory: Analysis and Design.* New York, NY, USA: Wiley-Interscience, 2005.

[69] D. J. Bem, "Electric-field distribution in the focal region of an offset paraboloid," *Proceedings of the Institution of Electrical Engineers*, vol. 116, no. 5, pp. 679–684, May 1969.

[70] A. El Alami, S. D. Bennani, A. Slimani, and A. Bendali, "Comparative study of the radiation patterns of circular patch antenna by using the model approach of the resonant cavity for microwave band rfid reader," in *2017 International Conference on Wireless Technologies, Embedded and Intelligent Systems (WITS)*, 2017, pp. 1–4.

[71] A. D. Olver and J. U. I. Syed, "Variable beamwidth reflector antenna by feed defocusing," *IEE Proceedings - Microwaves, Antennas and Propagation*, vol. 142, no. 5, pp. 394–, Oct 1995.

[72] S. K. Sharma, L. Shafai, B. Balaji, and A. Damini, "Beam scanning characteristics of an offset reflector by lateral displacements of multimode feed horn arrays for space borne radar," in *2006 IEEE Antennas and Propagation Society International Symposium*, July 2006, pp. 4335–4338.

[73] O. Yurduseven and D. Smith, "Symmetric/asymmetric h-plane horn fed offset parabolic reflector antenna with switchable pencil/fan-beam radiation characteristics," in *ISAPE2012*, Oct 2012, pp. 82–85.

[74] T. E. Charlton, K. E. Linehan, and D. B. Mowry, "2.3-metre offset antenna system for news gathering by satellite," *IEEE Transactions on Broadcasting*, vol. BC-32, no. 4, pp. 96–102, Dec 1986.

[75] T. Lindgren, O. Soutodeh, and P. . Kildal, "Study of cluster of hard horns feeding an offset multi-beam reflector antenna for dual band operation at 20/30 ghz," in *IEEE Antennas and Propagation Society Symposium, 2004.*, vol. 3, June 2004, pp. 3015–3018 Vol.3.

[76] C. Yu, S. He, P. Li, and Y. Wang, "A dual-band low-cost printed feed of offset parabolic reflector antennas for 2.4/5.5ghz wlan systems," in *2011 4th IEEE International Symposium on Microwave, Antenna, Propagation and EMC Technologies for Wireless Communications*, Nov 2011, pp. 132–135.

[77] L. G. Menndez, O. S. Kim, F. Persson, M. Nielsen, and O. Breinbjerg, "3d printed 20/30-ghz dual-band offset stepped-reflector antenna," in *2015 9th European Conference on Antennas and Propagation (EuCAP)*, April 2015, pp. 1–2.

[78] S. Y. Eom, S. H. Son, Y. B. Jung, S. I. Jeon, S. A. Ganin, A. G. Shubov, A. K. Tobolev, and A. V. Shishlov, "Design and test of a mobile antenna system with tri-band operation for broadband satellite communications and dbs reception," *IEEE Transactions on Antennas and Propagation*, vol. 55, no. 11, pp. 3123–3133, Nov 2007.

[79] C. Biurrun-Quel, E. Lacombe, F. Gianesello, C. Luxey, and C. Del-Ro, "Characterization of 3d-printed choke horn antenna for 5g backhaul applications," in *2019 13th European Conference on Antennas and Propagation (EuCAP)*, March 2019, pp. 1–4.

[80] W. Hong, Z. H. Jiang, C. Yu, J. Zhou, P. Chen, Z. Yu, H. Zhang, B. Yang, X. Pang, M. Jiang, Y. Cheng, M. K. T. Al-Nuaimi, Y. Zhang, J. Chen, and S. He, "Multibeam antenna technologies for 5g wireless communications," *IEEE Transactions on Antennas and Propagation*, vol. 65, no. 12, pp. 6231–6249, Dec 2017.

[81] Y. Yamada, K. M. Chatib Quzwain, I. I. Idrus, T. A. Latef, F. Ansarudin, M. K. Ishfaq, and T. A. Rahman, "Base station antennas for the 5g mobile system," in *2018 IEEE International RF and Microwave Conference (RFM)*, Dec 2018, pp. 1–4.

[82] S. E. El-khamy, R. M. El-Awadi, and E. . A. El-Sharrawy, "Simple analysis and design of annular ring microstrip antennas," *IEE Proceedings H - Microwaves, Antennas and Propagation*, vol. 133, no. 3, pp. 198–202, June 1986.

[83] Y. S. Wu and F. J. Rosenbaum, "Mode chart for microstrip ring resonators (short papers)," *IEEE Transactions on Microwave Theory and Techniques*, vol. 21, no. 7, pp. 487–489, Jul 1973.

List of Publications

Journal Publications

Published:

1. Kaushik Debbarma and Ratnajit Bhattacharjee, **" Matched feeds for offset reflector antenna using circular microstrip patch antenna** ," *International Journal of RF and Microwave Computer-Aided Engineering*, vol. 29, no. 11, July 2019.

2. Kaushik Debbarma and Ratnajit Bhattacharjee, **" Microstrip Patch Antenna Feed for Offset Reflector Antenna for Dual Band Application** ," *International Journal of RF and Microwave Computer-Aided Engineering*, vol. 29, no. 12, Sep 2019.

3. Kaushik Debbarma and Ratnajit Bhattacharjee, **" Small Offset Reflector with Matched Feed for 5G Application**," *IETE Journal of Research*, Taylor & Francis (Accepted, Jan 2021)

Communicated:

1. **Kaushik Debbarma** and Ratnajit Bhattacharjee, **" Design and Analysis of a Microstrip Matched Feed with Annular Ring Patch for Small Offset Reflectors**," (under review, major revision submitted) *IEEE Transactions on Antennas and Propagation.*

International Conferences

1. Kaushik Debbarma and Ratnajit Bhattacharjee,"**Comparative study of different types of antenna arrays as feed for an offset reflector antenna at 20GHz**," presented in *8th IEEE Indian Antenna Week 2017*, DIAT, Pune on 7th June 2017

2. Kaushik Debbarma and Ratnajit Bhattacharjee," **Analysis of Offset Reflector Performance Fed by 2×2 Microstrip Antenna Array using GO Technique**." presented in *3rd International Conference for Microwave and Photonics 2018*, ISM Dhanbad, 9-11 Feb, 2018.

3. Kaushik Debbarma and Ratnajit Bhattacharjee, "**2-D Circular Microstrip Patch Array Fed Offset Reflector Antenna for VSAT Application**," presented in *IEEE-INAE Workshop on Electromagnetics*, Trivandrum, 06-08 Dec, 2018.

4. Kaushik Debbarma and Ratnajit Bhattacharjee, "**Microstrip Antenna Feeds for Offset Reflector Antenna for Cross-polarization Reduction at both Diagonal and Asymmetric Planes**," presented in *Indian Conference on Antennas and Propagation*, Hyderabad, 16-19 Dec, 2018.

5. **Kaushik Debbarma** and Ratnajit Bhattacharjee, "**Pattern Shifting and Size Control in Offset Reflector Antennas with Microstrip Array as Matched Feed**," presented in *14th European Conference on Antennas and Propagation (EuCAP)*, Copenhagen, Denmark, 15-20 March, 2020.